INVESTIGATION OF CLONAL EVOLUTION IN CAPECITABINE RESISTANT CACO-2 AND IRINOTECAN RESISTANT HT-29 CELL LINES BY USING CELLULAR BARCODING TECHNOLOGY

A THESIS SUBMITTED TO
THE GRADUATE SCHOOL OF NATURAL AND APPLIED SCIENCES
OF
MIDDLE EAST TECHNICAL UNIVERSITY

BY

NURSEDA DANIŞIK

IN PARTIAL FULFILLMENT OF THE REQUIREMENTS
FOR
THE DEGREE OF MASTER OF SCIENCE
IN
BIOTECHNOLOGY

OCTOBER 2022

Approval of the thesis:

INVESTIGATION OF CLONAL EVOLUTION IN CAPECITABINE RESISTANT CACO-2 AND IRINOTECAN RESISTANT HT-29 CELL LINES BY USING CELLULAR BARCODING TECHNOLOGY

submitted by **NURSEDA DANIŞIK** in partial fulfillment of the requirements for the degree of **Master of Science** i**n Biotechnology, Middle East Technical University** by,

Prof. Dr. Halil Kalıpçılar
Dean, Graduate School of **Natural and Applied Sciences** _____

Assoc. Prof. Dr. Yeşim Soyer
Head of the Department, **Biotechnology** _____

Assist. Prof. Dr. Ahmet Acar
Supervisor, **Biotechnology, METU** _____

Assoc. Prof. Dr. Can Özen
Co-Supervisor, **Biotechnology, METU** _____

Examining Committee Members:

Assoc. Prof. Dr. Mecit Halil Öztop
Food Engineering, METU _____

Assist. Prof. Dr. Ahmet Acar
Biotechnology, METU _____

Assoc. Prof. Dr. Pelin Mutlu
Biotechnology, Ankara University _____

Date: 31.10.2022

I hereby declare that all information in this document has been obtained and presented in accordance with academic rules and ethical conduct. I also declare that, as required by these rules and conduct, I have fully cited and referenced all material and results that are not original to this work.

Name Last name : Nurseda Danışık

Signature :

ABSTRACT

INVESTIGATION OF CLONAL EVOLUTION IN CAPECITABINE RESISTANT CACO-2 AND IRINOTECAN RESISTANT HT-29 CELL LINES BY USING CELLULAR BARCODING TECHNOLOGY

Danışık, Nurseda
Master of Science, Biotechnology
Supervisor: Asst. Prof. Dr. Ahmet Acar
Co-Supervisor: Assoc. Prof. Dr. Can Özen

October 2022, 95 pages

The development of drug resistance in tumor cells is one of the biggest problems currently in the clinic. As the pace of drug discovery slows and each new drug becomes increasingly expensive to bring to market, it is becoming clearer that better model systems and an understanding of drug resistance mechanisms are needed for second-line therapies. The overall aim of this project is to investigate the clonal evolution and drug resistance in colorectal cancer cell lines Caco-2 and HT-29 by using cellular barcoding technology. It was hypothesized that the detection and tracking of the capecitabine-resistant clones in barcoded Caco-2 and irinotecan-resistant clones in barcoded HT-29 cell lines will unravel previously unidentified but key mechanisms. In parallel, studying the secondary drug responses and synergistic effects of drugs in resistant cell lines will help to identify new drug candidates and new treatment strategies. For these purposes, firstly Caco-2 and HT-29 cells were barcoded with unique barcode sequences by using a lentiviral vector system. Barcoded Caco-2 and HT-29 cells were treated with capecitabine and irinotecan respectively for six months to establish their drug-resistant derivatives. After

achieving capecitabine-resistant Caco-2 and irinotecan-resistant HT-29 cells, DNA barcode sequencing and bioinformatics analysis were performed. According to DNA barcode analysis, capecitabine-resistant Caco-2, and irinotecan-resistant HT-29 clones were detected and time-dependent frequencies of these resistant clones in the populations were tracked by sequencing of floating dead barcoded Caco-2 and HT-29 cells which were collected as pellets from harvested mediums in equal intervals during drug treatment. Additionally, secondary-drug response curves showed that the capecitabine-resistant Caco-2 cells were more sensitive to SN-38, cetuximab, and oxaliplatin whereas the irinotecan-resistant HT-29 cells were more sensitive to dabrafenib. The results indicate that well-design model systems are crucial to understanding and finding new feasible treatment strategies for drug-resistance problems in the clinic, additionally, further use of cellular barcoding technology in *in vivo* studies can play an important role to solve the clonal evolution mechanism of drug resistance.

Keywords: colorectal cancer, drug resistance, barcoding technology

ÖZ

KAPESİTABİNE DİRENÇLİ CACO-2 VE İRİNOTEKANA DİRENÇLİ HT-29 HÜCRE HATLARINDA KLONAL EVRİMİN HÜCRE BARKODLAMA TEKNOLOJİSİ KULLANILARAK ARAŞTIRILMASI

Danışık, Nurseda
Yüksek Lisans, Biyoteknoloji
Tez Yöneticisi: Dr. Öğretim Üyesi Ahmet ACAR
Ortak Tez Yöneticisi: Doç. Dr. Can Özen

Ekim 2022, 95 sayfa

Tümör hücrelerinde ilaç direncinin gelişmesi şu anda klinikteki en büyük sorunlardan biridir. İlaç keşfi hızı yavaşladıkça ve her yeni ilacın pazara sunulması giderek daha pahalı hale geldikçe, ikinci basamak tedaviler için daha iyi model sistemlerin ve ilaç direnç mekanizmalarının anlaşılmasının gerekli olduğu daha açık hale geliyor. Bu projenin genel amacı, hücresel barkodlama teknolojisini kullanarak kolorektal kanser hücre hatları Caco-2 ve HT-29 da klonal evrimi ve ilaç direncini araştırmaktır. Bu çalışmanın hipotezi, barkodlanmış Caco-2 hücrelerinde kapesitabine dirençli klonların ve barkodlanmış HT-29 hücrelerinde irinotekana dirençli klonların saptanması ve izlenmesinin daha önce tanımlanmamış anahtar mekanizmaları çözeceği üzerine oluşturuldu. Buna paralel olarak, dirençli hücre dizilerinde ilaçların ikincil ilaç tepkileri ve sinerjik etkilerinin incelenmesi, yeni ilaç adaylarının ve yeni tedavi stratejilerinin belirlenmesine yardımcı olacaktır. Bu amaçla öncelikle Caco-2 ve HT-29 hücreleri lentiviral vektör sistemleri kullanarak benzersiz barkod dizileriyle barkodlandı. Barkodlu Caco-2 ve HT-29 hücreleri, ilaca dirençli türevlerini oluşturmak için sırasıyla altı ay boyunca kapesitabin ve

irinotekan ile tedavi edildi. Kapesitabine dirençli Caco-2 ve irinotekana dirençli HT-29 hücreleri oluşturulduktan sonra DNA barkod dizilimi ve biyoinformatik analizler yapıldı. DNA barkod analizine göre, kapesitabine dirençli Caco-2 ve irinotekana dirençli HT-29 klonları tespit edildi ve bu dirençli klonların popülasyonlardaki zamana bağlı frekansları, ilaç uygulaması boyunca besiyerlerinden eşit aralıklarla pelet olarak toplanan ölü, barkodlu Caco-2 ve HT-29 hücrelerinin dizilenmesi ile takip edildi. Ek olarak, ikincil ilaç yanıt eğrileri, kapesitabine dirençli Caco-2 hücrelerinin SN-38, setuksimab ve oxaliplatine daha duyarlı olduğunu; irinotekana dirençli HT-29 hücrelerinin ise dabrafenibe daha duyarlı olduğunu gösterdi. Sonuçlar, klinikte ilaç direnci sorunu için yeni uygun tedavi stratejilerini anlamak ve bulmak için iyi tasarlanmış model sistemlerinin çok önemli olduğunu, ayrıca hücresel barkodlama teknolojisinin *in vivo* çalışmalarda daha fazla kullanılmasının ilaç direnci mekanizmalarının klonal evrimini anlamakta önemli bir rol oynayabileceğini göstermektedir.

Anahtar Kelimeler: kolorektal kanser, ilaç direnci, barkodlama teknolojisi

This thesis is dedicated to my family and my lovely husband,

For their endless love and support

ACKNOWLEDGMENTS

I would like to express my deepest gratitude to my supervisor Assist. Prof. Dr. Ahmet Acar, for the guidance, advice, criticism, encouragement, insight, and support throughout the research. I am very grateful for his time devoted to this study and sincerely appreciate his careful revision. I also would like to my co-supervisor Assoc. Prof. Dr. Can Özen for their guidance and advice throughout my graduate education.

I would like to thank the jury members, Assoc. Prof. Dr. Pelin Mutlu and Assoc. Prof. Dr. Mecit Halil Öztop for their valuable time and contributions.

I would like to thank Dr. Süleyman Coşkun and his lab members for their support throughout my graduate education.

I would like to express my thanks to Acar Lab members; Rana Can Baygın, Tuğçe Dilber, Can Ildız, Hakan Berk Aydın, Kübra Yılmaz and Erdi Can Kılıç for their support and contributions to this study.

I would like to express my special thanks to my colleagues Gizem Damla Yalçın and Arda Temena for their academic advice, sharing experience with me, and valuable contributions to this study and my life. I also would like to thank to Özlem Neyişci for her valuable friendship.

Finally, I wish to express my deepest love and gratitude to my husband and my family for their constant support, encouragement, and immeasurable sacrifices.

This work is funded by the Scientific and Technological Research Council of Turkey under grant number TUBİTAK 118C197.

This study was partially funded by the Scientific Research Projects Coordination Unit of Middle East Technical University. Project number: TEZ-YL-108-2022-10867.

TABLE OF CONTENTS

LIST OF TABLES

TABLES

LIST OF FIGURES

FIGURES

LIST OF ABBREVIATIONS

ABBREVIATIONS

CAF Cancer-Associated Fibroblasts

CAPE Capecitabine

CRC Colorectal Cancer

DMSO Dimethyl Sulfoxide

EGFR Epidermal Growth Factor Receptor

EMT Epithelial-Mesenchymal Transition

ERK Extracellular Signal Regulated Kinase

5-FU 5-Fluorouracil

IRI Irinotecan

MAPK Mitogen Activated Protein Kinase

MEK Mitogen Activated Protein Kinase Kinase

SDS Sodium Dodecyl Sulfate

PBS Phosphate Buffer Saline

TBS-T Tris-buffered saline and Tween-20

CHAPTER 1

INTRODUCTION

1.1 Colorectal Cancer

Cancer is a global health problem that can affect individuals of all ages and gender and is responsible for the second-highest disease-related death rate worldwide (Global Cancer Statistics 2020: GLOBOCAN Estimates of Incidence and Mortality Worldwide for 36 Cancers in 185 Countries | Enhanced Reader n.d.). Accumulation of genetic mutations and epigenetic alterations are the main factors for tumorigenesis (Hao, Wang, and Di 2015). Colorectal cancer is one of the five most common cancer types (breast, lung, colon-rectum, prostate, stomach) and the second cancer type that has the highest mortality rate with 935,000 estimated death in 2020 (9.4%) after lung cancer (18%) (Global Cancer Statistics 2020: GLOBOCAN Estimates of Incidence and Mortality Worldwide for 36 Cancers in 185 Countries | Enhanced Reader n.d.), (Sawicki et al. 2021).

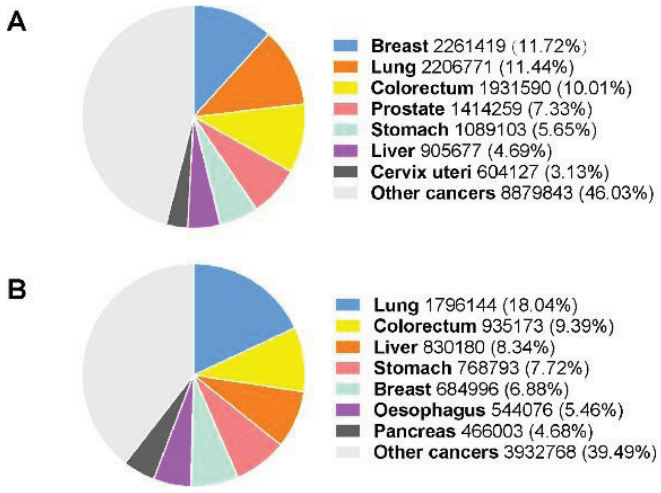

Figure 1.1 (A) Schematic representation of the ratio of most common cancer types, **(B)** Distributions of cancer types according to their mortality rates (taken by (Xi and Xu 2021))

Cancer types have close relations with the lifestyles of people and socioeconomic situations of societies/countries. Pollution of air and water, dietary patterns, and physical activities are important markers for determining which types of cancer have higher risks for the societies (Sawicki et al. 2021). Colorectal cancer is mainly described as structural malformation of the healthy colonic epithelium to adenomatous polyps as malignant (Banerjee et al. 2017). Colon polyps, chronic inflammation in the colorectal system, diabetes mellitus, and obesity can be evaluated as strong precursor markers for the development of the tumor structures (Sawicki et al. 2021). Tumor cells of malignant structures of the mucosal layer of the colon and/or rectum may spread to lymph nodes or metastasis sites like the liver (Anderson and Simon 2020). The tumor microenvironment is comprising the key factors such as autocrine and paracrine signals or Cancer-Associated Fibroblasts (CAFs) for the generation and proliferation of tumor cells resulting in tumorigenesis, angiogenesis, and involved in drug resistance to treatments (Anderson and Simon 2020). Although chemotherapy is a crucial part of treatment strategies for cancer patients according to the tumor stage to eliminate the tumorigenesis, intrinsic or de novo acquired drug resistance limits achieving successful results (T. Hu et al. 2016).

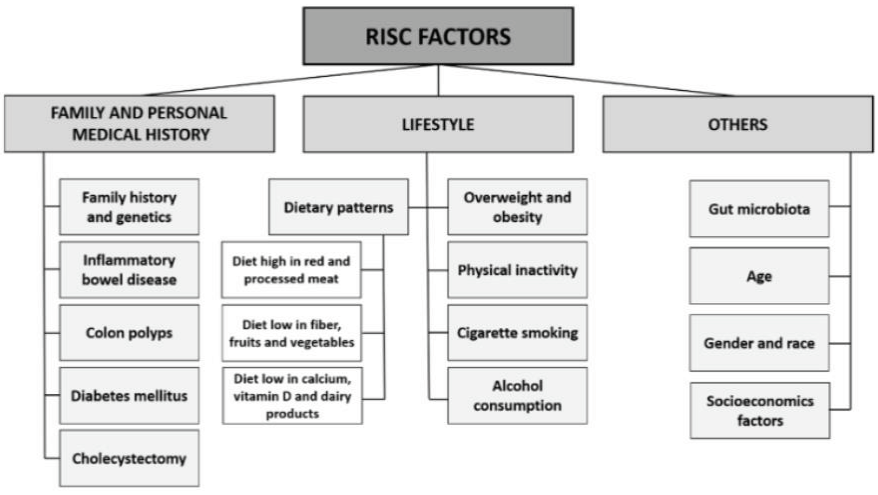

Figure 1.2 Schematic diagram of colorectal cancer risk factors **(**taken by (Sawicki et al. 2021))

1.2 Chemotherapy Drug Treatment in Colorectal Cancers

Colorectal cancer (CRC) treatment strategies are formed by surgery, radiotherapy, chemotherapy, and targeted therapies (Banerjee et al. 2017). Oxaliplatin (OX), Irinotecan (IRI), SN-38, 5-Fluorouracil (5-FU), and Capecitabine (CAPE) are the most commonly used non-site specific chemotherapeutic drugs for CRC patients and different combinations (Folinic acid-Fluorouracil-Oxaliplatin (FOLFOX), Folinic acid-Fluorouracil-Irinotecan (FOLFIRI), Capecitabine-Oxaliplatin (CAPOX)) of these drugs are used to increase the positive response rate to the treatment and prevent acquired drug-resistant against to monotherapeutic drugs (Banerjee et al. 2017). On the other hand, the idea of targeting the specific pathways which have roles in tumor proliferation, differentiation, metastasis, and apoptosis mechanisms has triggered the use of small molecules and monoclonal antibodies in CRC treatment (Xie, Chen, and Fang 2020). Pre-existing or de novo acquired resistance to drug therapies and side effects of drugs are the most important limiting factor against traditional cancer treatment strategies (Kciuk, Marciniak, and Kontek 2020).

The use of small molecules in the targeted therapy can enable the target of both surface proteins or intracellular downstream proteins in the tumor cells or tumor microenvironmental cells (Xie, Chen, and Fang 2020). Cetuximab (EGFR inhibitor), Panitumumab (EGFR inhibitor), Dabrafenib (BRAF inhibitor), Vemurafenib (BRAF inhibitor), and Bevacizumab (circulating VEGF-A inhibitor) are some of the important monoclonal antibodies which used alone, sequential or combined with the chemotherapies in CRC treatment (Xie, Chen, and Fang 2020). During treatment, exposure to the EGFR inhibitors mostly results in mutations in the RAS (KRAS or NRAS) gene in CRC cells that cause treatment failure by acquiring resistance to the inhibitors (Aleksakhina, Kashyap, and Imyanitov 2019).

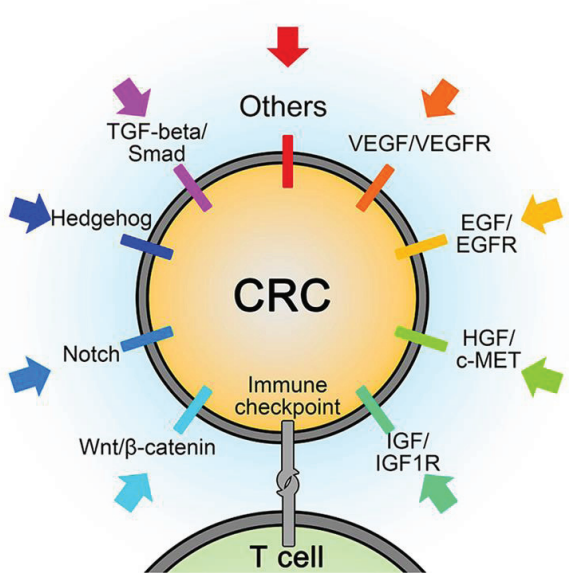

Figure 1.3 Schematic representation of main target pathways and receptors of targetted cancer therapy agents(taken by (Xie, Chen, and Fang 2020))

1.2.1 Action Mechanism of Capecitabine

One of the most preferred treatment methods for CRC patients is fluoropyrimidine-based chemotherapeutic drugs (Leicher et al. 2017). 5-fluorouracil (5-FU) is the most well-known member of these fluoropyrimidine-based first-line therapy options for patients and 5-FU was considered the only effective therapeutic drug for metastatic CRC patients until the 1990s (Leicher et al. 2017), (Luo et al. 2016). Capecitabine (Xeloda) is a pro-drug form of the 5-Fluorouracil that is available as an oral administration tablet for use of patients and preferred as single-agent therapy or in combination therapies instead of 5-FU due to their less cytotoxicity and more stable bioavailability properties [(Walko and Lindley 2005),(Saif, Katirtzoglou, and Syrigos n.d.), (Hirsch and Yousuf Zafar 2011). Capecitabine is the first approved oral form of 5-FU by the FDA (Hirsch and Yousuf Zafar 2011). Administrated Capecitabine is converted to Flurourocil in the liver as an active metabolite by three enzymatic reactions (Carboxylesterase, Cytidine deaminase, Thymidine Phosphorylase) (Walko and Lindley 2005). Several studies on 5-FU indicate that the

last step of this conversion occurs on the tumor side because upregulation of the Thymidine Phosphorylase (TP) enzyme in tumor tissue (Hirsch and Yousuf Zafar 2011). The main effect of 5-FU in cancer cells is inhibition of DNA and RNA synthesis and repair mechanisms by blocking deoxythymidine monophosphate (dTMP) production (Hirsch and Yousuf Zafar 2011).

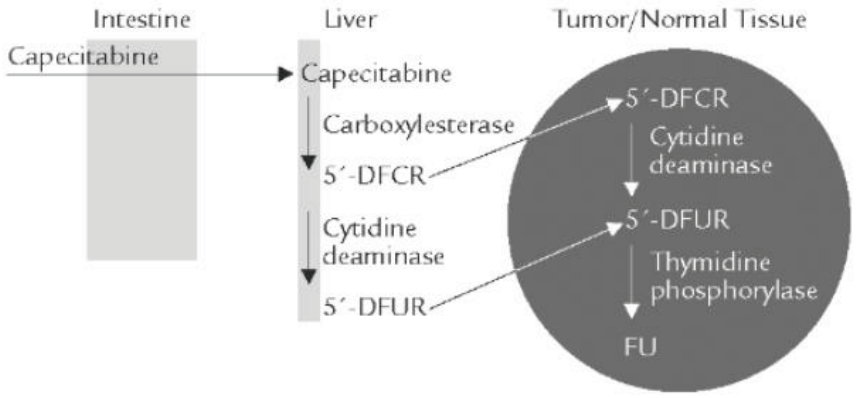

Figure 1.4 Schematic diagram of action mechanism of capecitabine (taken by (Walko and Lindley 2005))

1.2.2 Action Mechanism of Irinotecan

Irinotecan (IRI) is one of the most widely used chemotherapy drugs which was approved in 1994 in Japan as a medically usable anti-cancer agent (Bailly 2019). SN-38 is the active metabolite of the Irinotecan, Topoisomerase-1 (Topo-1) enzyme is the main target of the agent (Bailly 2019). Topo-1 has crucial importance during DNA replication and transcription for cancer cells' to continue their uncontrolled cell division (Kciuk, Marciniak, and Kontek 2020). Inhibition of Topo-1 by active agent SN-38 prevents the release of Topo-1 from the DNA double-strand and causes the formation of Double-Strand Breaks (DSB) and finally leads to apoptosis by inducing of DNA Damage Response (DDR) mechanism (Kciuk, Marciniak, and Kontek 2020). As some research reveals that Top1, ABCG2, PXR/SXR, and

CYP3A4 expression levels are important markers to understand whether there is an acquired resistance against irinotecan in the tumor cells resulting in treatment failure (Ozawa et al. 2021).

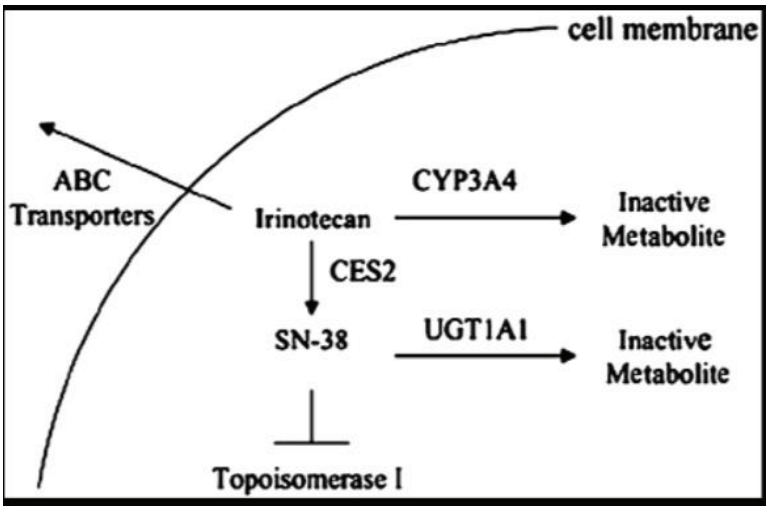

Figure 1.5 Schematic diagram of action mechanism of irinotecan (taken by (Parodi et al. 2008))

1.3 Drug Resistance in Cancer

Determination of the most effective treatment strategy is one of the vital steps to increase the overall survival rate in cancer patients. Statistically, 90% of cancer-related deaths are caused by intrinsic or acquired resistance against therapeutic drugs (X. Wang, Zhang, and Chen 2019). Definition of drug resistance is the ineffectiveness of the chemotherapeutic drugs in the inhibition of the tumor cells' proliferation and progression (Nikolaou et al. 2018). ATP-Binding cassette family (ABC) is one of the complexes which has an important role in multi-drug resistance mechanism; some studies on *ABCG2* indicate that overexpression of *ABCG2* is related to irinotecan resistance in breast cancer cells (Kciuk, Marciniak, and Kontek 2020), (Ozawa et al. 2021).

The heterogeneous nature of tumor cells and tumor microenvironments are the other two key factors in mediating drug resistance (Yalcin et al. 2020), (Vasan, Baselga, and Hyman 2019). Epigenetic and genetic alterations in the tumor cells and tumor microenvironmental cells (stromal cells, immune system cells, etc.) might induce the uncontrollable nature of the tumor cells by releasing some factors (NF-κB, IL-6, and IL-8) and increase the aggressiveness of tumor cells (Neophytou et al. 2021). One of the well-known examples of CAFs-related drug resistance in tumor cells is hyperactivation of Epithelial-Mesenchymal Transition (EMT) by releasing TGF-β, FGF, and EGF from CAFs (Son et al. 2017). Hyperactivation of the Wnt/β catenin signaling pathway is another important tumor microenvironment-related chemoresistance factor that leads to the overproduction of ATP-binding cassette G2 protein (ABCG2) (Son et al. 2017).

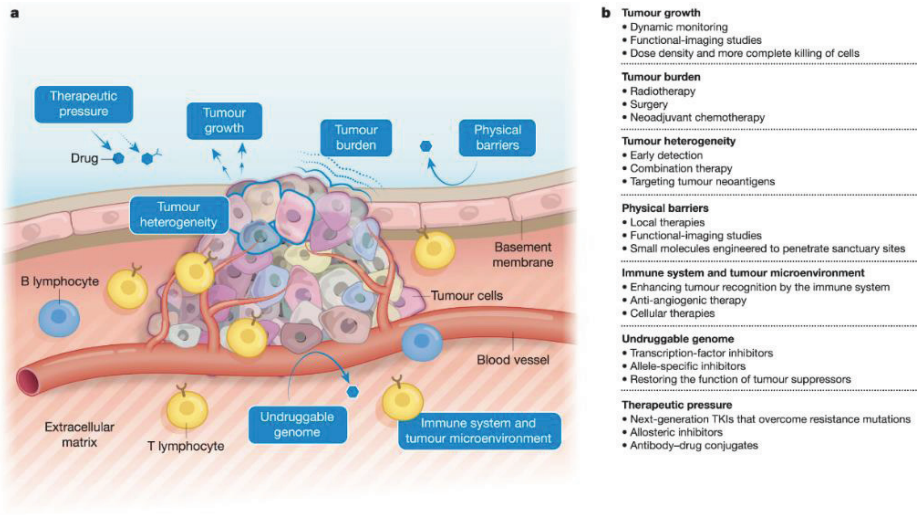

Figure 1.6 Schematic diagram of the drug resistance-driven factors in a tumor microenvironment (taken by (Vasan, Baselga, and Hyman 2019))

1.3.1 Tumor Heterogeneity

Morphologically, physiologically, and genetically heterogeneous nature of tumor cells are one of the leading causes of divergent tumor cell clones and drug resistance

(Marusyk and Polyak 2010). Expression differences in surface receptors, growth signals, and proliferation signals cause changes in response rate to cell division control signals of the tumor cells, and these determine the aggressiveness of the tumor cells and display differences from patient to patient even in the same cancer types (inter-tumoral heterogeneity)(Marusyk and Polyak 2010),(A. Zhang et al. 2022). Tumor cells are in continuous interaction with the extracellular matrix, vascular endothelial cells, stroma, and immune cells which form the tumor microenvironment and are one of the main reasons for heterogeneity (D. Wu et al. 2017). Studies indicate that hypoxic conditions formed by tumor microenvironmental cells cause tumor cell migration and invasion by increasing the expression of hepatocyte growth factor (Blank et al. 2018). As indicated in studies, clonal evolution of resistant cells is caused by continuous cross-talk between tumor cells themselves and tumor cells and microenvironmental cells. These interactions lead to alteration in expressions of key signals and target proteins that result in drug resistance(A. Zhang et al. 2022).

1.3.2 Second-Line Therapy in Drug Resistance

Drug resistance is a very critical factor in the first-line treatment period of cancer, and limits treatment strategies and effective drug options. In clinics, different chemotherapeutic agents are used as single agents, combinations or sequential therapies after tumor cells acquire resistance to the drugs in the first-line therapy (Guglielmi et al. n.d.). Second-line therapies are crucial to improve the life quality of the patients and survival rate; because almost 90% of the deaths during the first-line therapies are caused by pre-existing and de novo acquired drug resistance (X. Wang, Zhang, and Chen 2019). Tumor cells that have drug resistance to specific chemotherapeutic drugs may have more susceptibility to other chemotherapeutic drugs. Collateral sensitivity to other chemotherapeutics after acquired resistance to drugs in the first-line therapy determines the drugs which will be administrated during second-line or third-line therapies (Dhawan et al. 2017). Some studies reveal

that during second-line therapy, drug-free time periods between chemotherapeutic drug administration increase the rate of collateral sensitivity and successful results (Dhawan et al. 2017).

1.3.3 Combination Therapy in Drug Resistance

Combination therapy is one of the most important treatment strategies against intrinsic and acquired drug resistance by targeting more than one therapeutic promising target (A. Zhang et al. 2022). Since drug resistance can be originated from many different mechanisms: genetic/epigenetic changes, expression level changes, physiological changes, drug efflux, target alterations, alteration in tumor microenvironment compositions, etc., targeting different mechanisms and pathways is an important alternative strategy (Leary et al. 2018). Most cancer patients develop drug resistance by genetic alterations on MET, PD-L1, KRAS, ESR1, AKAP12, MKRN1, and BRAF genes during their chemotherapeutic treatment periods, therefore combination drug treatments target suppression of growth and progression mechanisms of these resistant clones (A. Zhang et al. 2022). The main purposes of combination therapies are preventing acquired drug resistance, decreasing side-effects of the drugs by using reduced doses, and inhibiting of proliferation and growth of tumor cells by targeting alternative pathways. At this point, the drugs administrated as combination therapy should exhibit a synergistic effect to enhance their efficiencies at lower doses (Leary et al. 2018), (Saputra et al. 2018).

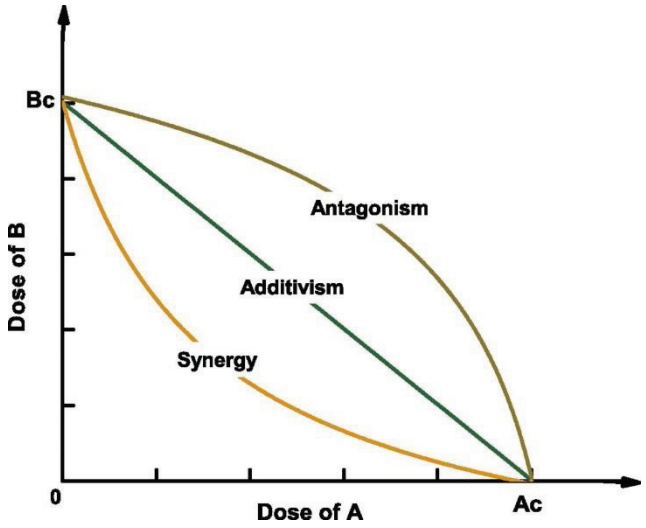

Figure 1.7 Schematic diagram of the drug interactions within drug combination therapies (taken by (Li et al. 2016))

1.4 Cellular DNA Barcoding Technology

The heterogeneous nature of tumor cells and tumor microenvironment has a significant role in drug resistance mechanisms to chemotherapeutic drugs (Kebschull and Zador 2018),(Dujardin et al. 2021). Tracking methods of clonal evolution of tumor cells have the power to investigate the acquired or de novo resistant cells against the treatment (Kebschull and Zador 2018), (Dujardin et al. 2021). Integration of short nucleic acid sequences to cellular DNA strategy started almost 30 years ago (Kebschull and Zador 2018).

Developments of high-throughput sequencing instruments have enabled the screening of a high number of cells at the same time and have provided more reliable results (Bramlett et al. 2020). All cell types appropriate for retroviral or lentiviral transduction can be labeled with these commercially available vectors (Bramlett et al. 2020). Those unique sequences embedded in nucleic acids also provide tracking of tumor cells' proliferation, progression, and metastasis in both *in vitro* and *in vivo* model systems (Bramlett et al. 2020).

1.4.1 Lentiviral and Retroviral Vector Systems for DNA Barcoding

Lentiviral and retroviral vector systems originated from human/ animal pathogen viruses and belong to the *Retroviridae* family (Dufait et al. 2012). Lentiviruses are subtypes of γ-retroviruses and have more complex genetic structures (Dufait et al. 2012). Genetic engineering studies have optimized the use of these vector systems for therapeutic and research purposes, therefore high transduction efficiencies and high integration stability of genes of interest into the host cells' genetic materials made them one of the most important tools in both research laboratories and clinics. Especially, a broad host range (infection capability on both dividing and non-dividing cells), higher virion stability with long-term gene expression, and capability of insertion of complex genetic elements are the main reasons why lentiviral vector systems are more feasible for research and medical applications (Dufait et al. 2012). One of the well-known applications of lentiviral and retroviral vectors is gene therapy applications in clinics and (chimeric antigen receptor) CAR-T cell immunotherapy in cancer treatment (Labbé, Vessillier, and Rafiq 2021).

Monitoring clonal dynamics in complex and heterogeneous cellular populations has always been a challenge. Until the recent technological and scientific developments, fluorescent markers had been preferred commonly for tracking single cells or the limited number of clones in both *in vitro* and *in vivo* studies (Porter et al. 2014). Integration of high-throughput technologies ‘‘- omics’’ science such as massively parallel sequencing into biology and genetics research has led to an increase in the use of DNA-based markers for clonal tracking and obtaining more sensitive and reliable analysis results (Porter et al. 2014),(Gerrits et al. 2010). Viral vector systems are important tools of cellular barcoding technology and are commonly preferred for tracking clonal dynamics and evolutions of even a million cells at the same time (Acar et al. 2020), (Bhang et al. 2015). Production of lentiviral vectors is performed by transfection of suitable packaging cells (HEK 293T, HEK 293) with these three plasmids: transfer vector, packaging vector, and envelope vector (Sinn, Sauter, and Mccray 2005).

1.5 Aim of Study

An ongoing project in our lab aims to investigate and reveal the clonal evolution of drug resistance in colorectal cancer. This thesis study is a part of this project and seeks the generation of capecitabine-resistant Caco-2 and irinotecan-resistant HT-29 colorectal cancer (CRC) cell lines to investigate and better understand of clonal evolution of chemotherapeutic drug resistance in CRC cells by using cellular barcoding technology. For these purposes;

1) To tag the Caco-2 and HT-29 cells with the unique sequences, Caco-2 and HT-29 cells were transduced with Lentiviruses to integrate unique barcodes into the cell lines' DNA
2) To generate the capecitabine-resistant Caco-2 and irinotecan-resistant HT-29 cell lines, barcoded Caco-2 and barcoded HT-29 cell lines were treated with capecitabine and irinotecan, respectively for six months.
3) To detect capecitabine-resistant Caco-2 and irinotecan-resistant HT-29 clones, isolated genomic DNA (gDNA) from initial, DMSO control and resistant cell lines were sequenced, and bioinformatics analyses were performed
4) To investigate the effect of drug resistance, cell viability assays were conducted in the presence of different chemotherapeutic drugs as monotherapy or combined therapy on capecitabine-resistant Caco-2 and irinotecan-resistant HT-29 cells

CHAPTER 2

MATERIALS AND METHODS

2.1 Cell Line Characteristics

Caco-2 cells are colorectal adenocarcinoma-originated intestinal model cell lines (Verhoeckx et al. 2015). Caco-2 cell line was established from a 72 years old colorectal patient. The cell line is heterogeneous and shows different characteristics and expression patterns (Verhoeckx et al. 2015). Caco-2 cells are able to exhibit enterocytic differentiation when they reach confluency without the need for other differentiation supplements in their culture medium (Verhoeckx et al. 2015). This differentiation of the Caco-2 cells occurs generally between 14-21 days culture period and polarized microvilli-like structures can be observed under a microscope (Verhoeckx et al. 2015). Caco-2 cells are mutant in terms of *P53*, while wild-type for *KRAS, BRAF, PIK3CA*, and *PTEN* genes (Ahmed et al. 2013). HT-29 cell line was established from a 44 years old female colorectal adenocarcinoma patient in 1964 (Cohen, Ophir, and Shaul 1999). HT-29 cell line has *BRAF* (p.V600E), *PIK3CA* (p.P449T) and *P53* (p.R273H) mutations (Verhoeckx et al. 2015). HT-29 cells are not able to differentiate in normal culture conditions but they can show polarized structures under the treatment of colchicine, nocodazole, taxol, and forskolin (Cohen, Ophir, and Shaul 1999).

2.2 Culture Conditions of Caco-2 and HT-29 Cell Lines

Caco-2 and HT-29 cell lines were obtained from ŞAP Institute, Ankara. Caco-2 cells were maintained in MEM-Eagle Earle's Salts medium (Biological Industries, Israel) supplemented with 20% (v/v) fetal bovine serum (Biological Industries, Israel) and 1% (v/v) Penicillin-Streptomycin, 1% (v/v) L-Glutamine and 1% (v/v) Non-

Essential Amino acids. HT-29 cells were maintained in DMEM High Glucose medium (Biological Industries, Israel) supplemented with 10% (v/v) fetal bovine serum (Biological Industries, Israel) and 1% (v/v) Penicillin-Streptomycin, 1% (v/v) L-Glutamine. Cells were incubated at 37˚C in a humidified atmosphere with 5% (v/v) CO_2 in an incubator (Nüve, Türkiye).

2.3 Sub-culturing and Counting of Cells

When the cells had 70-80% confluency in the 10 cm cell culture dishes, cell passaging protocols were applied to the cells. Firstly, the used medium in the dishes was discarded and the cells were washed with Phosphate Buffered Saline (PBS) (Biological Industries, Israel), then the Trypsin-EDTA (Biological Industries, Israel) solution was added onto the cells for inactivation of cell surface and cell-cell interactions and dissociation of the cells from the dishes' surfaces. The cells were incubated in a humidified incubator with 5% CO_2 at 37˚C for 4-6 minutes (the required time was different according to cell type). After, Trypsin-EDTA solution activity was inhibited with fresh medium, and cells were centrifuged at 180 x g for 3 minutes. Finally, supernatants were discarded, and cell pellets were dissociated with fresh mediums, and cells were seeded onto new 10 cm cell culture dishes.

Viable and dead cells were counted by using a Thoma hemocytometer (Marienfeld, Germany). Counted cells were prepared in a 1:10 ratio with Trypan Blue Dye (Biological Industries, Israel). Viable cells are in brownish color, while dead cells turn to blue color in Trypan Blue dye-cell mix solution (Strober 2015). The following equation was used to calculate the total number of the cells in 1 mL cell suspension.

Cell number/ mL= Average cell count per square x Dilution factor x 4 x 10^6

2.4 Cell Viability Assay (MTT Assay)

Estimation of the viable cells in the multi-well plates under specific circumstances is very important in *in vitro* studies. MTT [3-(4, 5-dimethylthiazol-2-yl)-2, 5-

diphenyltetrazolium bromide] assay is one of the most commonly used cell viability and proliferation assays (Riss et al. 2004). In this study, Caco-2 and HT-29 cells were seeded (10 x 10^3 / well in 96 well plates (for Caco-2 and HT-29 cell lines, 75 x 10^3 / well in 6 well plates (for Caco-2 cell line)) onto 96 well plates and/or 6 well plates according to the requirements of the experiments. The seeded cells were allowed to attach for 24 hrs., then the Caco-2 and HT-29 cells were treated with drugs of the specified assays and incubated for 72 hrs. in a humidified incubator with 5% CO_2 at 37^0 C incubator. After 72 hrs. incubation, 5 mg/mL MTT ((3-(4,5-dimethylthiazol-2-yl)-2,5-diphenyltetrazolium bromide) (Serva, Germany) solution was applied to each well, and the plates were incubated 4 hrs. in the incubator and 10% SDS solution was applied into the wells to solve the formazan crystals. After overnight incubation of the plates at 37^0 C incubator, absorbance values were measured by using a microplate spectrophotometer (Multiskan GO; Thermo Fisher Scientific, USA) at 570 nm wavelength. Cell viabilities in the solvent control groups were accepted as 100% and relative cell viability rates of the drug-treated groups were calculated accordingly.

2.5 Lentivirus Production

10 cm tissue cell culture plate was coated with 5 mL 0.1 mg/ mL Poly-L -Lysine (PLL) (Serva, Germany) for 30 min. at room temperature. Then, PLL was aspirated and the plate was dried at room temperature in a laminar flow hood. 2 x 10^6 HEK 293T cells were seeded onto the coated plate with 10 mL fresh full growth medium.

On the following day, 2.4 µg CloneTracker XP™ 1M Barcode-3' Library Pool 1 with RFP-Puro (Cellecta, USA Lot# 180817002), 0.6 µg pCMV-VSVG envelope vector (Addgene, USA # 8454), and 2.4 µg Delta 874.LV packaging vector (Addgene, USA # 8455) plasmids were added into DMEM Blank Media with 16.2 µL Lipofectamine 2000 (Invitrogen, USA), and the final volume was 600 µL. The Lipofectamine- DNA complex was incubated at room temperature for 30 min. and

the complex was added to the HEK 293T cell plate. On the other day, the medium of the HEK 293T cells was changed with 10 mL fresh medium.

On the fourth day, media was harvested and filtered with a 0.45 μm pore size filter and aliquoted into the cryovials to store at -80˚C.

2.6 Determination of Puromycin Concentration

The CloneTracker XP™ 1M Barcode-3' Library Pool 1 with RFP-Puro vector plasmid has a puromycin resistance gene. Due to this resistance gene, it is possible to eliminate the cells that are not transducted with any lentiviral vector with the treatment of puromycin selection concentration (CloneTracker XP^{TM} Lentiviral Barcode Libraries 2018). Therefore, puromycin selection concentrations were determined for the Caco-2 and HT-29 cell lines. Caco-2 cells were seeded into the 6 well plates (75x 10^3 / well) in 2 mL growth mediums. After 24 hrs. incubation, mediums were changed with fresh 2 mL full growth mediums which contained different Puromycin (Invivogen, France) doses, and mediums of the control wells were changed with fresh medium without puromycin. After 72 hrs. MTT cell viability assay protocol that explained in section 2.4 was applied. The cell viability rates in the puromycin-treated groups were calculated according to the drug-free control group. Puromycin concentration was determined for each cell line according to the analysis. Puromycin concentration experiments of the HT-29 cell line were conducted by our laboratory member, Rana Can Baygın.

Table 2.1 Determination of Caco-2 Puromycin Concentration Experiment Plate Set-up

Plate		
No Puromycin	*5 μg/mL Puromycin*	*7.5 μg/mL Puromycin*
10 μg/mL Puromycin	*12.5 μg/mL Puromycin*	*15 μg/mL Puromycin*

2.7 Determination of Multiplicity of Infection (MOI)

On the first day, 75 x 10^3 Caco-2 cells were seeded into the two six wells in 2 mL of growth mediums. On the following day, different amounts of lentivirus were added with 1 mL of growth mediums that contained 8 µg/mL Polybrene. In every six wells, one well was the ‘‘no virus’’ control group. Seeded cells were incubated with virus-contained mediums for 24 hrs. On the third day, previously determined puromycin concentration was added onto the cells in the fresh 2 mL mediums except ‘‘no puromycin’’ control wells. After 72 hrs. incubation with a selection medium containing appropriate puromycin doses, 200 *µL* MTT solution was added, after 4 hrs. 2 mL 10% SDS solution was applied to the 6 well plates and required amounts of the lentivirus for MOI ≤ 0.1 were determined with analysis of absorbance values for each cell lines. MOI experiments of the HT-29 cell line were conducted by Rana Can Baygın. The MOI experimental set-up of Caco-2 cells are indicated in **Table 2.2.**

Table 2.2 Caco-2 MOI Determination Six Well Plates Set-up

Plate 1		
No Puromycin (30 *µL virus*)	12 *µL virus*	24 *µL virus*
36 *µL virus*	48 *µL virus*	No virus
Plate 2		
No Puromycin (87,5 *µL virus*)	50 *µL virus*	75 *µL virus*
100 *µL virus*	125 *µL virus*	No virus

2.8 Barcoding of the Cell Lines

The Caco-2 cell lines were seeded into the 2x 15 cm cell culture dish (5 x 10^6 / cell culture dish) with 20 mL full growth medium. The following day, the cells were transducted with previously generated lentiviral vectors which have unique barcoding sequences in the presence of 8 µg/mL Polybrene in 15 mL medium. The amount of the lentivirus was determined by lentiviral titration results (MOI experiments) as ≤ 0.1 that each cell was transfected with maximum one lentiviral vector. Totally, 6.667 µL lentivirus was used for 2 x 15 cm cell culture dishes for barcoding of the Caco-2 cell line. Following infection, the used medium of the cells were changed with 12.5 µg/mL puromycin containing fresh medium. Due to the puromycin-resistant gene in the lentiviral vectors, barcoded Caco-2 cells with unique barcode sequences continued to proliferate while non-transducted cells were eliminated. When the barcoded Caco-2 cells reached to 80-90% confluency, the cells were frozen in cryovials (4 x 10^6 cells in each stock). The HT-29 cell line barcoding experiment was carried out by Rana Can Baygın.

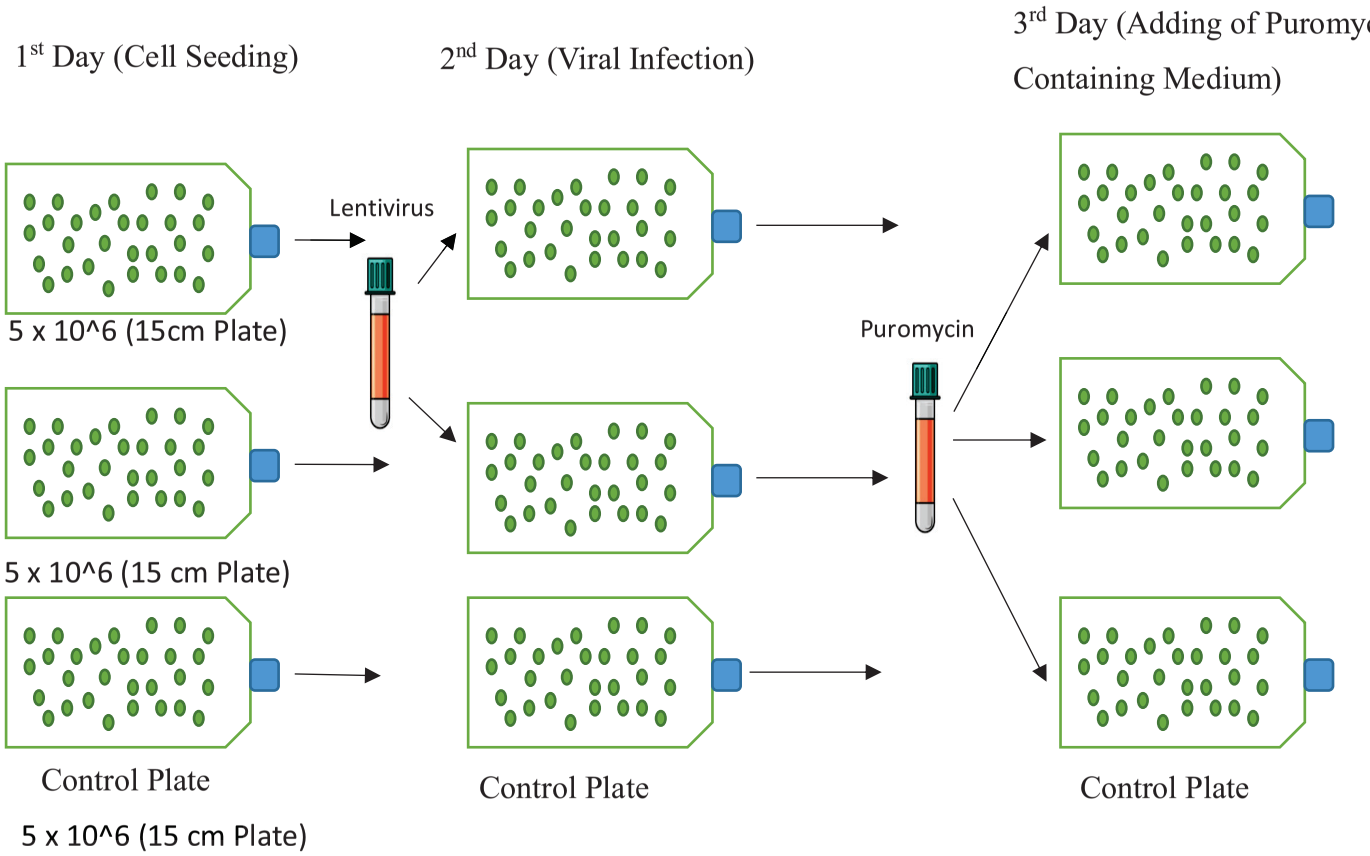

Figure 2.1 Schematic representation of the experimental set-up for barcoding of the cell lines

2.9 Determination of The Inhibitory Concentration 50 (IC50) values of Chemotherapeutic Drugs by MTT Assays

The Caco-2 and HT-29 cell lines were seeded into 96 wells (10 x 10^3 cells/ well). After 24 hrs. incubation, confluency of the cell lines was 70-80% in each well, and the Caco-2 and the HT-29 cells were treated with capecitabine (LC Laboratories) and irinotecan (AdooQ Bioscience) chemotherapy drugs respectively in different ranges to calculate the IC50 values of the drugs on the cell lines. After 72 hrs. incubation in a humidified incubator with 5% CO_2 at 37^0 C, the MTT cell viability assay protocol that explained in section 2.4 was applied. The cell viability rates in the drug-treated groups were calculated according to the solvent control groups. IC50 dose concentrations of the drugs were calculated by non-linear regression on the GraphPad Prism 8 (GraphPad Software Inc., USA).

2.10 Generation of Resistant Cell Lines

2.10.1 Generation of Capecitabine (CAPE)-Resistant Caco-2 Cell Line

Previously frozen a 4x 10^6 barcoded Caco-2 cell cryovial was thawed and seeded into 15 cm culture dishes. When the cells had 70-80% confluency, 2x 10^6 / dish cells were seeded into 4 different 15 cm dishes (DMSO Control, Replica A, B, C) with 25 mL medium. 2x 10^6 cell pellets were stocked to be used as initial control for unique-barcode sequencing and 2x 10^6 cells were frozen as initial cell control. During 6 months, mediums in the plates were changed twice in a week with fresh mediums with IC50 dose (4 months), 2x IC50 dose (2 months) capecitabine for the Caco-2 cell line. DMSO control Caco-2 cells were treated with the same amount of DMSO contained fresh medium. DMSO control cells were frozen after 3 passages, 4x 10^6 cells and 2x 10^6 cell pellets were stocked in each passaging. In each medium change, floating dead cells' pellets were collected from the used medium with centrifugation. End of the 6 months, 4x 10^6 capecitabine-resistant Caco-2 cells were

frozen and 2x 10^6 cell pellets were collected for end-point unique barcode sequencing analysis.

2.10.2 Generation of Irinotecan (IRI)-Resistant HT-29 Cell Line

Previously frozen a 4x 10^6 barcoded HT-29 cell cryovial was thawed and seeded into 15 cm culture dishes. When the cells had 70-80% confluency, 2x 10^6 / dish cells were seeded into 4 different 15 cm dishes (DMSO Control, Replica A, B, C) with 25 mL medium. 2x 10^6 cell pellets were stocked to be used as initial control for unique-barcode sequencing and 2x 10^6 cells were frozen as initial cell control. During 6 months, mediums in the plates were changed twice in a week with fresh mediums with IC50 dose irinotecan for the HT-29 cell line. DMSO control HT-29 cells were treated with the same amount of DMSO contained fresh medium. DMSO control cells were frozen after 3 passages, 4x 10^6 cells and 2x 10^6 cell pellets were stocked in each passaging. In each medium change, floating dead cells' pellets were collected from the used medium with centrifugation. End of the 6 months, 4x 10^6 irinotecan-resistant HT-29 cells were frozen and 2x 10^6 cell pellets were collected for end-point unique barcode sequencing analysis.

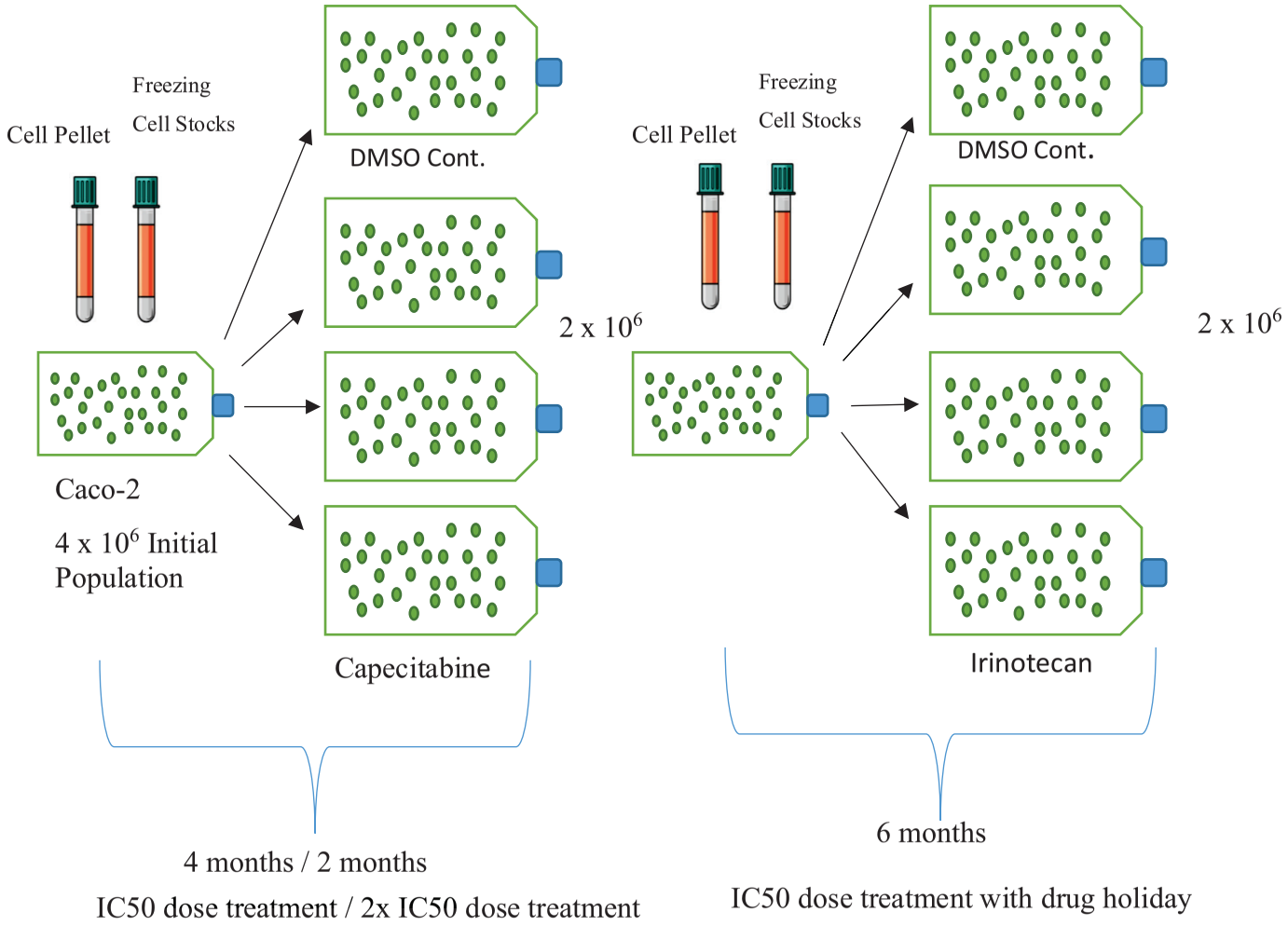

Figure 2.2 Schematic representation of the experimental set-up to generate drug resistant cell lines

2.11 Determination of Drug-Resistant Barcoded Cell Lines by MTT Assays

2.11.1 Determination of Capecitabine-Resistant Caco-2 Cell Line

Capecitabine-treated barcoded Caco-2 cell lines (A, B, C biological replicates), initial population, and DMSO control cell lines of these barcoded cells were seeded to 96 well plates (10 x 10^3 cells/ well). After 24 hrs. incubation, confluency of the cell lines was 70-80% in each well; Caco-2 cells were treated with capecitabine (LC Laboratories, USA) in different ranges to calculate the new IC50 values of the drug on the capecitabine-resistant cell lines. After 72 hrs. incubation in a humidified incubator with 5% CO_2 at 37^0, the MTT cell viability assay protocol that explained in section 2.4 was applied. The cell viability rates in the drug-treated groups were calculated according to the solvent control wells. The IC50 dose concentrations of the capecitabine on the control cells (DMSO and initial controls) and on the capecitabine-resistant Caco-2 cells were calculated by using GraphPad Prism 8 (GraphPad Software Inc., USA).

2.11.2 Determination of Irinotecan-Resistant HT-29 Cell Line

Irinotecan treated barcoded HT-29 cell lines (A, B, C biological replicates), initial population, and DMSO control cell lines of these barcoded cells we seeded in 96 well plates (10 x 10^3 cells/ well). After 24 hrs. incubation, confluency of the cell lines was 70-80% in each well; HT-29 cells were treated with irinotecan (AdooQ Bioscience, USA) in different ranges to calculate the new IC50 values of the drugs on the irinotecan-resistant cell lines. After 72 hrs. incubation in a humidified incubator with 5% CO_2 at 37^0, the MTT cell viability assay protocol that explained in section 2.4 was applied. The cell viability rates in the drug-treated groups were calculated according to the solvent control wells. The IC50 dose concentrations of the irinotecan on the control cells (DMSO and initial controls) and on the irinotecan-

resistant HT-29 cells were calculated by using GraphPad Prism 8 (GraphPad Software Inc., USA).

2.12 DNA Isolation

Genomic DNA isolation of barcoded initial control, barcoded DMSO control, and barcoded capecitabine-resistant Caco-2 and irinotecan-resistant HT-29 cells were conducted according to the manufacturer's instructions of the kit. GeneJET Genomic DNA purification Kit (ThermoFisher, USA) was used for isolation. The concentration of the isolated DNA samples was measured with BioDrop (Biochrom, UK), then stored at -20 ℃. A260/280 ratios of the samples in between 1.8- 2.0 values and the samples were considered pure DNA.

2.13 Barcode Detection with Next Generation Sequencing (NGS) System

Isolated genomic DNA samples from three biological replicates and initial, DMSO controls of the capecitabine-resistant Caco-2 and irinotecan-resistant HT-29 cells were used to detect unique barcode sequences with high-throughput NGS systems. Constructed libraries from these samples were sequenced on MiSeq Platform (Illumina, Inc.) by 150-bp paired-end mode following standard procedures in Intergen Genetics and Rare Diseases Diagnosis Research & Application Center (Ankara).

2.14 Bioinformatics Analysis of Barcode Sequencing

CloneTracker XP™ 10M Barcode-3' Library with RFP-Puro library pool has 1x 10^6 unique barcode sequences. The structure of one unique barcode is indicated in **Figure 2.3**. The variability of these barcode sequences is provided with 14 bp and 30 bp length variable nucleotide sequences. Bioinformatics analysis of the barcode

sequencing results was carried out by our laboratory member, M.Arda Temena and Erdi Can Kılıç.

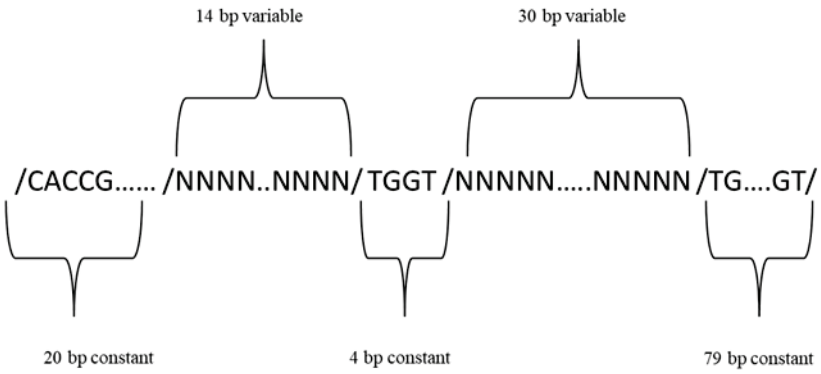

Figure 2.3 Schematic representation of the unique barcode sequence

2.14.1 Raw Data of Barcode Sequencing

The barcode sequencing results of the capecitabine-resistant Caco-2 replicate cells (A, B, C), irinotecan-resistant HT-29 replicate cells (A, B, C) and their initial and DMSO control cells were obtained in FASTQ format from Illumina MiSeq Platform. Reads were assessed by using FASTQC and the reads with Phred scores less than 20 were not included in further investigation.

2.14.2 Processing of the Raw Data

Firstly, the FASTQ reads were trimmed by using Trimmomatic (parameter MINLEN:147), and the pair-end reads less than 147 bp were eliminated (total number of constant and variable nucleotides) (Bolger, Lohse, and Usadel 2014). Following trimming, the constant nucleotides at both ends (20 bp and 79 bp) were cut off by using Trimmomatic (parameters HEADCROP:20 CROP:48 for the forward reads, HEADCROP:79 CROP:48 for the reverse reads) to detect variable unique barcodes (48 bp).

2.14.3 Generation and Alignment of the Barcodes

One million barcode sequences were re-generated computationally according to the Cellecta barcode library excel file (Cellecta-NGS-QC-CloneTracker-XP-10x1M-Barcode3-Lib-RFP.xlsx). Using the R package "insect", the regenerated sequences were written into a FASTA file. Individual barcode sequences were treated as transcripts. The detected barcode sequences from our samples were indexed with Salmon index function in Salmon with the -k 47 parameters (Patro 2017). The number of barcodes in forward and reverse reads was quantified and written an SF file by using Salmon function, then converted to json file. The built-in library JSON was utilized to write and read the counts of barcodes in JSON file format.

2.14.4 Classification of Barcode Phenotypes

The detected unique barcode counts were classified according to their frequencies in the biological replicates (A, B, C) of capecitabine-resistant Caco-2 and irinotecan-resistant HT-29 and their DMSO controls. The following growth rate formula was used to determine the phenotypes of the barcodes (Acar et al. 2020).

$$\text{Growth Rate} = \log(f_R/f_0)\ 1/T$$

Here, f_R represents the frequency of the barcode(s) in the replicate, f_0 represents the maximum frequency of all barcodes in the corresponding DMSO control and T represents the duration time (week) between the first drug treatment and the end of the experiment. To calculate the growth rate of the barcodes, the maximum frequency of all barcodes in the corresponding DMSO control was used as f_0 value. According to the calculated growth rates, the barcodes have a positive growth rate, and those detected at least two replicates were classified as 'resistant barcodes', the barcodes show a positive growth rate, and observed just in one replicate were classified as 'de novo barcodes'; the remaining detected barcodes were classified as 'sensitive barcodes', these barcodes show negative growth rate. The barcodes which

were observed in the replicates but not determined in the DMSO controls were classified as ‘not determined’(Acar et al. 2020).

2.14.5 Tracking of the Resistant and Sensitive Barcodes

During the establishment of capecitabine-resistant Caco-2 and irinotecan-resistant HT-29 cell lines, the used medium was changed with fresh medium twice in a week and the floating dead cells in the used mediums were collected as pellets in each medium change. DNA of these cell pellets from the five equal intervals (once in every four weeks) were isolated and sequenced to track the frequency changes of the resistant barcodes in the cell populations. Additionally, the sensitive barcodes were also tracked and plotted. Tracking of the ‘resistant barcodes’ and ‘sensitive barcodes’ was carried out only for Replicate B for both cell lines because replicates B of the two cell lines (CAPE-resistant Caco-2 and IRI-resistant HT-29) had the highest resistance fold change values.

2.15 Proliferation Assay

10 x 10^3 cells/ well capecitabine-resistant Caco-2, irinotecan-resistant HT-29 cells and their DMSO controls and initial cell population controls were seeded into 3 different 96 well plates. After 24 hrs., DMSO control Caco-2 and HT-29 cells and capecitabine-resistant Caco-2 and irinotecan-resistant HT-29 cells were treated with DMSO, capecitabine, and irinotecan respectively, while full fresh growth medium was added onto the initial control cells. MTT assay protocol was applied to plates after treatments at 24 hour., 48 hour and 72 hour incubation time in the incubator, absorbance values were measured by using a microplate spectrophotometer (Multiskan GO; Thermo Fisher Scientific, USA) at 570 nm wavelength. According to the absorbance values, proliferation cahnges of the cells were calculated by using GraphPad Prism 8 (GraphPad Software Inc., USA).

2.16 Drug Response Assays to Secondary Chemotherapeutic Drugs

2.16.1 Drug Response Assays of Secondary Chemotherapeutic Drugs on Capecitabine-resistant Caco-2 Cell Line

Capecitabine-resistant Caco-2 cells, and their DMSO and initial control cells were seeded into 96 well plates (10 x 10^3 cells/ well). After 24 hrs. cells were treated with chemotherapeutic drugs and inhibitors. Capecitabine-resistant, DMSO control, and initial control Caco-2 cells were treated with Irinotecan (Adooq, USA), SN-38 (Adooq, USA), Oxaliplatin (Adooq, USA), and Cetuximab (Merck, Germany). After 72 hrs. incubation under drug treatment, the MTT cell viability assay protocol that is explained in section 2.4 was applied.

2.16.2 Drug Response Assays of Secondary Chemotherapeutic Drugs on Irinotecan-resistant HT-29 Cell Line

Irinotecan-resistant HT-29 cells and their DMSO and initial control cells were seeded into 96 well plates (10 x 10^3 cells/ well). After 24 hrs. the cells were treated with chemotherapeutic drugs and inhibitors. Irinotecan-resistant, DMSO control, and initial control HT-29 cells were treated with SN-38(Adooq, USA), Oxaliplatin (Adooq, USA), Capecitabine (Adooq, USA), and Dabrafenib (Adooq, USA). After 72 hrs. incubation under drug treatment, the MTT cell viability assay protocol that is explained in section 2.4 was applied.

2.17 Drug Combination Assays

Capecitabine-resistant Caco-2 cells and irinotecan-resistant HT-29 cells and their DMSO and initial control cells were seeded into 96 well plates (10 x 10^3 cells/ well). After 24 hrs., capecitabine-resistant Caco-2 and its control cells were treated with oxaliplatin / capecitabine, SN-38 / capecitabine and cetuximab (Erbitux) /

capecitabine drug combinations; irinotecan-resistant HT-29 and its control cells were treated with dabrafenib/irinotecan and capecitabine/irinotecan drug combinations. In drug combination assays, capecitabine and irinotecan were background drugs and their doses were stable as 2 x IC50 and IC50 respectively; CAPE-resistant and control Caco-2 cells were treated with six doses in 1:2 dilution of oxaliplatin, and cetuximab, five doses in 1:2 dilution of SN-38 in combination with capecitabine; IRI-resistant and control HT-29 cells were treated with six doses in 1:2 dilution of dabrafenib and capecitabine in combination with irinotecan. After 72 hrs. incubation, the MTT cell viability assay protocol that explained in section 2.4 was applied. Cell viabilities of the cells were calculated according to control wells and synergy scores of the combined drug were calculated by using SynergyFinder 2.0 (University of Helsinki, Finland) and Combenefit (University of Cambridge, UK) software.

2.18 Protein Isolation and Quantification

Protein isolations from the cells were conducted with RIPA Buffer (SERVA, Germany), phosphatase, and protease inhibitors (SERVA, Germany) mixture. Firstly, $2x\ 10^6 - 5x\ 10^6$ cell pellets were collected from the resistant and control cells. The pellets were washed twice with cold PBS, and resuspended with the RIPA buffer-inhibitor mixture (100-150 μL). The suspensions were kept on ice for 25 min., and vortexed once every 5 minutes. Then, the samples were centrifuged at 14000 x g for 15 minutes, and protein contained supernatants were transferred into the prepared tubes. The proteins were stored at -80^0 for further analysis.

Quantification of the isolated proteins was determined by Bradford assay. Coomassie Protein Assay Reagent (Quick Start Bradford 1x Dye Reagent Bio-Rad, USA) was used in the 250:5 (μL) ratio reagent and sample, respectively. For the analyses, a standard curve generated from bovine serum albumin quantification was used.

2.19 Western Blot

The western blot protein analysis method was used to determine expression differences of p-MEK and p-ERK proteins between CAPE-resistant Caco-2 and DMSO and initial control Caco-2 cells; IRI-resistant HT-29 and DMSO and initial control HT-29 cells.

The experiment was conducted by using a Bio-Rad Western Blot setup. Total proteins isolated previously (60 μg- 80 μg) were loaded to 5% gel and separated by using SDS-PAGE at 90 V for 2 hrs. As a ladder, SERVA Triple Color Protein Standard 1 was preferred in the 15 to 180 kDa range (SERVA, Germany Cat no: 39251).

The wet transfer system Mini Trans-Blot Cell (BioRad, USA) was used to transfer the proteins from the SDS-PAGE gel to the polyvinylidene fluoride (PVDF) membrane (BioRad, USA). The transfer was carried out at 100 V for 90 minutes. The blocking of the membrane was carried out with 3% BSA at room temperature for 1 hrs.

The membrane was incubated with the primary antibodies (**Table 2.3**) for overnight at 4^0, then the membrane was washed three times with TBS-T for 15 minutes. Secondary antibody incubation was conducted for 2 hrs at room temperature. The membrane was visualized by using Chemi-Doc MP Imaging System (BioRad, USA) in the presence of Clarity^{TM} Western ECL substrate (BioRad, USA #1705060). Mild strip buffer was used to reprobe the membrane. The GAPDH antibody was used in this study as a loading control to verify equal protein loading in western blots.

Table 2.3 List of the Used Antibodies

Name of Antibody	***Company Catalog #***	***Host***	***Molecular Weight (kDa)***	***Dilution***	***Blocking Agent***
p-ERK	*Santa Cruz SC-7383*	goat	42/44	1:500	Skim Milk
p-MEK	*Santa Cruz SC-81503*	goat	45/47	1:500	3% BSA
GAPDH	*Santa Cruz*	goat	37	1:2000	Skim Milk

2.20 Statistical Analysis

All experiments were performed at least two or three biological replicates, and at least three technical replicates. All analyzes of the data were conducted on GraphPad Prism 8 (GraphPad Software Inc., USA). Student's t-test, two-way Annova and non-linear regression were applied according to the requirement of the analysis to determine significance. *p-value* <0.05 was considered as statistically significant. All results were expressed as mean ± SEM.

CHAPTER 3

RESULTS AND DISCUSSION

This study aimed to establish capecitabine-resistant Caco-2, and irinotecan-resistant HT-29 colorectal cancer cell models to investigate and better understand the clonal evolution of drug resistance by using a cellular barcoding technology with an ultimate aim to discover second line drugs sensitizing drug resistant cells.

3.1 Puromycin Selection Concentrations of Caco-2 and HT-29 Cell Lines

Due to the resistance gene in the used lentiviral vector system, the lethal purmoycin concentrations were determined to eliminate the non-transduced Caco-2 and HT-29 cell lines. Puromycin selection concentration for the Caco-2 cell line was determined as 12.5 µg/mL by MTT assay. The concentration range of puromycin was determined according to the previous studies (T. T. Hu et al. 2020). The HT-29 cell line puromycin selection concentration was determined as 1.5 µg/mL by Rana Can Baygın.

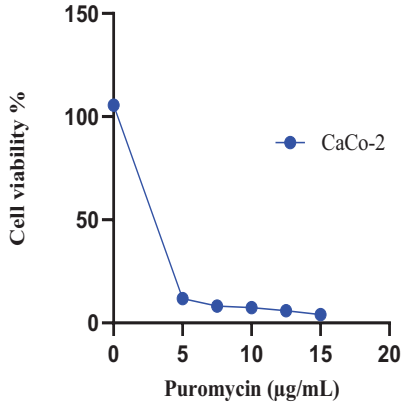

Figure 3.1 Dose-response curve of puromycin on Caco-2 cell line

3.2 MOI Determination of Caco-2 and HT-29 Cell Lines

The required lentivirus amount for MOI ≤ 0.1 was determined by MTT assay on the six-well plates. The experimental set-up was explained in **Table 2.2**. MOI 0.05 value was determined in the presence of 50 µL virus amount / 75 x 10^3 in the 6 well experiments for the Caco-2 cell line. The amount of virus was relatively calculated according to this amount, and 6.667 µL of the virus was used for 2 x 15 cm cell culture dish (5 x 10^6 / cell culture dish). For the HT-29 cell line, MOI 0.05 value was determined in the presence of 100 µL for 150 x 10^3 in the 6 well plates, and 6.666 µL of the virus was used for 2 x 15 cm cell culture dish (5 x 10^6 / cell culture dish).

Table 3.1 MOI Determination of Caco-2 Cell Line

Virus Amount	*No Puromycin (87,5 µL virus)*	*50 µL virus*	*75 µL virus*	*100 µL virus*	*125 µL virus*	*No Virus*
Cell Viability	*98.14%*	*4.22%*	*4.12%*	*4.61%*	*3.14%*	*2.5%*

3.3 IC50 Concentrations of Capecitabine on the Caco-2 Cell Line and Irinotecan on the HT-29 Cell Line

In this study, pro-drug form of 5-FU (capecitabine), and pro-drug form of SN-38 (irinotecan) were used to establish drug-resistant CRC cell line model systems. In the clinic, pro-drug froms of the chemotherapeutic drugs are generally preferred due to their less cytotoxicty, more tumor specificity, efficiency and safety (Ferguson, Ahmed, and Cassidy 2001),(Scheithauer et al. 2003). Pro-drugs are converted to their active metabolites through several chemical or enzymatic reactions in which liver and cancer cells (Mader et al. 2003),(J. Zhang et al. 2015),(Ferguson, Ahmed, and Cassidy 2001). Capecitabine is converted to its active metabolite 5-FU with three enzymatic reactions and two of them take place in liver. The last enzymatic reaction

occurs mainly in cancer cells in the tumor site by thymidine phosphorylase (TP) thanks to high TP concentration (J. Zhang et al. 2015). Zhang et al. demonstrated that co-culturing of breast cancer cells with liver cells increased the efficiency of capecitabine even at low concentrations, on the other hand, higher concentrations of capecitabine could still inhibit the proliferation of cancer cells without hepocyte co-culture (J. Zhang et al. 2015). Conversion of irinotecan to SN-38 is mainly mediated by liver carboxylesterases, on the other hand, the studies revealed that colon adenocarcinoma cells with CES2 (human carboxylesterase 2) expression mediate local conversion of irinotecan to its active metabolite SN-38 (Xu et al. 2002),(M. H. Wu et al. 2002).

The half-maximal inhibitory concentrations (IC50) of capecitabine and irinotecan on Caco-2 and HT-29 were determined by MTT assays, respectively. Firstly, the Caco-2 and HT-29 cells were seeded into 96 well plates ($10x10^3$ / well) and the cells were incubated under drug treatment in a humidified incubator at 37^0 for 72 hours. The capecitabine dose response curve of the Caco-2 and the irinotecan dose response curve of the HT-29 were graphed according to analysis of the absorbance values as indicated in **Figure 3.2**. The IC50 value of capecitabine on the Caco-2 was calculated as 2.12 mM; the IC50 value of irinotecan on the HT-29 was calculated as 8.851 μM by non-linear regression on GraphPad Prism 8 (GraphPad Software Inc., USA). Capecitabine is a prodrug form of 5-FU and has less cytotoxic effect. IC50 range of capecitabine depends on the used model cancer cell line, and can be calculated between 800 μM to 6 mM (Çakir and Eroglu 2021). Irinotecan is a Topoisomerase I inhibitor and prodrug form of the active metabolite SN-38. The irinotecan concentration range that HT-29 cells were treated to calculate IC50 concentration was determined according to literature (Pavillard et al. 2002).

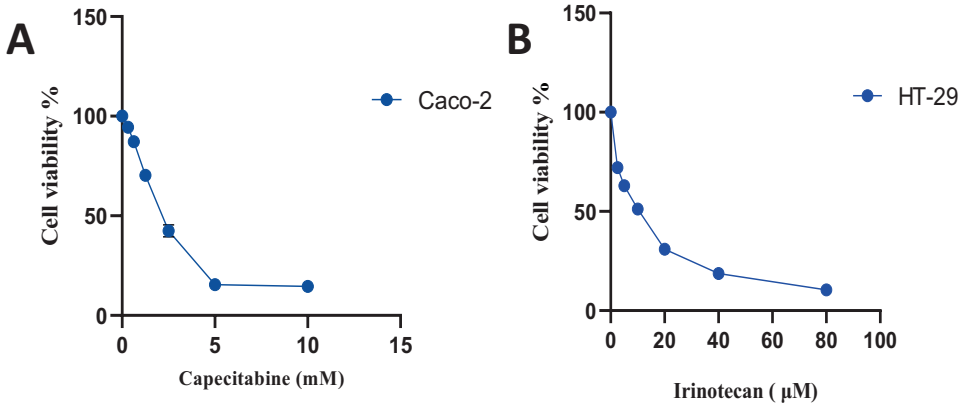

Figure 3.2 (**A**) Dose-response curve of capecitabine on the Caco-2 cell line (**B**) Dose-response curve of irinotecan on the HT-29 cell line (IC50 values were analyzed by non-linear regression)

3.4 Generation of Capecitabine – Resistant Caco-2 Cell Line

Previously barcoded Caco-2 cells were treated with IC50 concentration of capecitabine (2.12 mM) for 4 months and treated with 2x IC50 concentration of capecitabine for 2 months to establish capecitabine-resistant Caco-2 cell line. After 6 months capecitabine treatment in an increasing range, barcoded capecitabine-resistant Caco-2 cell line was established, and new IC50 concentrations of capecitabine on the CAPE-resistant Caco-2 cells (Replicates A B, C) were determined by cell viability assay (MTT assay). The resistant clones were detected by barcode sequencing and bioinformatic analysis, and finally the CAPE-resistant Caco-2 cells and their control cell lines (DMSO, initial population) were treated with other chemotherapeutics as single-agent and in combinations to control acquired cross-resistance and/or collateral sensitivity to other drugs.

3.4.1 Dose Response Curve of Capecitabine on Capecitabine-Resistant Caco-2 Cell Line and Resistance Fold Change Values

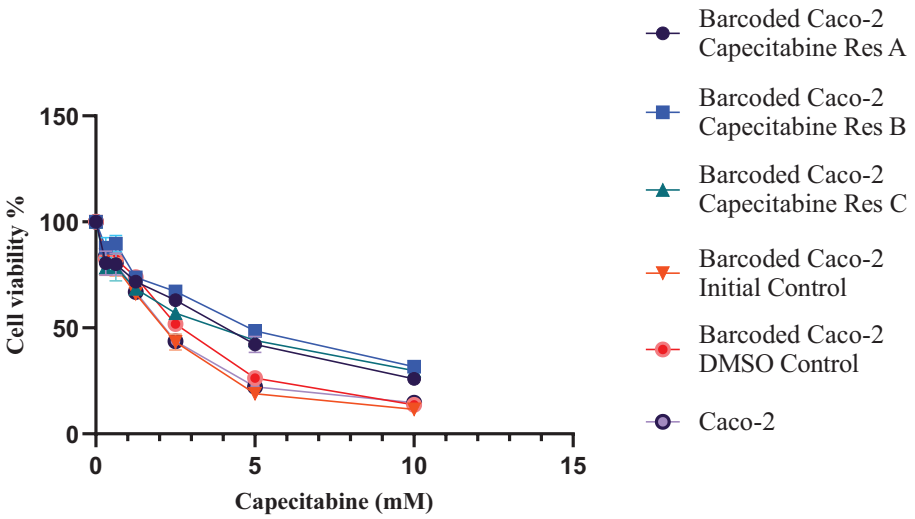

Figure 3.3 Drug dose response curve of capecitabine on CAPE-resistant Caco-2 cell line (Replicates A, B, C), DMSO control, initial population control, and parental control Caco-2 cell line

The CAPE-resistant Caco-2 cells (Replicates A, B, C) and their initial and DMSO control cell lines were seeded into 96 well plates (10 x 10^3 / well). After 24 hrs. the mediums of the cell lines were changed with capecitabine-containing medium in different concentrations (in a 1:2 dilution range). The cells were treated with capecitabine for 72 hrs., and the MTT assay protocol was applied. The new IC50 concentrations of capecitabine on CAPE-resistant Caco-2 cell lines were calculated by non-linear regression analysis as 3,417 mM, 4.555 mM, and 3.304 mM (Replicates A, B, C) respectively.

According to new IC50 values of the capecitabine-resistant Caco-2 cell line replicates, resistant fold-change values were calculated as indicated in **Table 3.2.** According to MTT cell viability assay results, replicate B has the highest IC50 dose

concentration (4.555 mM) and has the highest resistance fold change, therefore replicate B was used for further characterization assays.

Table 3.2 IC50 values of Control and CAPE-Resistant Caco-2 Cell Lines and Resistant Fold Change Values (* = p<0.05, ** = p<0.01, *** = p<0.001, **** = p<0.0001)

	CAPE- Res Caco-2	**Initial Cont.**	**DMSO Cont.**	**Caco-2**
IC50 Values (mM)	**Replicates** **(A)** 3.417 **(B)** 4.555 **(C)** 3.304	1.866	2.436	2.009
Fold Resistance	**IC50 of Res. Cell/ IC50 of Cont. Cell**	**(A)** 1.83 (****) **(B)** 2.44 (****) **(C)** 1.77 (****)	**(A)** 1.4 (***) **(B)** 1.87 (****) **(C)** 1.36 (**)	**(A)** 1.7 **(B)** 2.27 **(C)** 1.64

3.4.2 Proliferation Rate and Cell Morphology of the Capecitabine-Resistant Caco-2

MTT assay was carried out to investigate the effect of capecitabine on proliferation rate of the capecitabine-resistant Caco-2 cell line. For this, the capecitabine-resistant Caco-2 and control cell lines (DMSO and initial population) were seeded into 3 different 96 well plates (10 x 10^3 / well). The cells were allowed to attach in a humidified incubator with 5% CO_2 at 37°C for 24 hrs., then the cells were treated with capecitabine (for CAPE-resistant Caco-2), and the same concentration DMSO (DMSO control cell lines) while medium of the initial populations were changed with fresh growth medium. The MTT assay protocol was applied for each time point, and the absorbance values of the cells were measured at 24. hrs, 48. hrs., and 72. hrs. after treatment. According to measured absorbance values (at 570 nm) the proliferation rates were plotted by using GraphPad Prism 8 (GraphPad Software Inc., USA). The analysis was conducted by two-way Annova test (*** p<0.001).

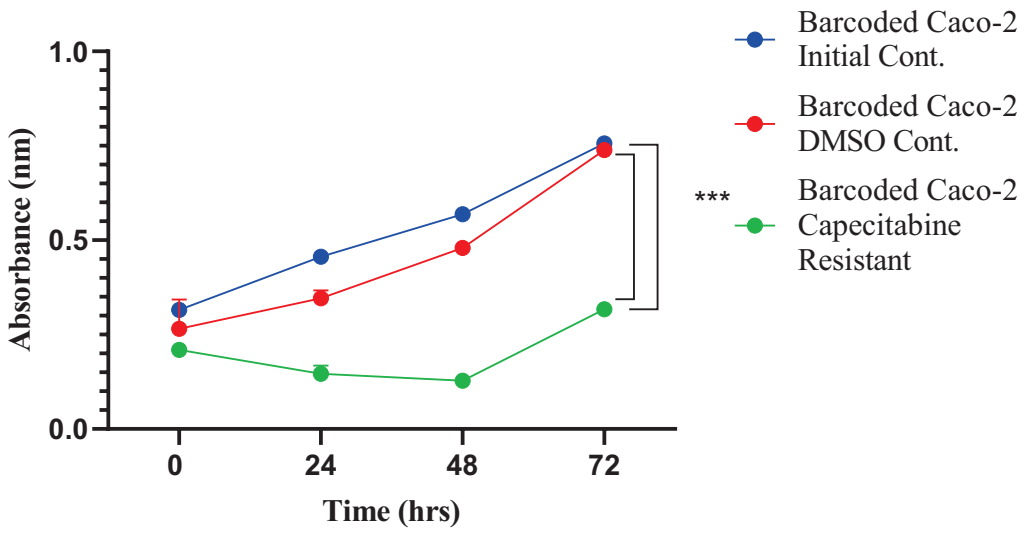

Figure 3.4 Time dependent absorbance values of CAPE-resistant Caco-2, DMSO control Caco-2 and Initial population control Caco-2

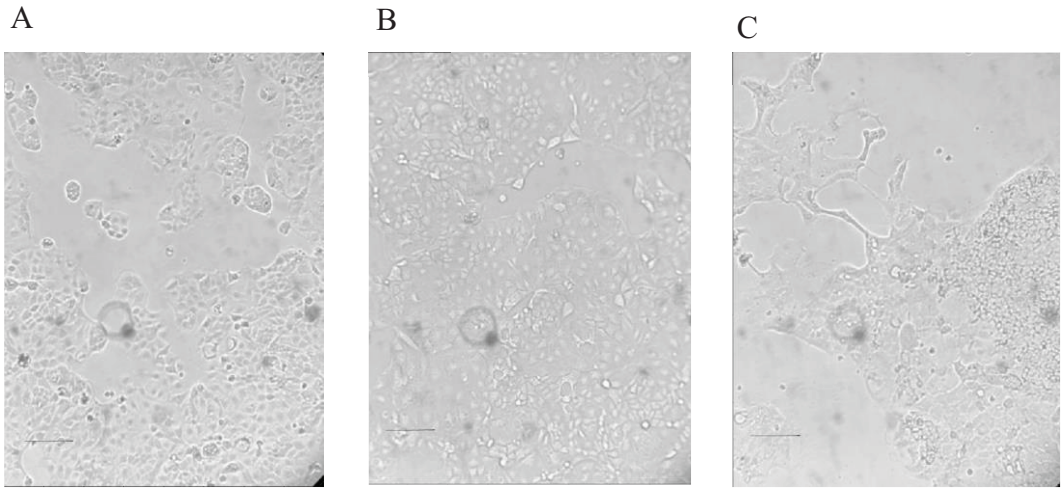

Figure 3.5 (A) Barcoded Caco-2 Initial Control, **(B)** Barcoded Caco-2 DMSO Control, **(C)** Barcoded CAP-Res Caco-2 Cells (10X) (1 mm)

As shown in **Figure 3.4**, capecitabine has an anti-proliferative effect on capecitabine-resistant cell line, and a significant proliferation inhibition was observed in the cells within capecitabine containing medium at the 72nd hrs (***$p<0.001$). As indicated in studies, drug-resistant cancer cell lines can show

differences in their morphologies, growth patterns, growth rates, doubling times, and cell cycles (Fu 2009). The study by Fu et al. indicated that there was 1.8 fold difference in doubling-time between the parental cell line and drug-resistant variant of esophageal squamous cell carcinoma cell line. Additioanlly, the drug-resistant variant cell line exhibited non-uniform structural patterns (Fu 2009). In this study, capecitabine treatment during 6 months without any drug-free breaks led to form of elongated structures in CAPE-resistant Caco-2 cells as seen in **Figure 3.5 (C)**.

3.4.3 Bioinformatics Analysis of Capecitabine – Resistant Caco-2 Cell Line Barcode Sequencing

The cell pellets collected from capecitabine-resistant Caco-2 replicate plates, DMSO and initial population Caco-2 cell lines were used for DNA isolation. Due to these cells were barcoded with unique barcode sequences in their genome by using lentiviral vectors, the isolated DNA samples were sequenced to detect and analyze unique barcodes in CAPE-resistant and control Caco-2 cell lines. Additionally, DNA isolation was performed from dead cell pellets which were collected from used medium in equal time points for tracking of frequencies of the detected unique barcodes during establishment of CAPE-resistant Caco-2 clones.

3.4.3.1 Barcode Analysis of the Detected Clones in the Capecitabine-Resistant Caco-2 Cell Line

To annotate each barcode with a phenotype, an approximate growth rate under each condition were first determined according to the frequencies and similar rules were applied as in Acar et al(Acar et al. 2020). The formula below is used to calculate growth rate:

$$\text{Growth Rate} = \log(f_R/f_0)\ 1/T$$

The barcodes have positive growth rate at least two replicates were classified as 'Resistant barcode'; the barcodes have positive growth rate and were detected only in one replicate were classified as 'De novo barcodes' and remaining barcodes were named as 'Sensitive barcodes' and these barcodes exhibit negative growth rate (Acar et al. 2020). According to bioinformatics analysis of barcode sequencies of control and CAPE-resistant Caco-2 cell lines; the red bar in **Figure 3.6** represents the distributions of the barcode frequencies in the populations. The numbers of the detected resistant barcodes in the replicates are 4, 4, and 7 (A, B, C), and total number of the detected unique resistant barcode is 7. The numbers of the detected de novo barcodes in the replicate A, B, C populations are 3, 3 and 0 respectively. In Figure 3.5 the grey bars represent 'Not determined barcodes which were found in the replicates but were not detected in the DMSO control population (Acar et al. 2020).

Intrinsic (pre-existing) drug resistance is originated from genetic/epigenetic mutations which have roles in apoptosis, cell growth, and proliferation mechanisms. Intrinsic resistance cause ineffectiveness to drugs, ultimately failure of treatment (X. Wang, Zhang, and Chen 2019). For example, *HER2* overexpression is related with cisplatin resistance in gastric cancer patients (X. Wang, Zhang, and Chen 2019). Acquired de novo resistance is different from pre-existing resistance, tumor microenvironment has also an important role in acquired drug resistance. The efficiency of drugs decreases over time, therefore tumor growth, proliferation, and metastasis can continue even under drug treatment (X. Wang, Zhang, and Chen 2019). Determination of which type of resistance cells dominate the tumor cell population is important to follow the most efficient treatment strategies. Studies indicate that tracking of clonal evolution of pre-existing and acquired resistant clones can provide pre-information about resistance profiles of the tumor cells, and target pathways can be decided according to these results. Currently, these studies are mainly conducted on cell lines but there are also important studies that patient-derived xenografts are used (Merino et al. 2019),(Bhang et al. 2015). As shown in the barcode sequencing frequency plot (**Figure 3.6 B**), in CAPE-resistant Caco-2 cell line replicates (A, B, C) the majority of the resistant clones formed by pre-

existing resistant clones and dominated the populations. CAPE-resistant Caco-2 A, B, C replicates have ∼50 %,∼75%, >75% frequency in terms of resistant barcodes that have positive growth rates and shared with at least one other replicates; on the other hand, replicate C has not any de novo resistant clones, and the frequency of de novo resistant clones in replicates A and B are less than pre-existing ones. The frequency analysis indicates that pre-existing clones dominated the capecitabine drug resistance for these CAPE-resistant Caco-2 populations (Acar et al. 2020).

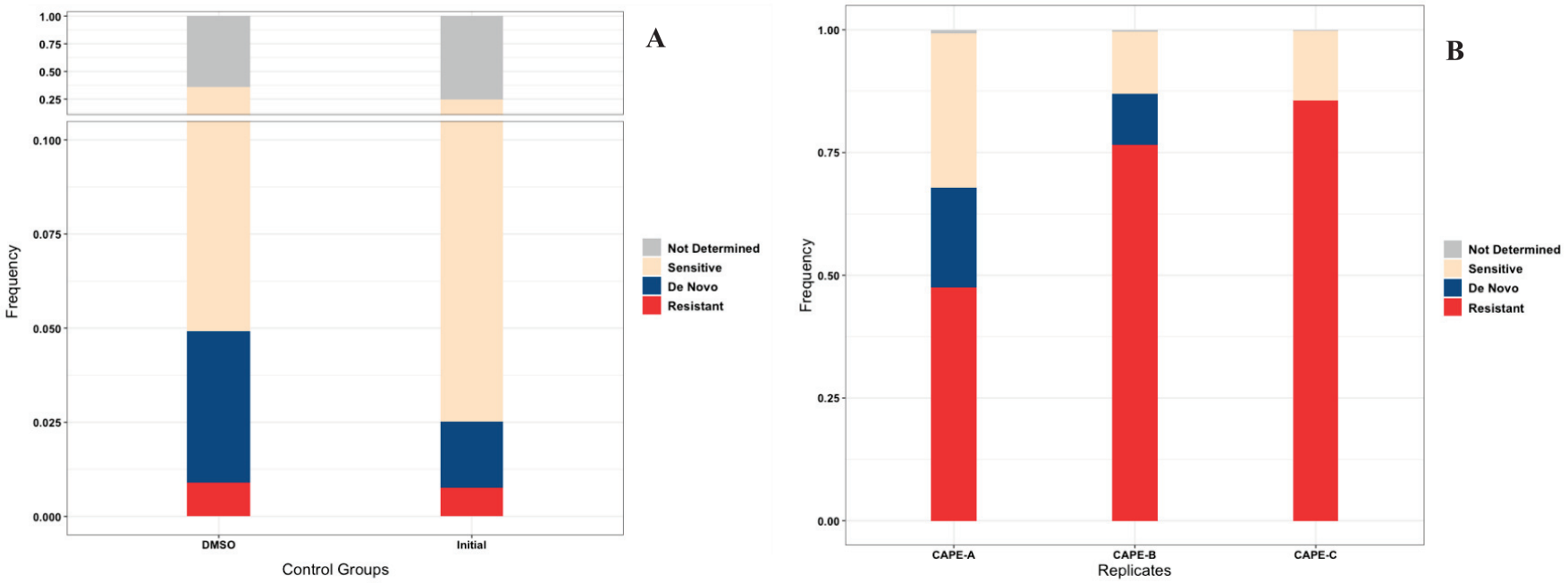

Figure 3.6 (A) Barcode frequency distributions of DMSO and Initial Caco-2 cell line controls and **(B)** Capecitabine-resistant Caco-2 cell line (Replicates A, B, C)

3.4.3.2 Tracking of the Capecitabine – Resistant Caco-2 Clones in the Population

The barcode frequencies in five different mediums collected at equal intervals (each month) were determined in order to track the resistant barcodes (only for Replicate B). Resistant barcodes with positive growth rate are plotted. Likewise, the tracking line graph of the frequencies in the middle and end points has been obtained for sensitive barcodes so that they can be compared with resistant barcodes. As indicated in **Figure 3.7** (A), a total of 4 resistant barcodes were tracked by sequencing of the floating dead cells from used medium, and one of these resistant clones which had unique barcode ID number 82195 dominated the capecitabine-resistant Caco-2 cells with highest barcode frequency ratio in the population (Replicate B). Because of the treatment of the barcoded Caco-2 cells were switched to 2 x IC50 from 1 x IC50 capecitabine concentration after 4 months, frequencies of the 2 resistant barcodes (ID numbers: 168122 and 545550) were found as a decreasing pattern in their frequencies. As seen in the plot, the fourth resistant clone which has unique barcode (ID number 119218) maintained and increased its frequency ratio in the capecitabine-resistant Caco-2 population even under higher capecitabine concentration treatment.

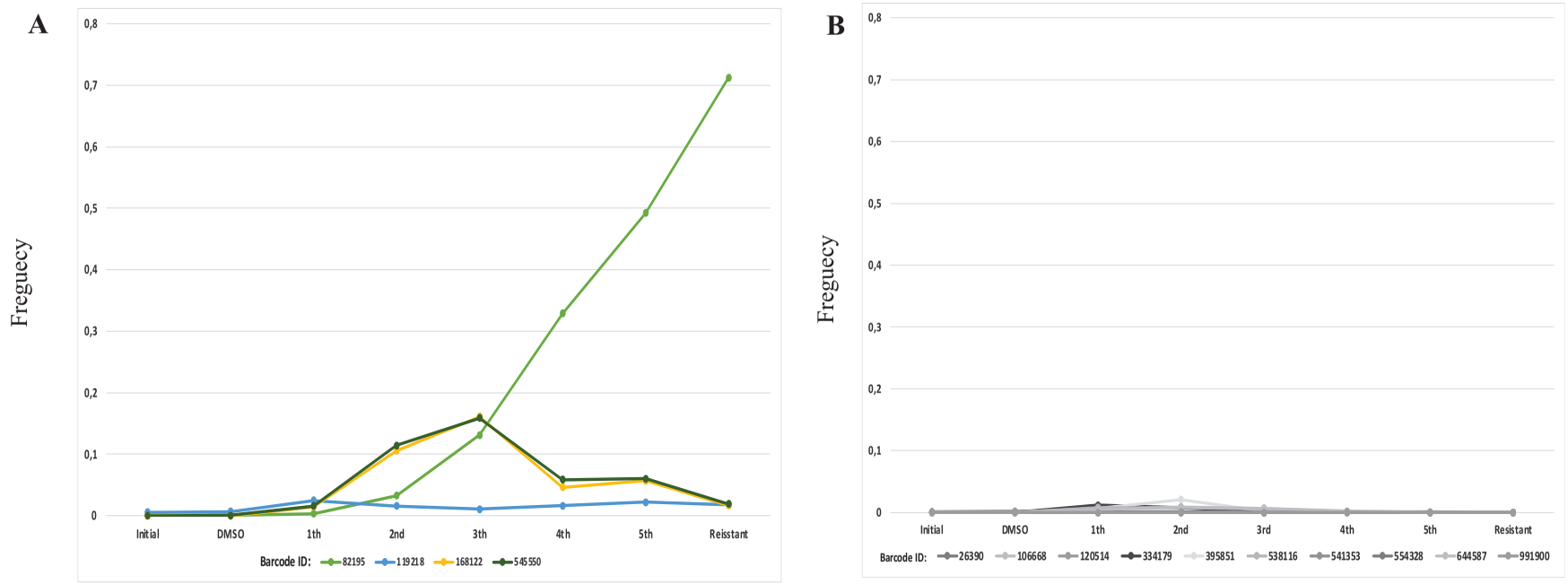

Figure 3.7 (A) Frequency distributions of the resistant barcodes in DMSO, Initial cell line controls and Capecitabine resistant Caco-2 cell line (Replica B) and dead cells in the mediums (Replica B mediums) **(B)** Frequency distributions of the sensitive barcodes in DMSO, Initial cell line controls and Capecitabine resistant Caco-2 cell line (Replica B) and dead cells in the mediums (Replica B mediums)

3.4.4 Secondary Drug Dose-Response Curves of Capecitabine – Resistant Caco-2 Cell Line

Drug-resistance to chemotherapeutics and targeted- molecular agents in tumor cells still represents one of the most important obstacle in the clinic, and prevents providing successfull and efficient results in cancer therapies (Holohan et al. 2013). To offer potential solution to this problem, targeting different molecules and use of combinations of chematherapeutic agents which are not overlap in a pathway are preferred as a second-line / third-line therapy strategy after failure in a first-line therapy (Holohan et al. 2013). To investigate the effects of secondary chematherapeutic drugs on capecitabine-resistant Caco-2 cells; Capecitabine-resistant Caco-2 cells, and their DMSO and initial control cells were seeded into 96 well plates (10 x 10^3 cells/ well). After 24 hrs. incubation, the cells were treated with oxaliplatin, irinotecan, SN-38 and cetuximab in different concentrations. The capecitabine-resistant Caco-2 and their control cells were treated with the drugs for 72 hrs., and MTT assay protocol was applied. As indicated in **Figure 3.8**, capecitabine-resistant Caco-2 cells exhibit sensitivity to SN-38, cetuximab and oxaliplatin while sensitivity was not observed to irinotecan. The IC50 concentration of SN-38 was calculated as 1.8 μM on capecitabine-resistant Caco-2, and the following concentrations were calculated as 4.14 μM and 3.25 μM for DMSO and initial Caco-2 control cells respectively. IC50 concentrations of Oxaliplatin on Cape-resistant Caco-2, DMSO and initial controls were calculated as 1.8 μM, 3.8 μM and 3.3 μM, respectively. IC50 concentration of cetuximab on the capecitabine-resistant Caco-2 cannot be calculated but cell viability differences especially in low concentrations were calculated as significant between CAPE-resistant Caco-2 and control cell lines (**p <0.01) by using student's t-test on GraphPad Prism 8 (GraphPad Software Inc., USA).

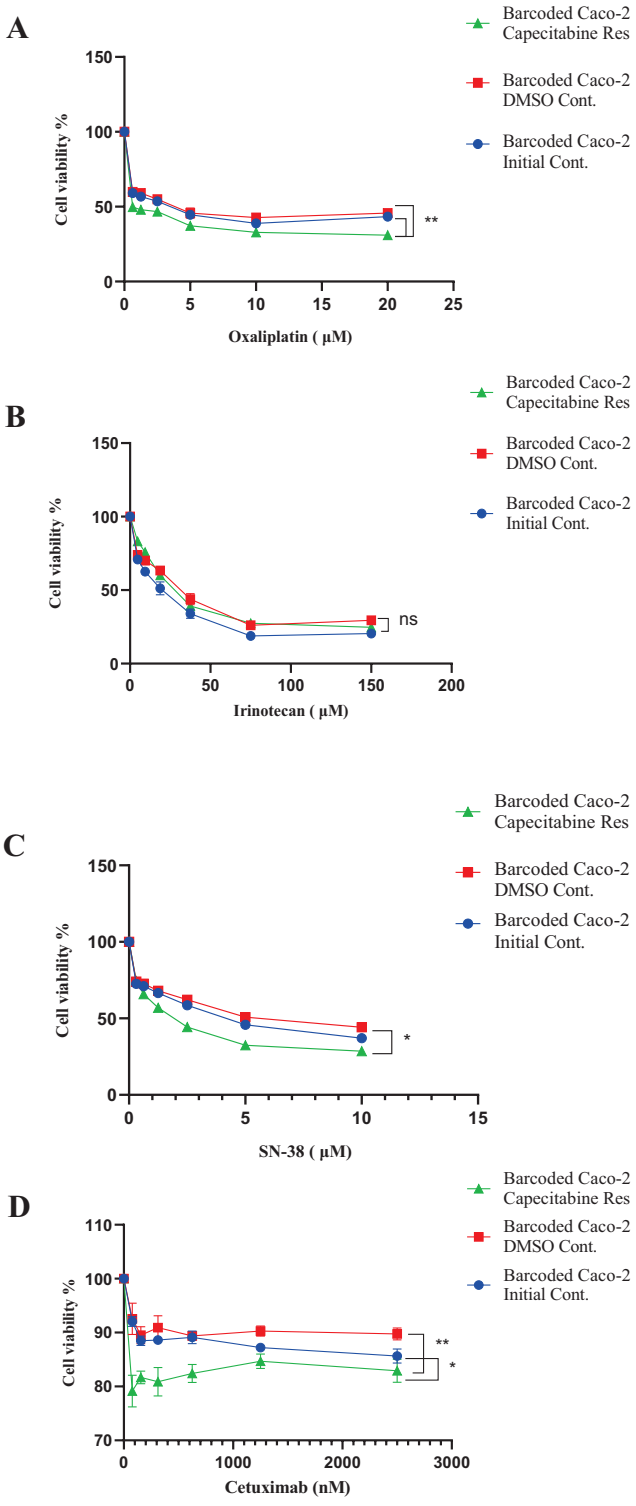

Figure 3.8 (A) Oxaliplatin, **(B)** Irinotecan, **(C)** SN-38 **(D)** Cetuximab dose-response curve of DMSO, Initial CaCo-2 cell line controls and Capecitabine-resistant CaCo-2 cell lines

3.4.5 Drug Combination Assays on Capecitabine-Resistant Caco-2 Cell Line

Since drug resistance is still one of the limiting factors for developing life qualities of cancer patients and increasing progression-free survival ratio; more sustainable and effective therapy strategies are required. Therefore, in clinics, one of the effective therapy strategies is the treatment of tumor cells with combinations of chemotherapeutic drugs with chemotherapeutics or site-specific inhibitors and agents (Jaaks et al. 2022). Despite, the main purposes of drug combinations are the elimination of drug resistance, increasing the efficiency of treatment by targeting different mechanisms, and decreasing the side effects and toxicity of the drugs by using low doses; the co-administration of drugs may show antagonistic effects and may lead to unexpected worse results (Riechelmann and Krzyzanowska 2019). Capecitabine is one of the most commonly used fluorouracil-based drugs as a first-line and second-line therapy agent. In clinics, capecitabine is mainly combined with oxaliplatin and irinotecan (XELOX, XELIRI) (L. Wang et al. 2020). In this study, capecitabine was used as a background drug and its concentration fixed at 2x IC50 (4.2 mM) and combined with different doses of cetuximab, SN-38, and oxaliplatin. To investigate the combination effects of capecitabine/cetuximab, capecitabine/SN-38 and capecitabine/oxaliplatin on the CAPE-resistant Caco-2 cell line, MTT assay protocol was applied as indicated in section 2.4. As shown in **Figure 3.9** and **Figure 3.10**, cell viability rates of CAPE-resistant Caco-2 decreased under combination therapy **(Figure 3.9 A, Figure 3.10 A)** when compared with cetuximab and SN-38 single-agent therapies. On the other hand, combination of capecitabine and oxaliplatin at specified concentrations exhibited weak antagonistic effect and increased the cell viability rates as shown in **Figure 3.11 (A)**. The synergy/ antagonism interactions of these drugs in used concentrations were calculated by using SynergyFiner 2.0 version (University of Helsinki, Finland) **(Figure 3.9 B, Figure 3.10 B, Figure 3.11 B)**. The interactions between -10 and 10 synergy scores were evaluated as additive (Zheng et al. 2022). The results were evaluated according

to two most commonly used drug interaction models: Bliss independence model and Loewe additivity model (Anastasio et al. 2015),(Kashif et al. 2017).

In metastatic colorectal cancer therapy, capecitabine (fluoropyrimidine-based therapies), EGFR inhibitors (cetuximab, panitumumab), irinotecan (SN-38), and oxaliplatin have very important roles and are used as single chemotherapeutic drugs and/or in combination with other therapeutic agents (Cassidy et al. 2004),(Cao, Durrani, and Rustum 2005). XELOX (CAPOX), XELIRI (CAPIRI) are two examples to the most administrated combined treatment regimens, and studies indicate that oxaliplatin and 5-FU based drugs have an enrichment effect on their anti-cancer properties, and enhance their therapeutic benefits, especially at specific concentrations (Cassidy et al. 2004). Cetuximab is a targeted cancer drug as an EGFR inhibitor, and effective in KRAS wild type cells. When compared with normal cells, tumor cells have higher EGFR expression (Mahtani and Macdonald 2008). The studies indicate that the use of cetuximab as a cancer therapy agent increases the sensitivity of tumor cells to radiotherapy and chemotherapy, additionally the use of cetuximab in combinations therapies induces tumor growth suppression and apoptosis (Reynolds and Wagstaff 2004). In drug combination therapies 'more-is-better' approach does not convenient, and the combined drugs tend to exhibit antagonistic effects at high concentrations while exhibiting synergistic effects at low concentrations. This is based on molecular and pharmacokinetic interactions of the drugs, and additionally, target pathways and target molecules of the drugs are also important to enhance or inhibit their effects (Mayer and Janoff 2007),(Zoetemelk, Ramzy, and Rausch 2020). In clinics, capecitabine + oxaliplatin (CAPOX/XELOX), capecitabine + irinotecan (CAPIRI/XELIRI) combination therapies are commonly preferred for advanced metastatic CRC patients. Studies indicate that even in elderly patients, side effects of the drugs can be tolerated, and these combination treatments are safe and effective (Comella et al. 2009),(Feliu et al. 2006),(Cao, Durrani, and Rustum 2005). Synergistic effects of the combinations of these drugs based on used drug concentrations, and these interactions are dose dependent. Studies indicates that 5-FU based drugs exhibit more synergistic and/or additive interactions with other

drugs at low concentrations (Cells et al. 2022). In this study, combination effects of capecitabine/ cetuximab, capecitabine / SN-38 and capecitabine / oxaliplatin on the CAPE-resistant Caco-2 cell line were investigated. Capecitabine was used as a background drug at 2x IC50 concentration, and six different doses of cetuximab, five different doses of SN-38 and six different doses of oxaliplatin were combined with this concentration of capecitabine. The MTT assay protocol was conducted, and cell viability rates of CAPE-resistant Caco-2 cell lines under combination therapies and single agent therapies were calculated. The IC50 concentration was calculated as 0.4 μM for CAPE/SN-38 combination, on the other hand it was calculated as 1.9 μM for single agent SN-38 treatment. The IC50 concentration of combined (CAPOX) drug treatment was calculated as 2.1 μM while IC50 concentration of oxaliplatin was calculated as 1.8 μM, any significant difference was not observed in terms of IC50 concentration of CAPOX treatment on CAPE-resistant Caco-2 cells.

The history of combination therapies for different diseases is based on pre-modern medicine stages, but the first applications of co-administration of anti-cancer drugs to the patients are based in the1960s (Gilad et al. 2021). Despite, the four main drug synergy models are commonly used to calculate the interactions between combined drugs, there is still no certain, accepted guideline about which synergy model is the most accurate, and applicable one (Correia, Gärtner, and Vale 2021),(Ma and Motsinger-Reif 2019),(Tang, Wennerberg, and Aittokallio 2015). In this study, synergistic/ antagonistic interactions of the combined drugs were evaluated by using two different approaches: Bliss Independence Model and Loewe Additivity model. Bliss independence model assumes that two drugs act independently in a combination, and there is no interaction between them; on the other hand, Loewe additivity model idea is based on the combination of a drug with itself (Correia, Gärtner, and Vale 2021). As seen in **Figures 3.9 (B), 3.10 (B)**, Cetuximab/Capecitabine combinations have additive effects at all used concentrations in terms of both approaches, SN-38/Capecitabine combinations have additive effects according to Bliss model, have synergistic effects at the lowest three SN-38 concentrations according to Loewe model on CAPE-resistant Caco-2 cells

(Zheng et al. 2022). Despite, most of the *in vitro* and clinic studies indicate that CAPOX (capecitabine/oxaliplatin) combinations have an enrichment effect in terms of their cytotoxicity, in our study according to Bliss model ‘‘weak antagonisim’’ was observed for all oxaliplatin concentrations, according to Loewe model, ‘‘weak antagonism’’ and additive effects were observed (Caesar et al. 2019).

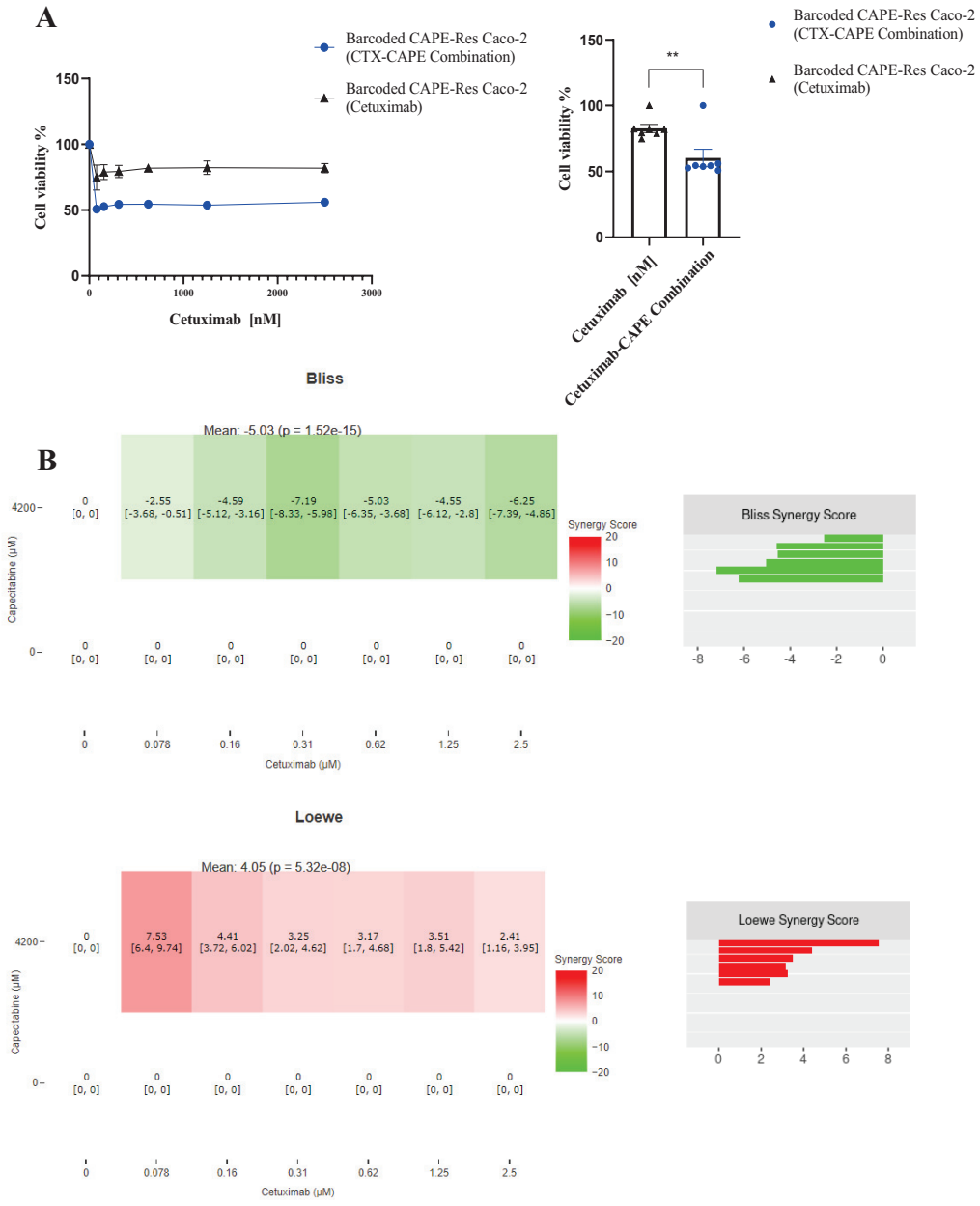

Figure 3.9 (A) Cell viability rates of CAPE-resistant Caco-2 cell line under cetuximab and capecitabine (2 x IC50 conc.) drug combinations **(B)** Visualization of calculated synergy map and synergy scores of cetuximab and capecitabine drug combinations on CAPE-resistant Caco-2 cell line (SynergyFinder 2.0 (University of Helsinki, Finland))

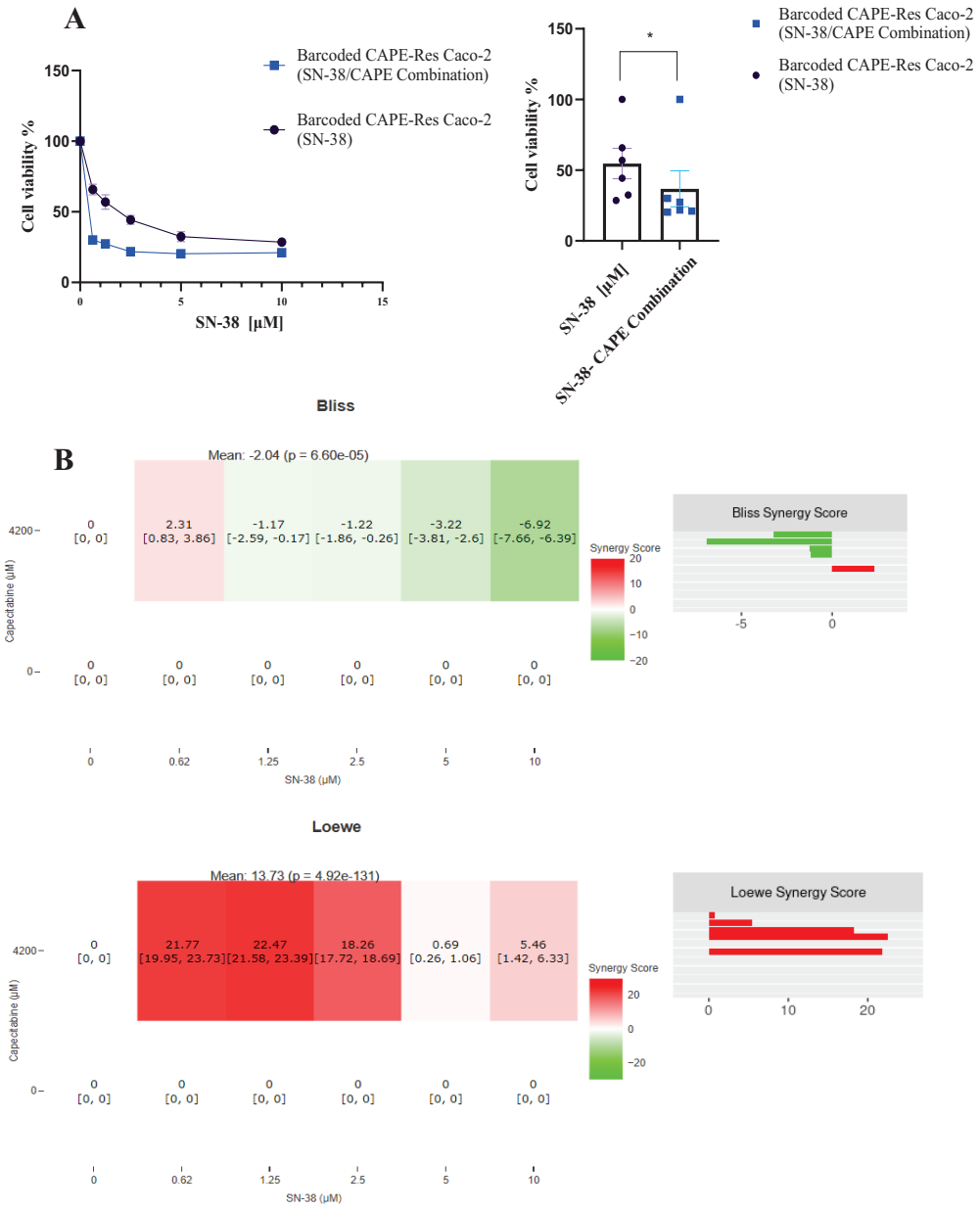

Figure 3.10 (A) Cell viability rates of CAPE-resistant Caco-2 cell line under SN-38 and capecitabine (2x IC50 conc.) drug combinations **(B)** Visualization of calculated synergy map and synergy scores of SN-38 and capecitabine drug combinations on CAPE-resistant Caco-2 cell line (SynergyFinder 2.0 (University of Helsinki, Finland))

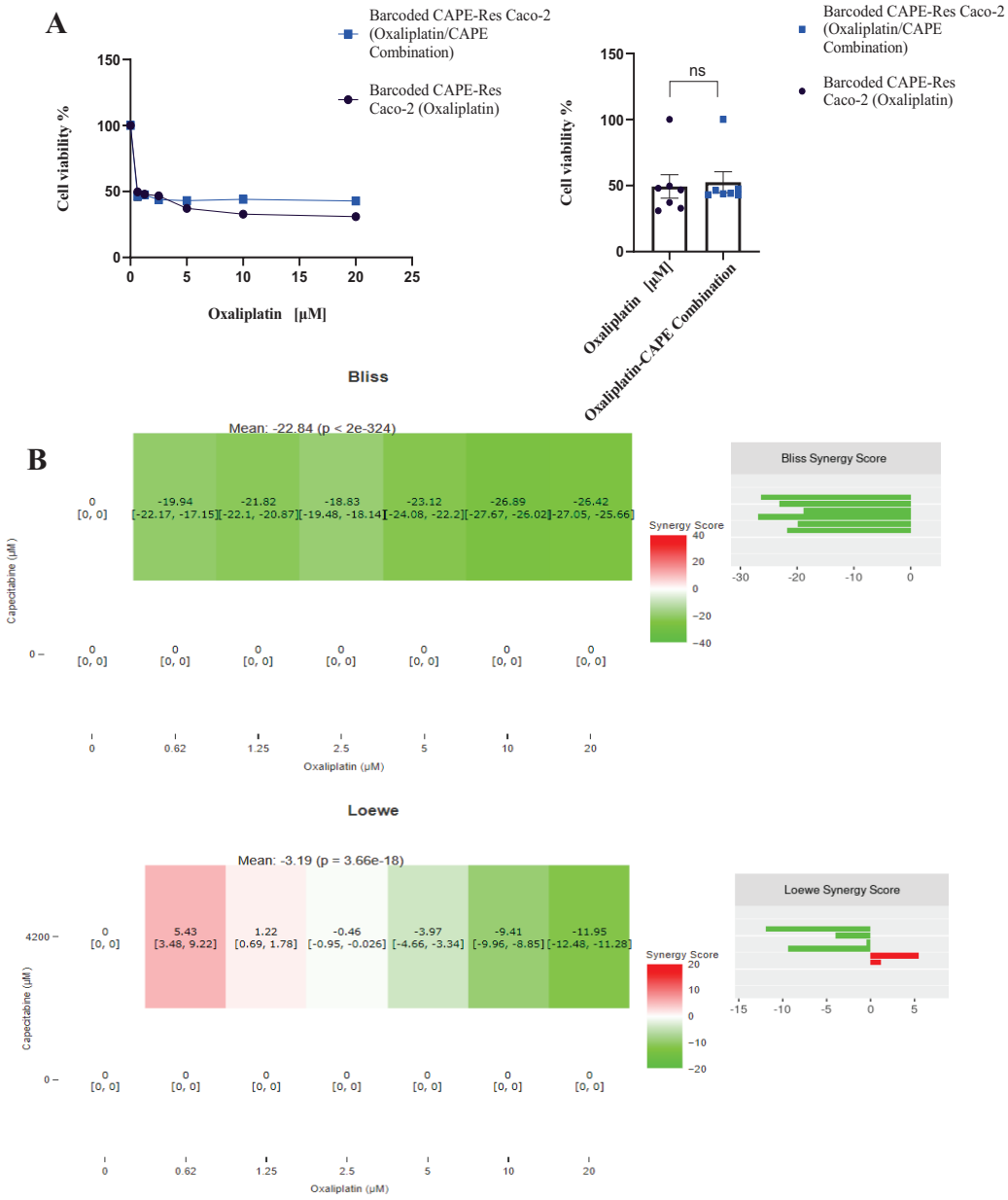

Figure 3.11 (A) Cell viability rates of CAPE-resistant Caco-2 cell line under oxaliplatin and capecitabine (2x IC50 conc.) drug combinations **(B)** Visualization of calculated synergy map and synergy scores of oxaliplatin and capecitabine drug combinations on CAPE-resistant Caco-2 cell line (SynergyFinder 2.0 (University of Helsinki, Finland))

3.5 Generation of Irinotecan – Resistant HT-29 Cell Line

Barcoded HT-29 cells were treated with IC50 concentration of irinotecan (8.851 μM) for 6 months to generate irinotecan-resistant HT-29 cell line. After 6 months irinotecan treatment at IC50 concentration, a barcoded irinotecan-resistant HT-29 cell line was established, and new IC50 concentration of irinotecan on the IRI-resistant HT-29 cells were determined by cell viability assay (MTT assay). Resistant clones were detected by barcode sequencing and bioinformatics analysis, and finally the IRI-resistant HT-29 cells and its control cell lines (DMSO, initial population) were treated other chemotherapeutics as single-agent and in combinations to control acquired cross-resistance or collateral sensitivity to other drugs.

3.5.1 Drug Dose Response Curve of Irinotecan on Irinotecan-Resistant HT-29 Cell Line and Resistance Fold Change Values

The IRI-resistant HT-29 cells (evolutionary replicates A, B, C) and their initial and DMSO control cell lines were seeded into 96 well plates (10 x 10^3 / well). After 24 hrs. the mediums of the cell lines were changed with irinotecan-containing medium in different concentration (in 1:2 dilution range). The cells were treated with irinotecan for 72 hrs., and MTT assay protocol was applied. The new IC50 concentration of irinotecan on IRI-resistant HT-29 cell lines were calculated by non-linear regression analysis as 44,57 μM, 55.96 μM, and 49,42 μM (Replicates A, B, C) respectively.

According to new IC50 values of the irinotecan-resistant HT-29 cell line replicates, resistant fold-change values were calculated as indicated in **Table 3.3**. According to MTT cell viability assay results, the replicate B has the highest IC50 dose concentration (55,96 μM) and has the highest resistance fold change over control cell lines, therefore replicate B was used for further characterization assays.

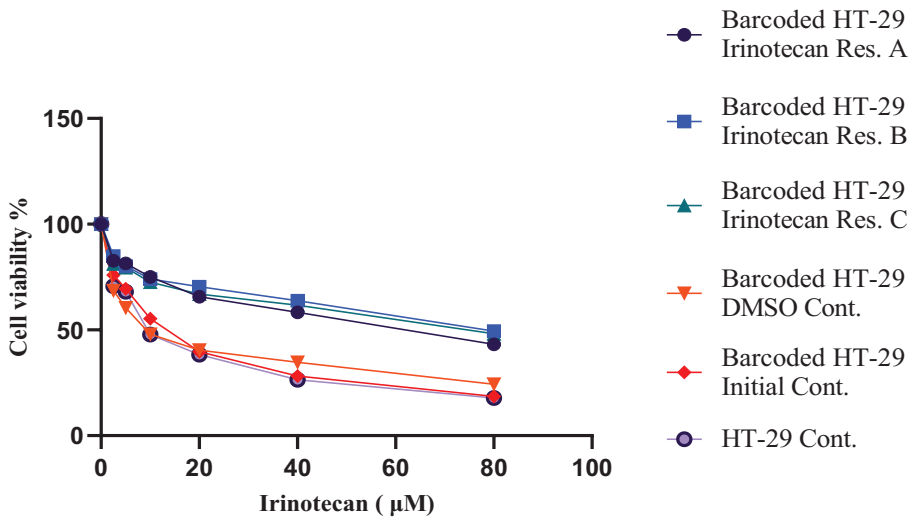

Figure 3.12 Drug dose response curve of irinotecan on IRI-resistant HT-29 cell line (Replica A, B, C), DMSO control, initial population control and parental control HT-29 cell line

Table 3.3 IC50 values of Control and IRI-Resistant HT-29 Cell Lines and Resistant Fold Changes (* = p<0.05, ** = p<0.01, *** = p<0.001, **** = p<0.0001)

	IRI- Res HT-29	**Initial Cont.**	**DMSO Cont.**	**HT-29**
IC50 Values (µM)	**Replicates** **(A)** 44.57 **(B)** 55.96 **(C)** 49.42	12.62	10.87	10.55
Fold Resistance	**IC50 of Res. Cell/ IC50 of Cont. Cell**	**(A)** 3.53 (****) **(B)** 4.43(****) **(C)** 3.9 (****)	**(A)** 4.1(****) **(B)** 5.15(****) **(C)** 4.55(****)	**(A)** 4.22 **(B)** 5.30 **(C)** 4.68

3.5.2 Proliferation Rate and Cell Morphology of the Irinotecan-Resistant HT-29

MTT assay was carried out to investigate the effect of irinotecan on proliferation rate of the irinotecan-resistant HT-29 cell line. For this, the irinotecan-resistant HT-29 and control cell lines (DMSO and initial population) were seeded into 3 different 96 well plates (10 x 10^3 / well). The cells were allowed to attach in a humidified incubator with 5% CO_2 at 37°C for 24 hrs., then the cells were treated with irinotecan (for IRI-resistant HT-29), and the same concentration DMSO (DMSO control cell lines) while medium of the initial populations were changed with fresh growth medium. The MTT assay protocol was applied for each time point, and the absorbance values of the cells were measured at 24. hrs, 48. hrs., and 72. hrs. after treatment. According to measured absorbance values (at 570 nm) the proliferation rates were plotted by using GraphPad Prism 8 (GraphPad Software Inc., USA). The analysis was conducted by two-way Annova test (****p<0.0001).

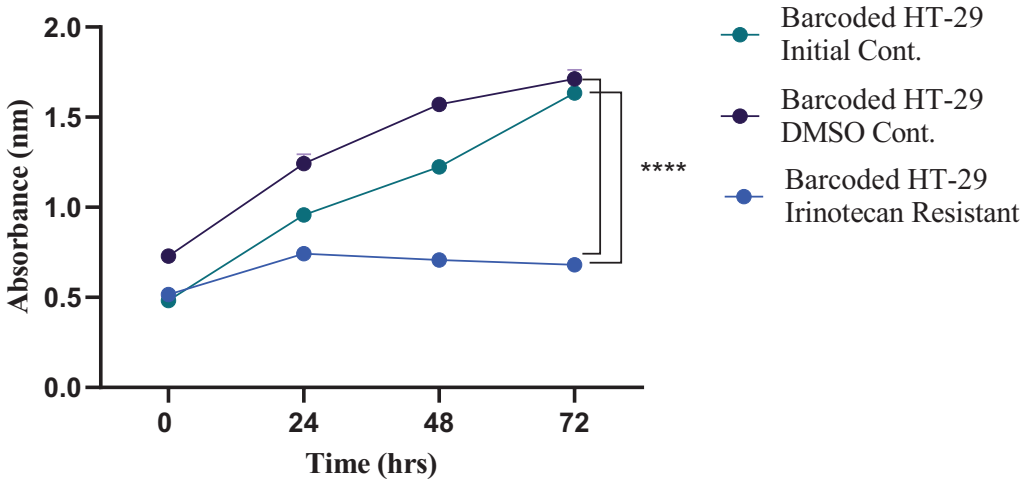

Figure 3.13 Time dependent absorbance values of IRI-resistant HT-29, DMSO control HT-29 and Initial population control HT-29

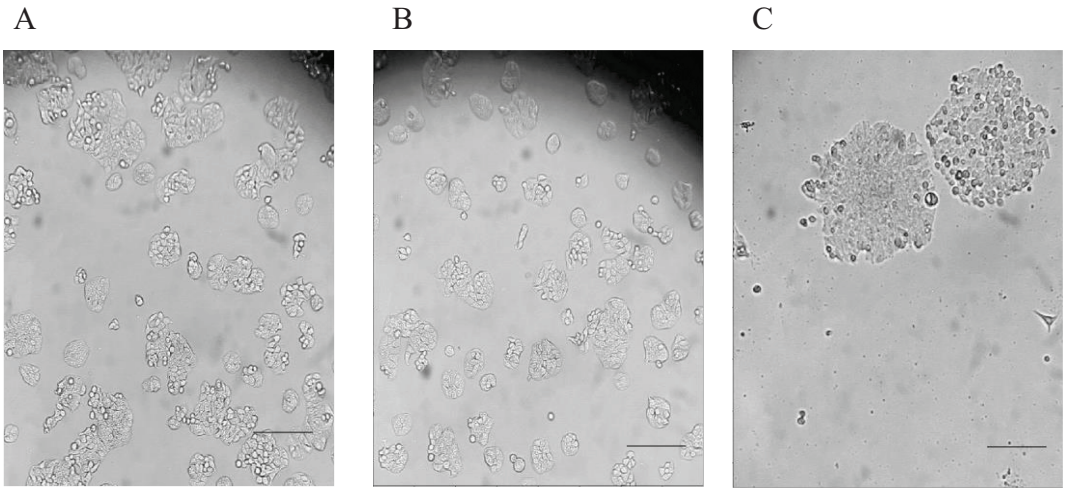

Figure 3.14 (A) Barcoded HT-29 Initial Control, **(B)** Barcoded HT-29 DMSO Control, **(C)** Barcoded IRI-Res HT-29 Cells (10X) (1 mm)

As shown in **Figure 3.13**, irinotecan has an anti-proliferative effect on irinotecan-resistant HT-29 cell line, and a significant proliferation inhibition was observed in the cells within irinotecan containing medium at the 72nd hrs (****$p<0.0001$). Additionally, the clones that acquired resistance to irinotecan during irinotecan treatment for 6 months formed colony-like structures and dominated the population as seen in **Figure 3.14 (C)**.

3.5.3 Bioinformatics Analysis Results of Irinotecan – Resistant HT-29 Cell Line

The cell pellets collected from irinotecan-resistant HT-29 replicate plates, DMSO and initial population HT-29 cell lines were used for DNA isolation. Due to these cells were barcoded with unique barcode sequences in their genome by using lentiviral vectors, the isolated DNA samples were sequenced to detect and analyze unique barcodes in IRI-resistant and control HT-29 cell lines. Additionally, DNA isolation was performed from floating cell pellets which were collected from used

mediums in equal time points for tracking of frequencies of the detected unique barcodes during establishment of IRI-resistant HT-29 clones.

3.5.3.1 Barcode Analysis of the Detected Clones in the Irinotecan-Resistant HT-29 Cell Population

The approximate growth rates of the detected barcodes in irinotecan-resistant HT-29 replicates and their DMSO and initial cell controls were calculated by using the same formula that is indicated in session 3.4.2.1. The barcodes have positive growth rate at least two replicates were classified as 'Resistant barcode'; the barcodes have positive growth rate and were detected only in one replicate were classified as 'De novo barcodes' and remaining barcodes were named as 'Sensitive barcodes' and these barcodes exhibit negative growth rate (Acar et al. 2020). According to bioinformatics analysis of barcode sequencies, the red bars shown in **Figure 3.15** represents the frequencies of the resistant barcodes in the populations. The numbers of the detected resistant barcodes in the replicates 20, 24, and 24 (A, B, C) respectively, and total number of the detected unique resistant barcode is 32 while detected de novo barcode numbers are 137, 120, 126 (A, B, C) in the irinotecan-resistant HT-29 replicates. In **Figure 3.15** the grey bars represent 'Not determined barcodes which were found in the replicates but were not detected in the DMSO and/or Initial control populations (Acar et al. 2020). As shown in the barcode sequencing frequency plot (**Figure 3.15 B**), in IRI-resistant HT-29 cell line replicates (A, B, C) the majority of the resistant clones formed by de novo (acquired) resistant clones and dominated the populations. IRI-resistant HT-29 A, B, C replicates have higher frequency in terms of de novo resistant barcodes that have positive growth rates and detected only in one replicate. The frequency analysis indicates that de novo resistant clones dominated the irinotecan drug resistance for these IRI-resistsnt HT-29 populations (Acar et al. 2020).

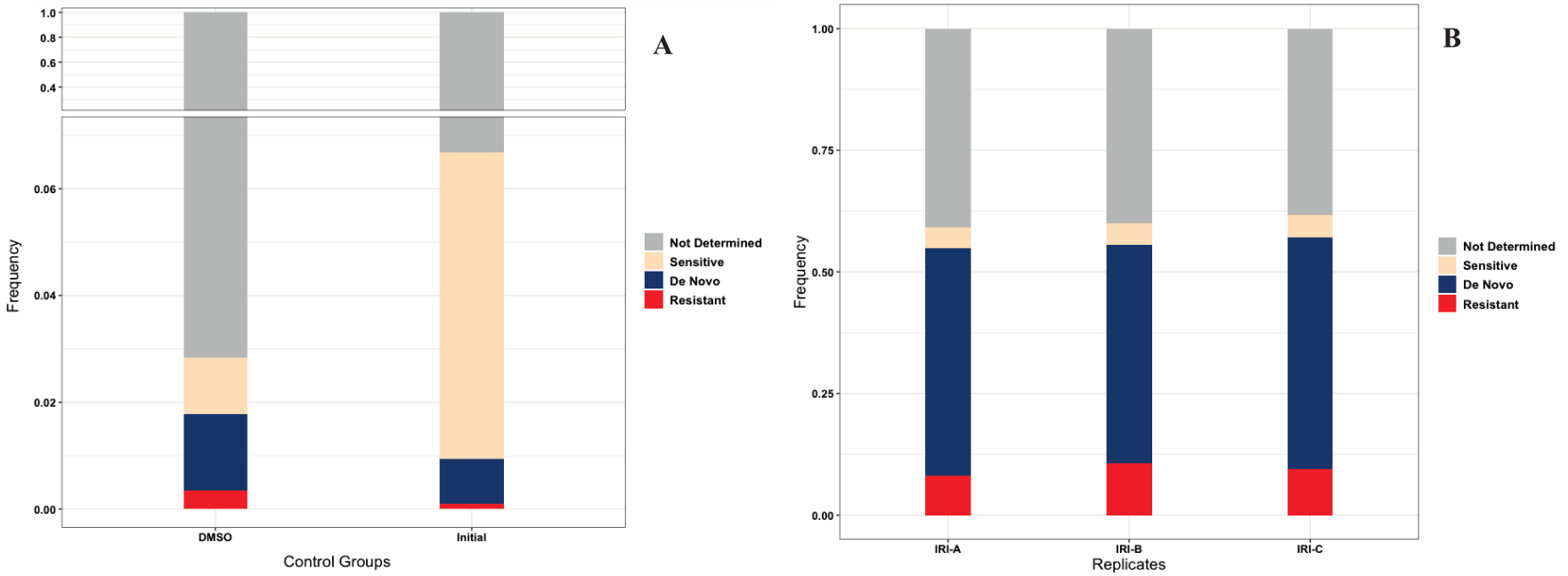

Figure 3.15 **(A)** Barcode frequency distributions of DMSO and Initial HT-29 cell line controls and **(B)** Irinotecan-resistant HT-29 cell lines (Replicates A, B, C)

3.5.3.2 Tracking of the Irinotecan – Resistant HT-29 Clones in the Population

The barcode frequencies in five different medium collected at equal intervals (once in every four weeks) were determined in order to track the resistant barcodes (only for Replicate B). Resistant barcodes with positive growth rate are plotted. Likewise, the tracking line graph of the frequencies in the middle and end points has been obtained for sensitive barcodes so that they can be compared with resistant barcodes. As indicated in **Figure 3.16 (A)**, a total of 9 resistant barcodes were tracked by sequencing of the floating dead cells from used medium. As seen in the figure, all tracked resistant barcodes have an increasing pattern according to the first time point. At the beginning of the experiment, collected dead cell pellets from used medium mostly formed from the irinotecan sensitive cells, and collected cell pellet amount decreased in time. Through the end of the experiments, resistant-cell confluency in the plate increased and resistant cells began to detach. Tracking of the resistant clones from floating dead cells provided information about temporal dynamics in the population, this method can be thought of as using the circulating tumor DNA in the cancer patients (Acar et al. 2020).

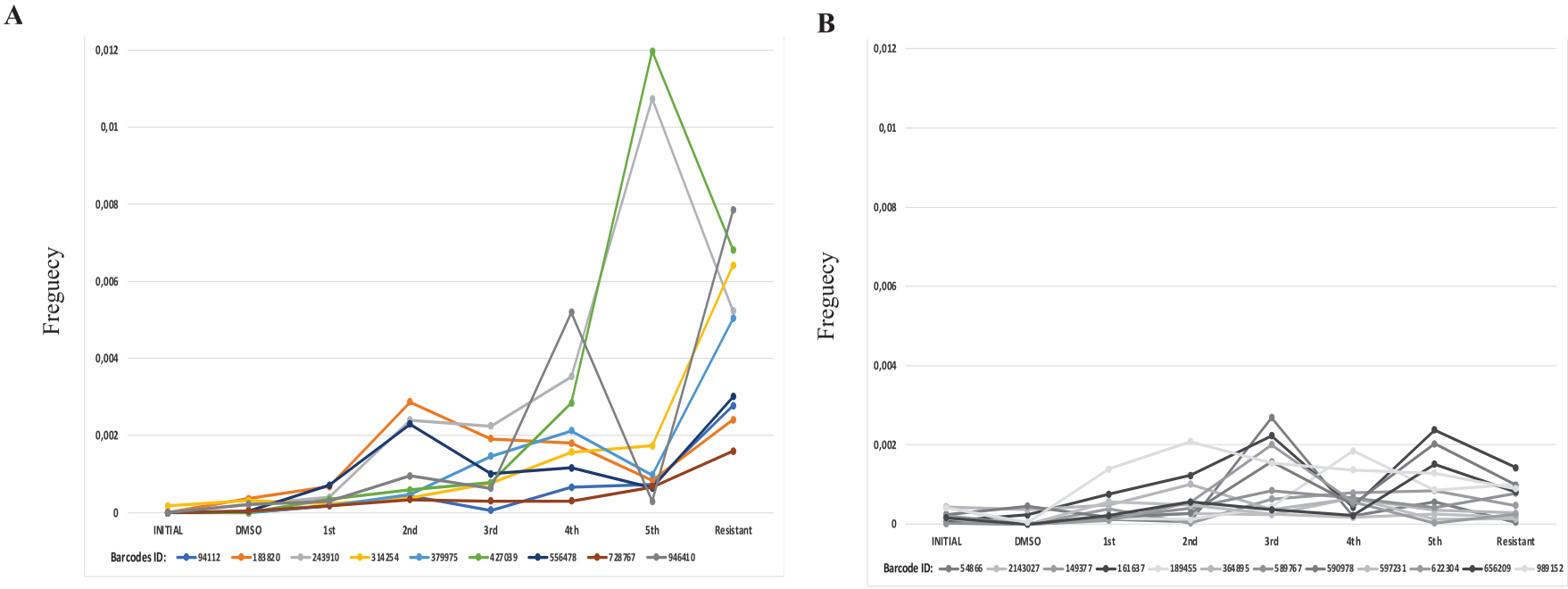

Figure 3.16 **(A)** Frequency distributions of the resistant barcodes in DMSO, Initial cell line controls and Irinotecan resistant HT-29 cell line (Replica B) and dead cells in the mediums (Replica B mediums) **(B)** Frequency distributions of the sensitive barcodes in DMSO, Initial cell line controls and Irinotecan resistant HT-29 cell line (Replica B) and dead cells in the mediums (Replica B mediums)

3.5.4 Secondary Drug Dose Response Curves of Irinotecan – Resistant HT-29 Cell Line

To investigate the effects of secondary chemotherapeutic drugs on irinotecan-resistant HT-29 cells; IRI-resistant HT-29 cells, and their DMSO and initial control cells were seeded into 96 well plates (10×10^3 cells/ well). After 24 hrs. incubation, the cells were treated with capecitabine, SN-38, oxaliplatin and dabrafenib in different concentrations. The irinotecan-resistant HT-29 and their control cells were treated with the drugs for 72 hrs., and MTT assay protocol was applied. As indicated in **Figure 3.17**, irinotecan-resistant HT-29 cells exhibit sensitivity to dabrafenib (BRAF inhibitor) (*$p < 0.05$) while sensitivity was not observed to capecitabine and oxaliplatin. Due to SN-38 is the active metabolite of irinotecan, irinotecan-resistant HT-29 cells were less sensitive to SN-38 than DMSO and initial HT-29 control cells. Irinotecan-resistant HT-29 cells also exhibited cross-resistant to SN-38 drug. IC50 concentrations of SN-38 were calculated as 0.44 μM and 0.46 μM for initial and DMSO control, respectively; on the other hand, it was calculated as 0.99 μM for IRI-resistant HT-29 cells.

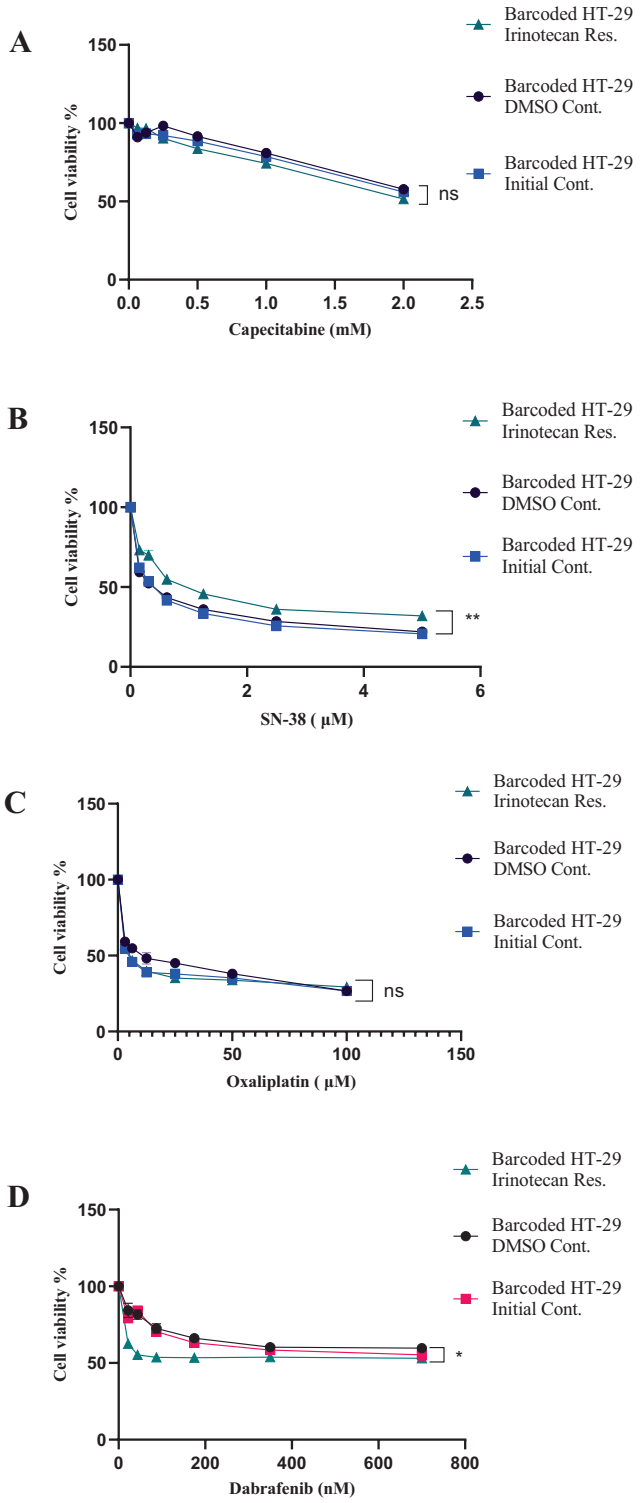

Figure 3.17 **(A)** Capecitabine, **(B)** SN-38, **(C)** Oxaliplatin **(D)** Dabrafenib dose-response curve of DMSO, Initial HT-29 cell line controls and Irinotecan- resistant HT-29 cell lines

3.5.5 Drug Combination Assays on Irinotecan-Resistant HT-29 Cell Line

Irinotecan is one of the drugs that form the backbone of colorectal cancer therapy regimens. Irinotecan and its active metabolite SN-38 are commonly used as a single agent and/or combination with other drugs at first-line and second-line therapies in advanced colorectal cancer patients' treatments thanks to their proliferation inhibiting effects by suppressing DNA replication (Kciuk, Marciniak, and Kontek 2020). Despite the response rate changes according to the factors such as stage of the cancer, mutation types, metastatic situation; irinotecan based combination therapies are commonly administrated: FOLFIRI, CAPIRI, FOLFIRINOX, TEMIRI, etc. (Bailly 2019) Approximately 8-10% of advanced colorectal cancer patients have alterations on their BRAF gene, and V600E alteration has the highest frequency. Chemotherapy response rates of the patients have BRAF mutations are very limited ,therefore these alterations are considered as negative prognostic biomarkers in clinics (Grassi et al. 2021). These alterations play important roles on efficiency of the applied treatment regimens, drug response, tumor progression-free time, overall survival rate (Grassi et al. 2021). Dabrafenib is BRAF inhibitor, and administrated with combination of 5-FU, Leucovorin, oxaliplatin and irinotecan (FOLFOXIRI) as a standard therapeutic approach for BRAF ^{mt} colorectal cancer patients (Grothey, Fakih, and Tabernero 2021). Studies indicate that, dabrafenib is not effective as a monotherapeutic agent on BRAF^{mt} CRC patients, on the other hand combination of dabrafenib with EGFR inhibitors (cetuximab), and other chemotherapeutic (oxaliplatin, irinotecan, capecitabine) may exhibit the expected therapeutic effects (Grothey, Fakih, and Tabernero 2021),(Grassi et al. 2021), (Imai, Ohmori, and Fukuda 2014). Dabrafenib/irinotecan combination treatment is considered for both advanced colorectal cancer patients and advanced melanoma patients in clinics (Z. Wang et al. 2022). In this study, irinotecan-resistant HT-29 (BRAF V600E cell line model) cells were treated with irinotecan/dabrafenib and irinotecan/capecitabine combinations. As indicated in section 3.4.5, combination therapies tend to exhibit synergistic and additive effects at low doses of the combined drugs. As seen in

Figure 3.18 (A) treatment of IRI-resistant HT-29 cells with combination of dabrafenib/irinotecan decreased the cell viability rate, and additive effect was observed at the lowest dabrafenib concentration (irinotecan concentration was stable at IC50) according to Bliss model (**Figure 3.18 (B)**). As mentioned in section 3.4.5, capecitabine and irinotecan (CAPIRI) combination is one of the most important treatment regimens in advanced colorectal cancer patients, and studies exhibit that dose-dependent synergistic effect of these two drugs play important role in achieving positive response to the treatment. As seen in **Figure 3.19 (B)**, capecitabine/irinotecan combination exhibited additive effects at almost all capecitabine concentrations (irinotecan concentration was stable at IC50) according to the both synergy models.

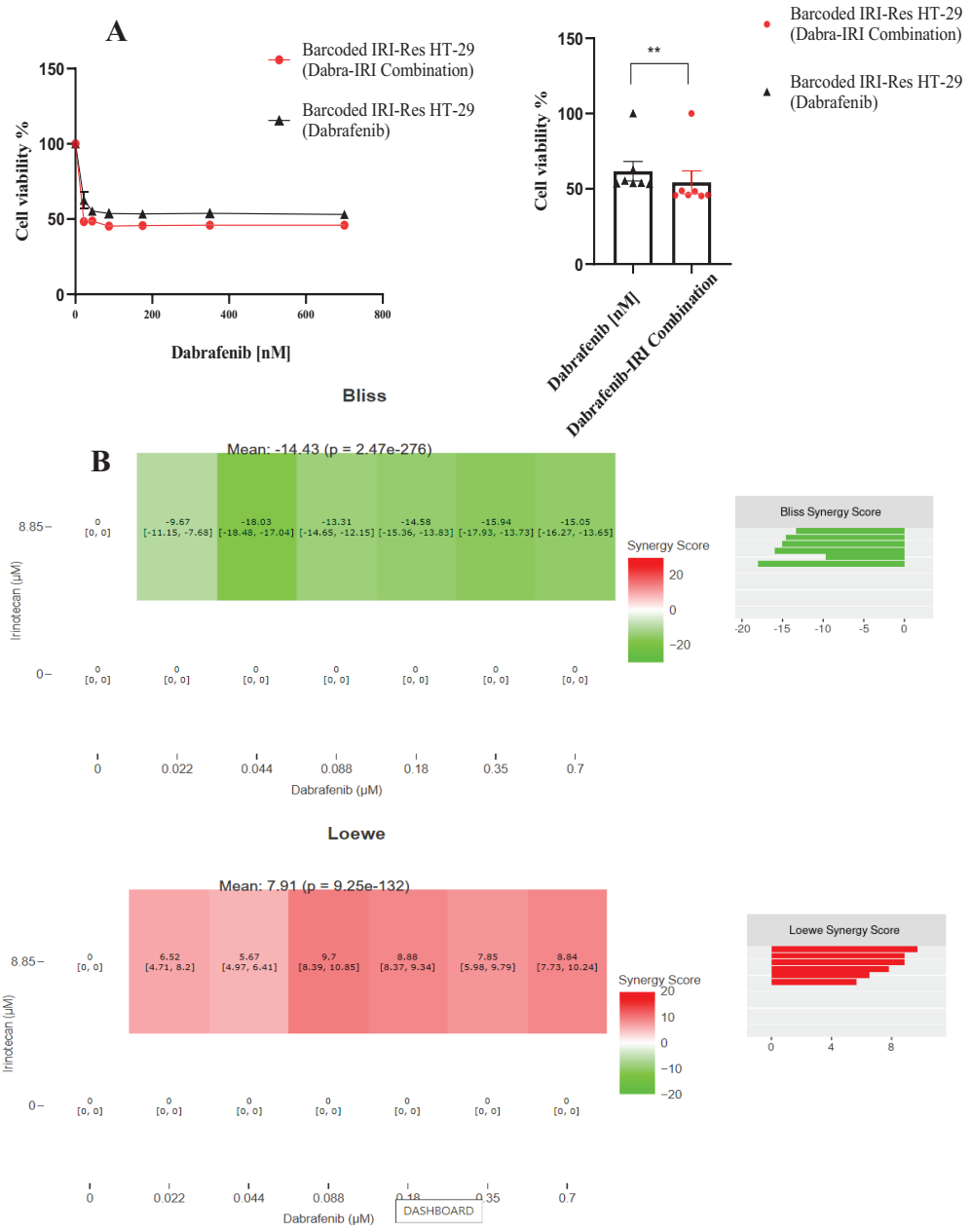

Figure 3.18 **(A)** Cell viability rates of IRI-resistant HT-29 cell line under dabrafenib and irinotecan (IC50 conc.) drug combinations **(B)** Visualization of calculated synergy map and synergy scores of dabrafenib and irinotecan drug combinations on IRI-resistant HT-29 cell line (SynergyFinder 2.0 (University of Helsinki, Finland))

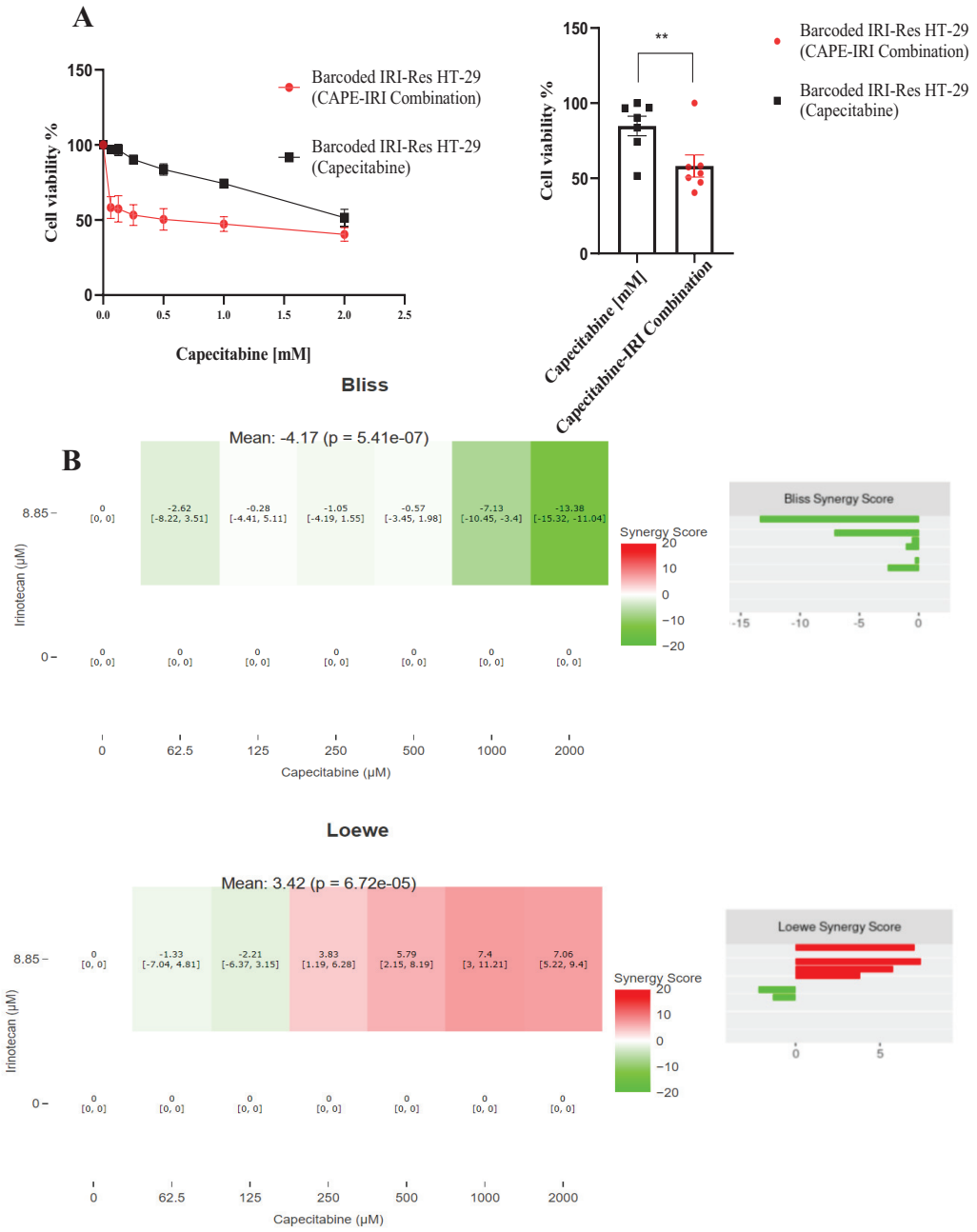

Figure 3.19 **(A)** Cell viability rates of IRI-resistant HT-29 cell line under capecitabine and irinotecan (IC50 conc.) drug combinations **(B)** Visualization of calculated synergy map and synergy scores of capecitabine and irinotecan drug combinations on IRI-resistant HT-29 cell line (SynergyFinder 2.0 (University of Helsinki, Finland))

3.6 Western Blot

Mitogen-activated protein kinases (MAPK) is very important member of serine-threonine kinases family, and play a crucial role in interaction between cell surface mediators and nucleus (Fang and Richardson 2005). Three major pathways of MAPK are: ERK MAPK pathway (Ras-Raf1-Mek-Erk), JNK/SAPK and MAPK14. ERK MAPK pathway mediates cell proliferation, cell growth, and differentiation, therefore hyperactivation of this pathway is directly related with the tumor formation. Studies indicate that all kinases in ERK MAPK pathway have a role on profile, progression and aggressiveness of colorectal cancer cells and all of these kinases are also promising targets to treatment of colorectal cancer (Fang and Richardson 2005). 30-40% of colorectal cancer patients harbor KRAS mutation, and 85-90% of this mutation are found on codon 12 and 13; 8-10% of colorectal cancer patients harbor B-RAF mutation on their genomes (Roock et al. 2011), (Grassi et al. 2021). Studies indicate that KRAS and B-RAF mutations decrease the drug sensitivity of tumor cells and cause drug resistance, therefore combination therapies with KRAS/BRAF target inhibitors increase the efficiency of chemotherapeutic drugs (Lee, Rauch, and Kolch 2020), (Yang et al. 2011). In this study, western blot experiment was conducted to investigate the p-MEK and p-ERK expression differences in CAPE-resistant Caco-2, IRI-resistant HT-29 and their control cell lines. According to western blot analysis results, overexpression of p-MEK was observed in irinotecan-resistant HT-29 cell line, while no significant differences were observed in p-ERK expression in between the resistant cell lines and their controls (**Figure 3.20**). Activation of MAPK pathway, ultimately overexpression of p-MEK1/2 in IRI-res HT-29 can be one of the potentiate factors for acquired resistance to irinotecan in HT-29 cell line and potential targeting of MEK1/2 using FDA approved drug trametinib may act as second-line therapeutic approach sensitizing IRI-resistant HT-29 cell line (Imai, Ohmori, and Fukuda 2014), (Patel et al. 2021).

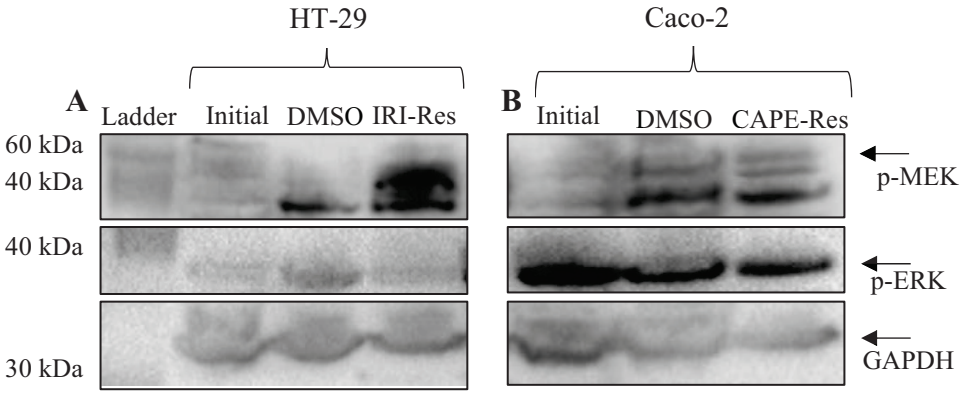

Figure 3.20 (A) p-MEK and p-ERK expression differences between IRI-resistant HT-29 cell line and DMSO, initial HT-29 control cell lines; **(B)** p-MEK and p-ERK expression differences between CAPE-resistant Caco-2 cell line and DMSO, initial Caco-2 control cell lines

CHAPTER 4

CONCLUSION AND FUTURE PROSPECTS

The overall aim of this study was the investigation and better understanding of clonal evolution of drug resistance in tumor cells to provide new model systems and evolutionary perspectives for drug resistance in cancer.

In this study, firstly two colorectal cancer cell line models Caco-2 and HT-29 cells were barcoded with DNA-based unique barcode sequences by lentiviral vector systems. Then, the barcoded Caco-2 cell lines were treated with capecitabine for 6 months and capecitabine-resistant Caco-2 cell lines were generated. The same experimental protocol was performed for the HT-29 cell line by using irinotecan, and at the end of the 6 months irinotecan treatment, irinotecan – resistant HT-29 cell line was established. The primary results of this study are presented below;

IC50 concentration of capecitabine on the CAPE-resistant Caco-2 cell lines was at least 1.4 times higher than DMSO control Caco-2 cell line; IC50 concentration of irinotecan on the IRI-resistant HT-29 cell lines was at least 4.1 times higher than DMSO control HT-29 cell line.

Barcode sequencing was performed by using isolated DNAs from cell pellets of CAPE-resistant Caco-2 and IRI-resistant HT-29 cell lines and their control cell lines (DMSO and initial control cells). In CAPE-resistant Caco-2 cell line replicates; 4 resistant, 3 de novo barcodes dominated the replicate A cell population, 4 resistant 3 de novo barcodes dominated the replicate B cell population, and 7 resistant barcodes dominated the replicate C population. Detected unique barcodes indicated that capecitabine resistance was dominated by pre-existing resistant clones in the CAPE-resistant Caco-2 cell line.

In IRI-resistant HT-29 cell line replicates, the numbers of the detected resistant barcodes were very consistent. The number of the detected resistant barcodes was 20, 24, and 24 (replicates A, B, and C), respectively. The number of de novo barcodes was 137, 120, and 126 in replicates A, B, and C, respectively indicating that de novo barcode selection dominated the populations.

Under capecitabine treatment, CAPE-resistant Caco-2 cells exhibited an elongated structure, under irinotecan treatment IRI-resistant HT-29 cells formed colony-like structures. It indicates that under long-term drug treatment, cells can have morphological changes besides potential genetic and epigenetic changes. Phenotypic changes associated with cancer progression are considered one of the driving forces behind drug-resistance, and therefore morphological changes that I observed in Caco-2 cells and HT-29 cells may be one of the possible mechanisms driving drug-resistance mechanism in our experimental model system.

Capecitabine-resistant Caco-2 cells were treated with oxaliplatin, irinotecan, SN-38 and cetuximab to see the effects of secondary drug treatment on capecitabine-resistant Caco-2 cells. Under these conditions, capecitabine-resistant Caco-2 cells exhibited collateral sensitivity to oxaliplatin, SN-38 and cetuximab. Furthermore, irinotecan-resistant HT-29 cells treated with oxaliplatin, SN-38, dabrafenib and capecitabine exhibited collateral sensitivity to dabrafenib. Since SN-38 is active metabolite of irinotecan, irinotecan-resistant HT-29 cells were co-resistant to SN-38. The genetic alterations on the cancer cells play important roles on the determinaton of the sensitivity and/or resistance to chemotherapeutic drugs. The cancer cells carrying KRAS/BRAF mutations may exhibit resistance to most of the anti-cancer drugs when they are administrated as monotherapy. Secondary- drug response assays can help to understand new therapy regimens after cancer cells show resistance to the drugs at the first-line therapy.

Capecitabine-resistant Caco-2 cells were treated with capecitabine/oxaliplatin, capecitabine/ SN-38 and capecitabine/cetuximab drug combinations. In all combinations, capecitabine concentration was maintained at 2x IC50 (4.2 mM)

which they were initially became resistant to capecitabine. Except for capecitabine/oxaliplatin (CAPOX) combination, almost all combinations exhibited additive effects according to Bliss and Loewe synergy scores. Capecitabine/SN-38 combination had a synergistic effect on Cape-resistant Caco-2 cells in low concentrations. The highest synergy was observed at 4.2 mM / 0.625 μM (Capecitabine/ SN-38, respectively) drug concentration combination.

Irinotecan-resistant HT-29 cells were treated with irinotecan/capecitabine and irinotecan/dabrafenib drug combination. In all combinations, irinotecan concentration was maintained at IC50 (8.85 μM) which they were initially became resistant to irinotecan. Almost all combinations exhibited additive effects according to Bliss and Loewe synergy scores.

According to p-MEK and p-ERK western blot analyses, overexpression of p-MEK was observed in IRI-resistant HT-29 while; significant expression differences were not observed in CAPE-resistant Caco-2. Expression differences may therefore be likely due to acquired drug-resistance levels achieved in each cell line.

As indicated in this study, experimental evolution model systems to investigate the clonal evolution of drug-resistant tumor cells can provide valuable information about resistance-driving clones. Since 2D cell line culture model systems lack mimicking the presence of tumor microenvironment and interactions between tumor cells and stromal cells, better model systems considering stromal cells such as CAFs and immune cells will be needed. Alongside with using of cellular barcoding technology in co-cultured experimental model systems will likely to more patient-relevant understanding of the underlying molecular determinants of drug resistance.

REFERENCES

Acar, Ahmet et al. 2020. "Exploiting Evolutionary Steering to Induce Collateral Drug Sensitivity in Cancer." *Nature Communications* 11(1): 1–14. http://dx.doi.org/10.1038/s41467-020-15596-z.

Ahmed, D et al. 2013. "Epigenetic and Genetic Features of 24 Colon Cancer Cell Lines." (2). www.nature.com/oncsis.

Aleksakhina, Svetlana N., Aniruddh Kashyap, and Evgeny N. Imyanitov. 2019. "Mechanisms of Acquired Tumor Drug Resistance." *Biochimica et Biophysica Acta - Reviews on Cancer* 1872(2): 188310. https://doi.org/10.1016/j.bbcan.2019.188310.

Anastasio, Thomas J et al. 2015. "What Is Synergy? The Saariselkä Agreement Revisited." *Frontiers in Pharmacology | www.frontiersin.org* 6: 181. www.frontiersin.org.

Anderson, Nicole M, and M Celeste Simon. 2020. 30 Current Biology *The Tumor Microenvironment*.

Bailly, Christian. 2019. "Irinotecan: 25 Years of Cancer Treatment." *Pharmacological Research* 148.

Banerjee, Antara et al. 2017. "Strategies for Targeted Drug Delivery in Treatment of Colon Cancer: Current Trends and Future Perspectives." *Drug Discovery Today* 22(8): 1224–32.

Bhang, Hyo Eun C. et al. 2015. "Studying Clonal Dynamics in Response to Cancer Therapy Using High-Complexity Barcoding." *Nature Medicine* 21(5): 440–48.

Blank, Annika et al. 2018. "Tumor Heterogeneity in Primary Colorectal Cancer and Corresponding Metastases. Does the Apple Fall Far from the Tree?" *Frontiers in Medicine* 5(AUG): 1–8.

Bolger, Anthony M, Marc Lohse, and Bjoern Usadel. 2014. "Genome Analysis Trimmomatic: A Flexible Trimmer for Illumina Sequence Data." 30(15):

2114–20. http://www.usadellab.org/cms/index.

Bramlett, Charles et al. 2020. “Throughput Sequencing.” 15(4): 1436–58.

Caesar, Lindsay K et al. 2019. “Synergy and Antagonism in Natural Product Extracts: When 1 + 1 Does Not Equal 2.” 36(6): 845–936. https://mcsquared.uncg.edu/.

Çakir, Hacer Kaya, and Onur Eroglu. 2021. “In Vitro Anti-Proliferative Effect of Capecitabine (Xeloda) Combined with Mocetinostat (MGCD0103) in 4T1 Breast Cancer Cell Line by Immunoblotting.” *Iranian Journal of Basic Medical Sciences* 24(11): 1515–22.

Cao, Shousong, Farukh A. Durrani, and Youcef M. Rustum. 2005. “Synergistic Antitumor Activity of Capecitabine in Combination with Irinotecan.” *Clinical Colorectal Cancer* 4(5): 336–43. http://dx.doi.org/10.3816/CCC.2005.n.007.

Cassidy, Jim et al. 2004. “XELOX (Capecitabine plus Oxaliplatin): Active First-Line Therapy for Patients with Metastatic Colorectal Cancer.” *Journal of Clinical Oncology* 22(11): 2084–91.

Cells, Cancer, Sareh Kamran, Ajantha Sinniah, and Zamri Chik. 2022. “Diosmetin Exerts Synergistic Effects in Combination With.”

CloneTracker XP™ Lentiviral Barcode Libraries. 2018.

Cohen, Esther, Ilana Ophir, and Yehuda Ben Shaul. 1999. “Induced Differentiation in HT29, a Human Colon Adenocarcinoma Cell Line.” *Journal of Cell Science* 112(16): 2657–66.

Comella, Pasquale et al. 2009. “Role of Oxaliplatin in the Treatment of Colorectal Cancer.” *Therapeutics and Clinical Risk Management* 5(1): 229–38.

Correia, Ana Salomé, Fátima Gärtner, and Nuno Vale. 2021. “Drug Combination and Repurposing for Cancer Therapy: The Example of Breast Cancer.” *Heliyon* 7(1).

Dhawan, Andrew et al. 2017. “Collateral Sensitivity Networks Reveal Evolutionary Instability and Novel Treatment Strategies in ALK Mutated

Non-Small Cell Lung Cancer." *Scientific Reports* 7(1): 1–9. http://dx.doi.org/10.1038/s41598-017-00791-8.

Dufait, Inès et al. 2012. "Retroviral and Lentiviral Vectors for the Induction of Immunological Tolerance." *Article ID* 2012: 14. http://dx.doi.org/10.6064/2012/694137.

Dujardin, Philip, Anna K. Baginska, Sebastian Urban, and Barbara M. Grüner. 2021. "Unraveling Tumor Heterogeneity by Using DNA Barcoding Technologies to Develop Personalized Treatment Strategies in Advanced-Stage PDAC." *Cancers 2021, Vol. 13, Page 4187* 13(16): 4187. https://www.mdpi.com/2072-6694/13/16/4187/htm (March 14, 2022).

Fang, Jing Yuan, and Bruce C Richardson. 2005. "Biological Effects of the MAPK Pathways." *Lancet Oncology* 6(May): 322–27. http://oncology.thelancet.com.

Feliu, J. et al. 2006. "XELOX (Capecitabine plus Oxaliplatin) as First-Line Treatment for Elderly Patients over 70 Years of Age with Advanced Colorectal Cancer." *British Journal of Cancer* 94(7): 969–75.

Ferguson, Michelle J., Fareeda Y. Ahmed, and Jim Cassidy. 2001. "The Role of Pro-Drug Therapy in the Treatment of Cancer." *Drug Resistance Updates* 4(4): 225–32.

Fu. 2009. "Establishment and Biological Analysis of the EC109/CDDP Multidrug-Resistant Esophageal Squamous Cell Carcinoma Cell Line." *Oncology Reports* 22(01): 861–67. http://www.spandidos-publications.com/or/23/3/861.

Gerrits, Alice et al. 2010. "Cellular Barcoding Tool for Clonal Analysis in the Hematopoietic System." *Blood* 115(13): 2610–18. http://ashpublications.org/blood/article-pdf/115/13/2610/1324089/zh801310002610.pdf.

Gilad, Yosi, Gary Gellerman, David M. Lonard, and Bert W. O'malley. 2021. "Drug Combination in Cancer Treatment—from Cocktails to Conjugated Combinations." *Cancers* 13(4): 1–26.

"Global Cancer Statistics 2020: GLOBOCAN Estimates of Incidence and Mortality Worldwide for 36 Cancers in 185 Countries | Enhanced Reader."

Grassi, Elisa et al. 2021. "Current Therapeutic Strategies in BRAF-Mutant Metastatic Colorectal Cancer." *Frontiers in Oncology* 11(June): 1–6.

Grothey, A., M. Fakih, and J. Tabernero. 2021. "Management of BRAF-Mutant Metastatic Colorectal Cancer: A Review of Treatment Options and Evidence-Based Guidelines." *Annals of Oncology* 32(8): 959–67. https://doi.org/10.1016/j.annonc.2021.03.206.

Guglielmi, Alessandra P, Alberto F Sobrero, A P Guglielmi, and A F Sobrero. 1 Gastrointest Cancer Res *Second-Line Therapy for Advanced Colorectal Cancer*. www.myGCRonline.org.

Hao, Dapeng, Li Wang, and Li-Jun Di. 2015. "Distinct Mutation Accumulation Rates among Tissues Determine the Variation in Cancer Risk OPEN." www.nature.com/scientificreports.

Hirsch, Bradford R, and S Yousuf Zafar. 2011. "Cancer Management and Research Dovepress Capecitabine in the Management of Colorectal Cancer." *Cancer Management and Research*: 3–79. https://www.dovepress.com/.

Holohan, Caitriona, Sandra Van Schaeybroeck, Daniel B Longley, and Patrick G Johnston. 2013. "Cancer Drug Resistance: An Evolving Paradigm." www.nature.com/reviews/cancer.

Hu, Tao, Zhen Li, Chun-Ying Gao, and Chi Hin Cho. 2016. "Mechanisms of Drug Resistance in Colon Cancer and Its Therapeutic Strategies." *World J Gastroenterol* 22(30): 6876–89. http://www.wjgnet.com/esps/HelpDesk:http://www.wjgnet.com/esps/helpdesk.aspx.

Hu, Ting Ting et al. 2020. "Detection of Genes Responsible for Cetuximab Sensitization in Colorectal Cancer Cells Using CRISPR-Cas9." *Bioscience Reports* 40(10): 1–10.

Imai, Yasuo, Kyoko Ohmori, and Kazunori Fukuda. 2014. “The Activated MEK / ERK Pathway May Potentiate Breast Cancer Resistance Protein / ABCG2 Function in SN38-Selected MCF-.” 2(Topo I): 1–7.

Jaaks, Patricia et al. 2022. “Effective Drug Combinations in Breast, Colon and Pancreatic Cancer Cells.” *Nature* 603(7899): 166–73.

Kashif, Muhammad et al. 2017. “Bliss and Loewe Interaction Analyses of Clinically Relevant Drug Combinations in Human Colon Cancer Cell Lines Reveal Complex Patterns of Synergy and Antagonism.” *Oncotarget* 8(61): 103952–67.

Kciuk, Mateusz, Beata Marciniak, and Renata Kontek. 2020. “Irinotecan—Still an Important Player in Cancer Chemotherapy: A Comprehensive Overview.” *International Journal of Molecular Sciences* 21(14): 1–21.

Kebschull, Justus M., and Anthony M. Zador. 2018. “Cellular Barcoding: Lineage Tracing, Screening and Beyond.” *Nature Methods* 15(11): 871–79. http://dx.doi.org/10.1038/s41592-018-0185-x.

Labbé, Roman P, Sandrine Vessillier, and Qasim A Rafiq. 2021. “Viruses Lentiviral Vectors for T Cell Engineering: Clinical Applications, Bioprocessing and Future Perspectives.” https://doi.org/10.3390/v13081528.

Leary, Meghan, Sarah Heerboth, Karolina Lapinska, and Sibaji Sarkar. 2018. “Sensitization of Drug Resistant Cancer Cells: A Matter of Combination Therapy.” *Cancers* 10(12): 1–18.

Lee, Shannon, Jens Rauch, and Walter Kolch. 2020. “Targeting MAPK Signaling in Cancer: Mechanisms of Drug Resistance and Sensitivity.” *International Journal of Molecular Sciences* 21(3): 1–29.

Leicher, Laura W. et al. 2017. “Tolerability of Capecitabine Monotherapy in Metastatic Colorectal Cancer: A Real-World Study.” *Drugs in R and D* 17(1): 117–24.

Li, Runze et al. 2016. “Synergistic Reaction of Silver Nitrate, Silver Nanoparticles,

and Methylene Blue against Bacteria." *Proceedings of the National Academy of Sciences of the United States of America* 113(48): 13612–17.

Luo, H. Y. et al. 2016. "Single-Agent Capecitabine as Maintenance Therapy Afterinduction of XELOX (or FOLFOX) in First-Line Treatmentof Metastatic Colorectal Cancer: Randomized Clinical Trialof Efficacy and Safety." *Annals of Oncology* 27(6): 1074–81.

Ma, Jun, and Alison Motsinger-Reif. 2019. "Current Methods for Quantifying Drug Synergism." *Proteomics & bioinformatics : current research* 1(2): 43–48. http://www.ncbi.nlm.nih.gov/pubmed/32043089%0Ahttp://www.pubmedcentral.nih.gov/articlerender.fcgi?artid=PMC7010330.

Mader, R. M. et al. 2003. "Penetration of Capecitabine and Its Metabolites into Malignant and Healthy Tissues of Patients with Advanced Breast Cancer." *British Journal of Cancer* 88(5): 782–87.

Mahtani, Reshma L., and John S. Macdonald. 2008. "Synergy Between Cetuximab and Chemotherapy in Tumors of the Gastrointestinal Tract." *The Oncologist* 13(1): 39–50.

Marusyk, Andriy, and Kornelia Polyak. 2010. "Tumor Heterogeneity: Causes and Consequences." *Biochimica et Biophysica Acta - Reviews on Cancer* 1805(1): 105–17. http://dx.doi.org/10.1016/j.bbcan.2009.11.002.

Mayer, Lawrence D., and Andrew S. Janoff. 2007. "Optimizing Combination Chemotherapy by Controlling Drug Ratios." *Molecular Interventions* 7(4): 216–23.

Merino, D. et al. 2019. "Barcoding Reveals Complex Clonal Behavior in Patient-Derived Xenografts of Metastatic Triple Negative Breast Cancer." *Nature Communications* 10(1). http://dx.doi.org/10.1038/s41467-019-08595-2.

Neophytou, Christiana M, Myrofora Panagi, Triantafyllos Stylianopoulos, and Panagiotis Papageorgis. 2021. "Cancers The Role of Tumor

Microenvironment in Cancer Metastasis: Molecular Mechanisms and Therapeutic Opportunities." https://doi.org/10.3390/cancers.

Nikolaou, Michail, Athanasia Pavlopoulou, Alexandros G Georgakilas, and Efthymios Kyrodimos. 2018. "The Challenge of Drug Resistance in Cancer Treatment: A Current Overview." *Clinical & Experimental Metastasis* 35: 309–18. https://doi.org/10.1007/s10585-018-9903-0.

Ozawa, Shogo, Toshitaka Miura, Jun Terashima, and Wataru Habano. 2021. "Cellular Irinotecan Resistance in Colorectal Cancer and Overcoming Irinotecan Refractoriness through Various Combination Trials Including DNA Methyltransferase Inhibitors: A Review." *Cancer Drug Resistance* 4(4): 946–64.

Parodi, Luis et al. 2008. "Utility of Pretreatment Bilirubin Level and UGT1A1 Polymorphisms in Multivariate Predictive Models of Neutropenia Associated with Irinotecan Treatment in Previously Untreated Patients with Colorectal Cancer." www.blackwell-synergy.com.

Patel, Hima et al. 2021. "Igf1r/Ir Mediates Resistance to Braf and Mek Inhibitors in Braf-Mutant Melanoma." *Cancers* 13(22).

Patro, Rob. 2017. "Salmon Provides Fast and Bias-Aware Quantification of Transcript Expression." http://www.nature.

Pavillard, Valérie et al. 2002. "Determinants of the Cytotoxicity of Irinotecan in Two Human Colorectal Tumor Cell Lines." *Cancer Chemotherapy and Pharmacology* 49(4): 329–35.

Porter, Shaina N., Lee C. Baker, David Mittelman, and Matthew H. Porteus. 2014. "Lentiviral and Targeted Cellular Barcoding Reveals Ongoing Clonal Dynamics of Cell Lines in Vitro and in Vivo." *Genome biology* 15(5): R75.

Reynolds, Neil A, and Antona J Wagstaff. 2004. 64 Drugs *ADIS DRUG PROFILE Cetuximab In the Treatment of Metastatic Colorectal Cancer*.

Riechelmann, Rachel P., and Monika K. Krzyzanowska. 2019. "Drug Interactions

and Oncological Outcomes: A Hidden Adversary." *Ecancermedicalscience* (13): 1–4.

Riss, Terry L et al. 2004. "Cell Viability Assays." *Assay Guidance Manual* (Md): 1–25. http://www.ncbi.nlm.nih.gov/pubmed/23805433.

Roock, Wendy De et al. 2011. "KRAS, BRAF, PIK3CA, and PTEN Mutations: Implications for Targeted Therapies in Metastatic Colorectal Cancer." *The Lancet Oncology* 12(6): 594–603. http://dx.doi.org/10.1016/S1470-2045(10)70209-6.

Saif, Muhammad Wasif, Nikos A Katirtzoglou, and Kostas N Syrigos. *Capecitabine: An Overview of the Side Effects and Their Management*.

Saputra, Elysia C., Lu Huang, Yihui Chen, and Lisa Tucker-Kellogg. 2018. "Combination Therapy and the Evolution of Resistance: The Theoretical Merits of Synergism and Antagonism in Cancer." *Cancer Research* 78(9): 2419–31.

Sawicki, Tomasz et al. 2021. "Cancers A Review of Colorectal Cancer in Terms of Epidemiology, Risk Factors, Development, Symptoms and Diagnosis." https://doi.org/10.3390/cancers13092025.

Scheithauer, Werner et al. 2003. "Oral Capecitabine as an Alternative to i.v. 5-Fluorouracil-Based Adjuvant Therapy for Colon Cancer: Safety Results of a Randomized, Phase III Trial." *Annals of Oncology* 14(12): 1735–43. https://doi.org/10.1093/annonc/mdg500.

Sinn, P L, S L Sauter, and P B Mccray. 2005. "Gene Therapy Progress and Prospects: Development of Improved Lentiviral and Retroviral Vectors-Design, Biosafety, and Production." *Gene Therapy* 12: 1089–98. www.nature.com/gt.

Son, Beomseok et al. 2017. 8 Oncotarget *Oncotarget 3933 Www.Impactjournals.Com/Oncotarget The Role of Tumor Microenvironment in Therapeutic Resistance*. www.impactjournals.com/oncotarget/.

Strober, Warren. 2015. “Trypan Blue Exclusion Test of Cell Viability.” *Current Protocols in Immunology* 111(1): A3.B.1-A3.B.3.

Tang, Jing, Krister Wennerberg, and Tero Aittokallio. 2015. “What Is Synergy? The Saariselkï¿½ Agreement Revisited.” *Frontiers in Pharmacology* 6(SEP): 1–5.

Vasan, Neil, José Baselga, and David M Hyman. 2019. “A View on Drug Resistance in Cancer.” *Nature* 575. https://doi.org/10.1038/s41586-019-1730-1.

Verhoeckx, Kitty et al. 2015. The Impact of Food Bioactives on Health: In Vitro and Ex Vivo Models *The Impact of Food Bioactives on Health: In Vitro and Ex Vivo Models*.

Walko, Christine M, and Celeste Lindley. 2005. “Capecitabine: A Review.” *Clinical Therapeutics* 27(1).

Wang, Lu et al. 2020. “Effect of Reduced-Dose Capecitabine plus Cetuximab as Maintenance Therapy for RAS Wild-Type Metastatic Colorectal Cancer: A Phase 2 Clinical Trial.” *JAMA Network Open* 3(7).

Wang, Xuan, Haiyun Zhang, and Xiaozhuo Chen. 2019. “Drug Resistance and Combating Drug Resistance in Cancer.” *Cancer Drug Resistance* 2(2): 141–60.

Wang, Zhe et al. 2022. “Prediction of Drug–Drug Interaction Between Dabrafenib and Irinotecan via UGT1A1-Mediated Glucuronidation.” *European Journal of Drug Metabolism and Pharmacokinetics* 47(3): 353–61. https://doi.org/10.1007/s13318-021-00740-x.

Wu, Duojiao et al. 2017. “Roles of Tumor Heterogeneity in the Development of Drug Resistance: A Call for Precision Therapy.” *Seminars in Cancer Biology* 42: 13–19. http://dx.doi.org/10.1016/j.semcancer.2016.11.006.

Wu, Michael H., Bingfang Yan, Rod Humerickhouse, and M. Eileen Dolan. 2002. “Irinotecan Activation by Human Carboxylesterases in Colorectal

Adenocarcinoma Cells." *Clinical Cancer Research* 8(8): 2696–2700.

Xi, Yue, and Pengfei Xu. 2021. "Global Colorectal Cancer Burden in 2020 and Projections to 2040." *Translational Oncology* 14(10).

Xie, Yuan Hong, Ying Xuan Chen, and Jing Yuan Fang. 2020. "Comprehensive Review of Targeted Therapy for Colorectal Cancer." *Signal Transduction and Targeted Therapy* 5(1). http://dx.doi.org/10.1038/s41392-020-0116-z.

Xu, Guang, Wanghai Zhang, Margaret K. Ma, and Howard L. McLeod. 2002. "Human Carboxylesterase 2 Is Commonly Expressed in Tumor Tissue and Is Correlated with Activation of Irinotecan." *Clinical Cancer Research* 8(8): 2605–11.

Yalcin, Gizem Damla, Nurseda Danisik, Rana Can Baygin, and Ahmet Acar. 2020. "Systems Biology and Experimental Model Systems of Cancer." *Journal of Personalized Medicine* 10(4).

Yang, Shi Yu et al. 2011. "Inhibition of the P38 MAPK Pathway Sensitises Human Colon Cancer Cells to 5-Fluorouracil Treatment." *International Journal of Oncology* 38(6): 1695–1702.

Zhang, Aiping, Kai Miao, Heng Sun, and Chu Xia Deng. 2022. "Tumor Heterogeneity Reshapes the Tumor Microenvironment to Influence Drug Resistance." *International Journal of Biological Sciences* 18(7): 3019–33.

Zhang, Jie et al. 2015. "An in Vitro Liver Model on Microfluidic Device for Analysis of Capecitabine Metabolite Using Mass Spectrometer as Detector." *Biosensors and Bioelectronics* 68: 322–28.

Zheng, Shuyu et al. 2022. "SynergyFinder Plus: Toward Better Interpretation and Annotation of Drug Combination Screening Datasets." *Genomics, Proteomics & Bioinformatics* (January). https://doi.org/10.1016/j.gpb.2022.01.004.

Zoetemelk, Marloes, George M Ramzy, and Magdalena Rausch. 2020. "Folinic Acid and Oxaliplatin and Its Activity In." *Molecules* 25.

APPENDICES

A. MAP OF VECTOR USED IN THIS STUDY

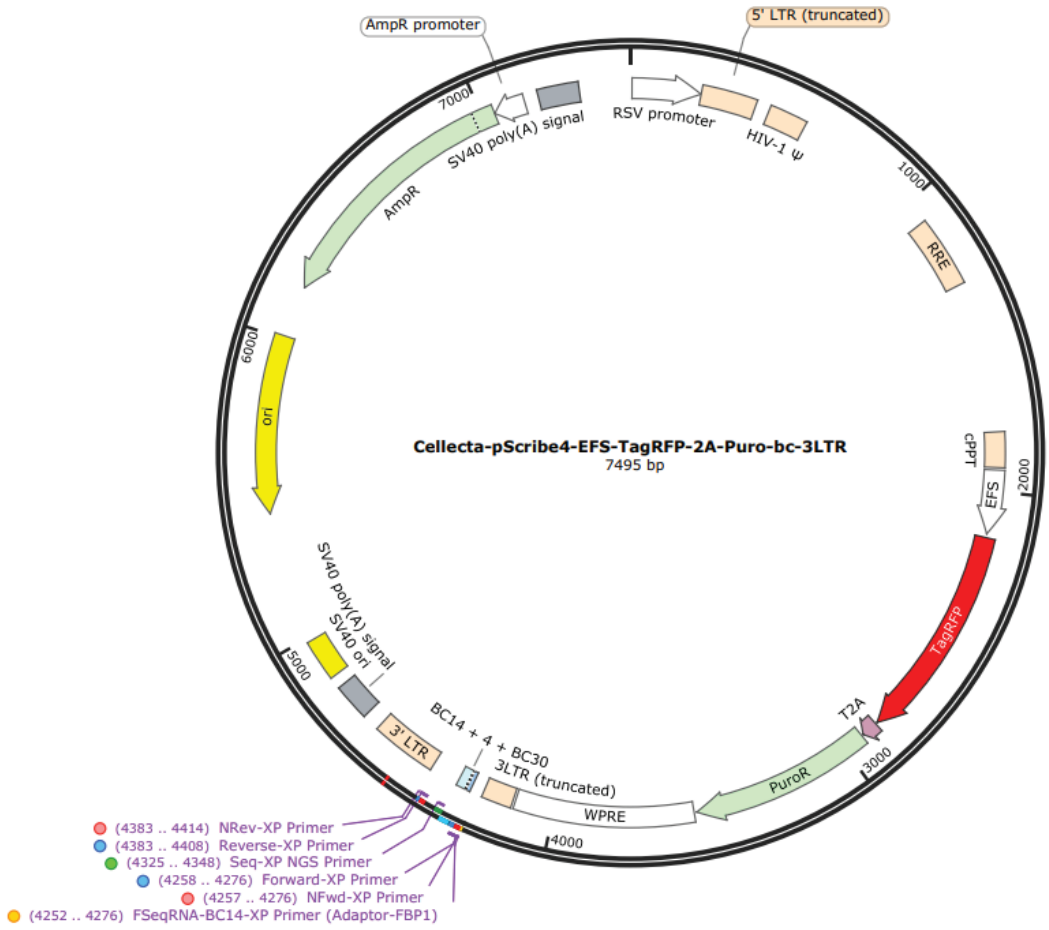

Figure A.1 The vector map of CloneTracker XP 1M Barcode-3' Library with RFP-Puro (plasmid) (Cellecta, # BCXP1M3RP-XS-P)

B. TRACKING OF DE NOVO BARCODES OF CAPECITABINE-RESISTANT CACO-2 AND IRINOTECAN-RES HT-29 CELL LINES

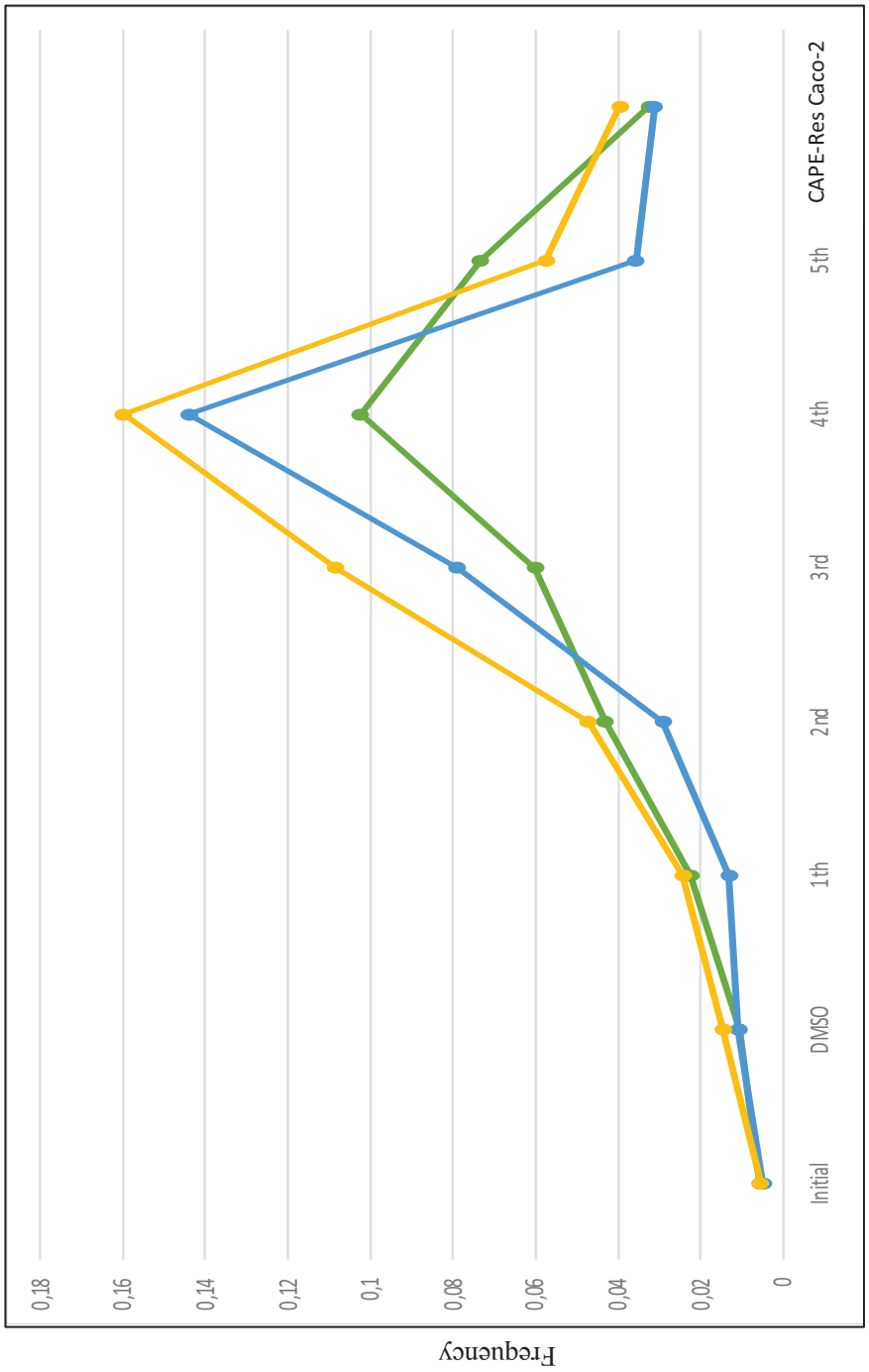

Figure B.1 Frequency distributions of the de novo barcodes in DMSO, Initial cell line controls and capecitabine-resistant Caco-2 cell line (Replica B) and dead cells in the mediums (Replica B mediums)

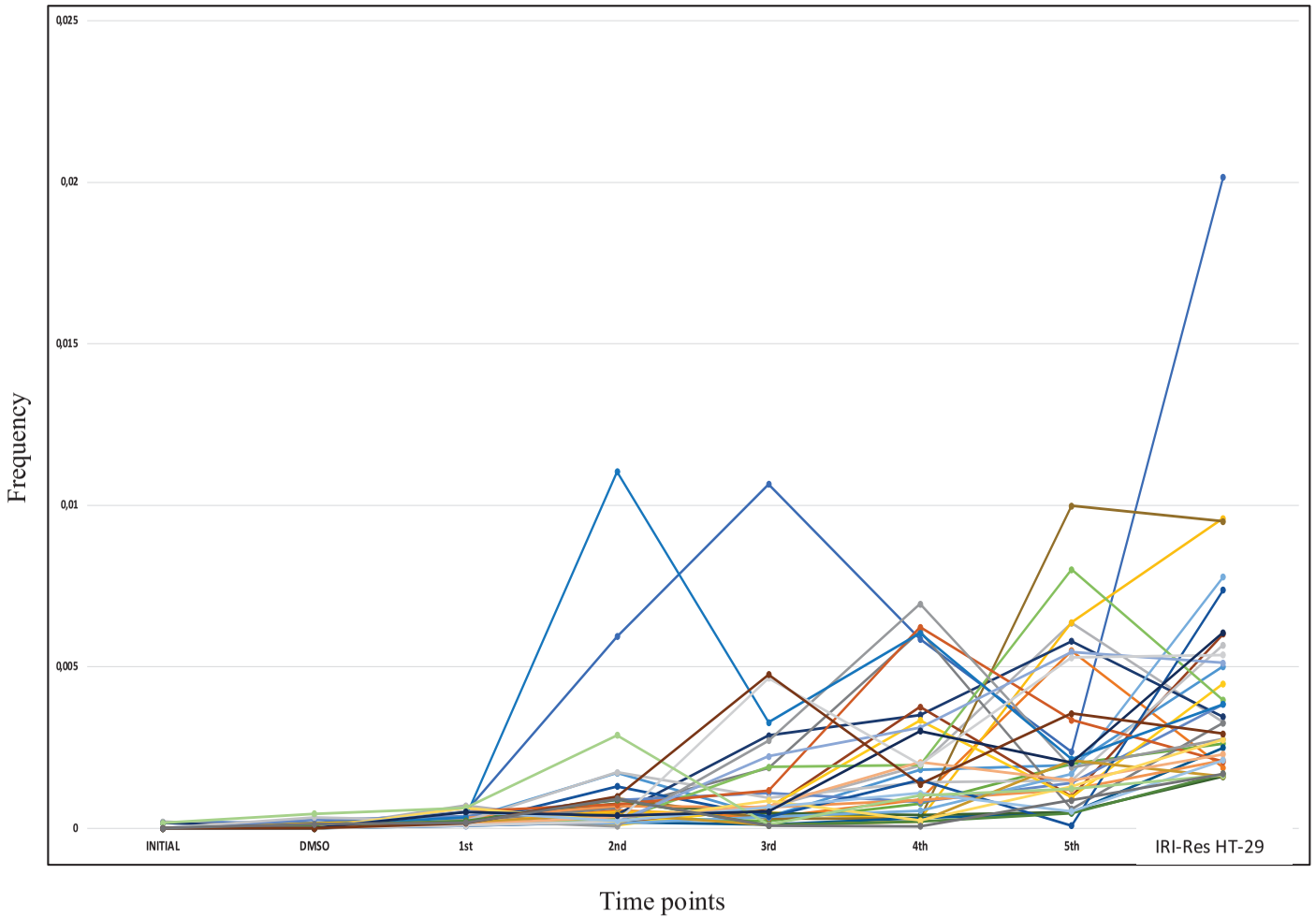

Figure B.2 Frequency distributions of the de novo barcodes in DMSO, Initial cell line controls and irinotecan-resistant HT-29 cell line (Replica B) and dead cells in the mediums (Replica B mediums)

C. TRACKING OF SENSITIVE BARCODES OF CAPECITABINE-RESISTANT CACO-2 AND IRINOTECAN-RES HT-29 CELL LINES

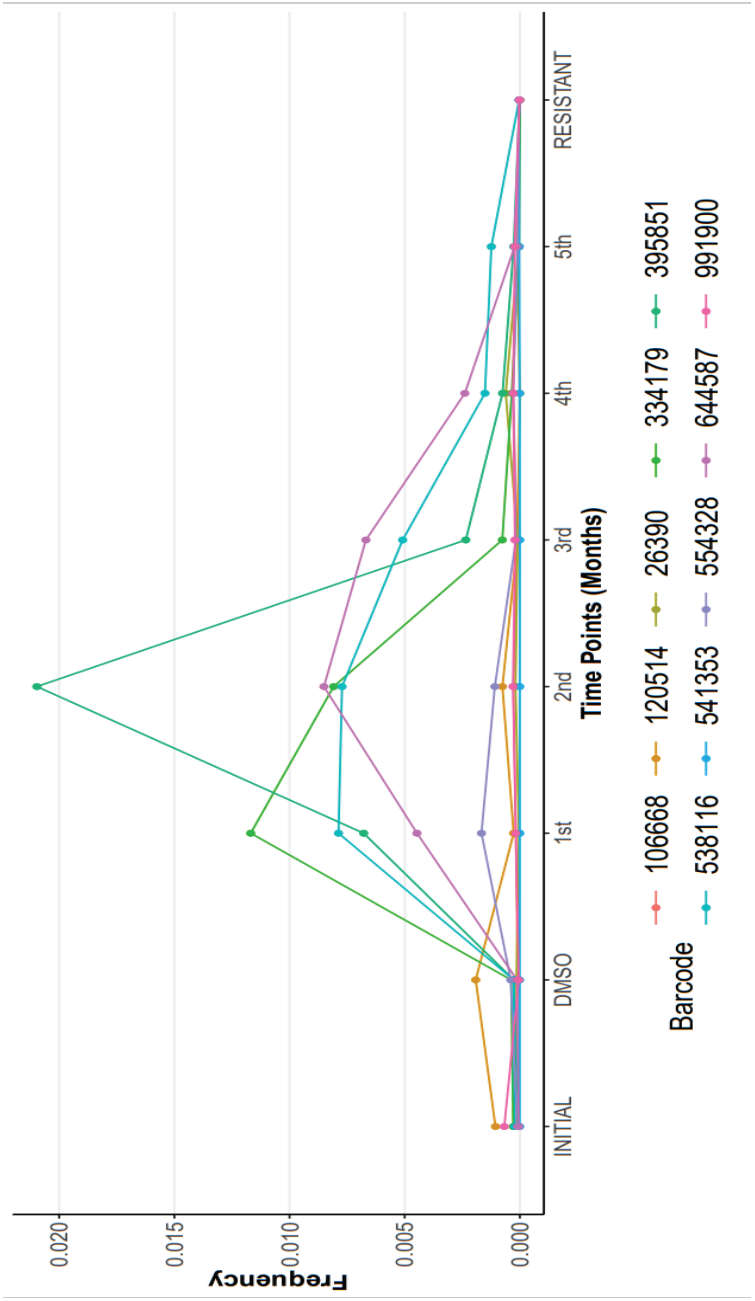

Figure C.1 Representation of Figure 3.7 with the smaller y-axis range. Frequency distributions of the sensitive barcodes in DMSO, Initial cell line controls and capecitabine resistant Caco-2 cell line (Replica B) and dead cells in the mediums (Replica B mediums)

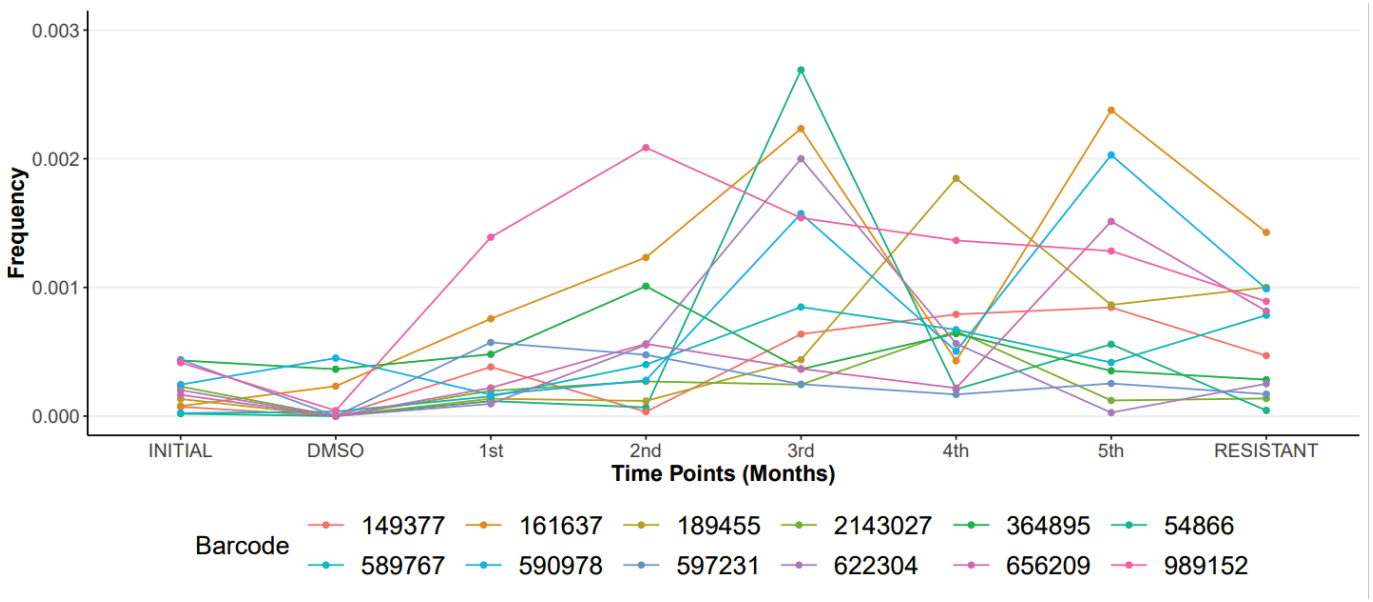

Figure C.2 Representation of Figure 3.16 with the smaller y-axis range. Frequency distributions of the sensitive barcodes in DMSO, Initial cell line controls and irinotecan resistant HT-29 cell line (Replica B) and dead cells in the mediums (Replica B mediums)

D. THE NUMBER OF DETECTED BARCODES IN BARCODED INITIAL, DMSO AND CAPE-RESISTANT CACO-2 CELL POPULATIONS

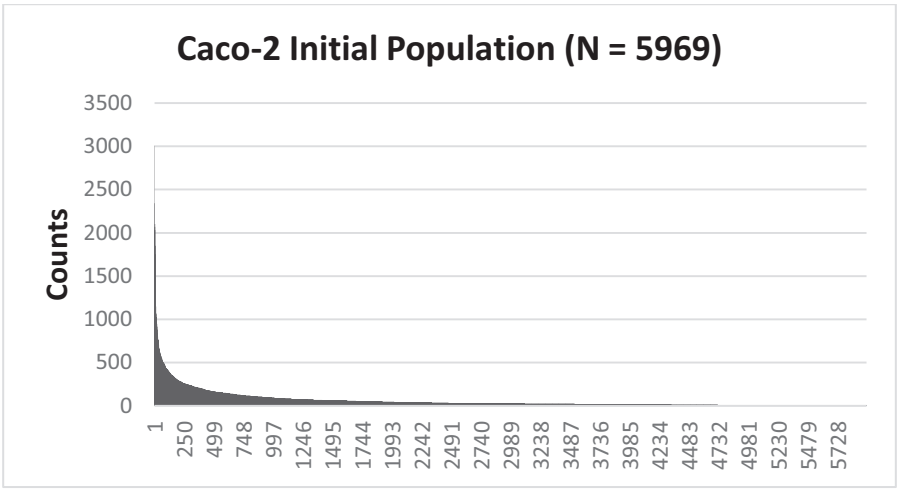

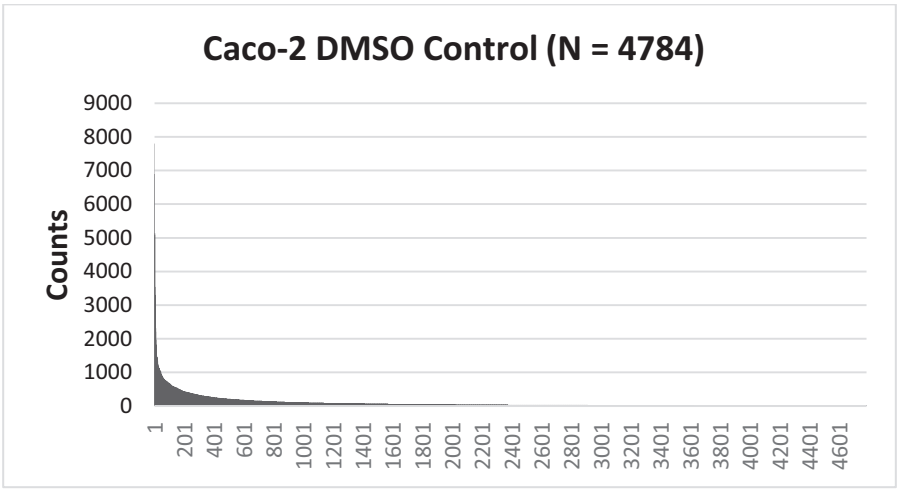

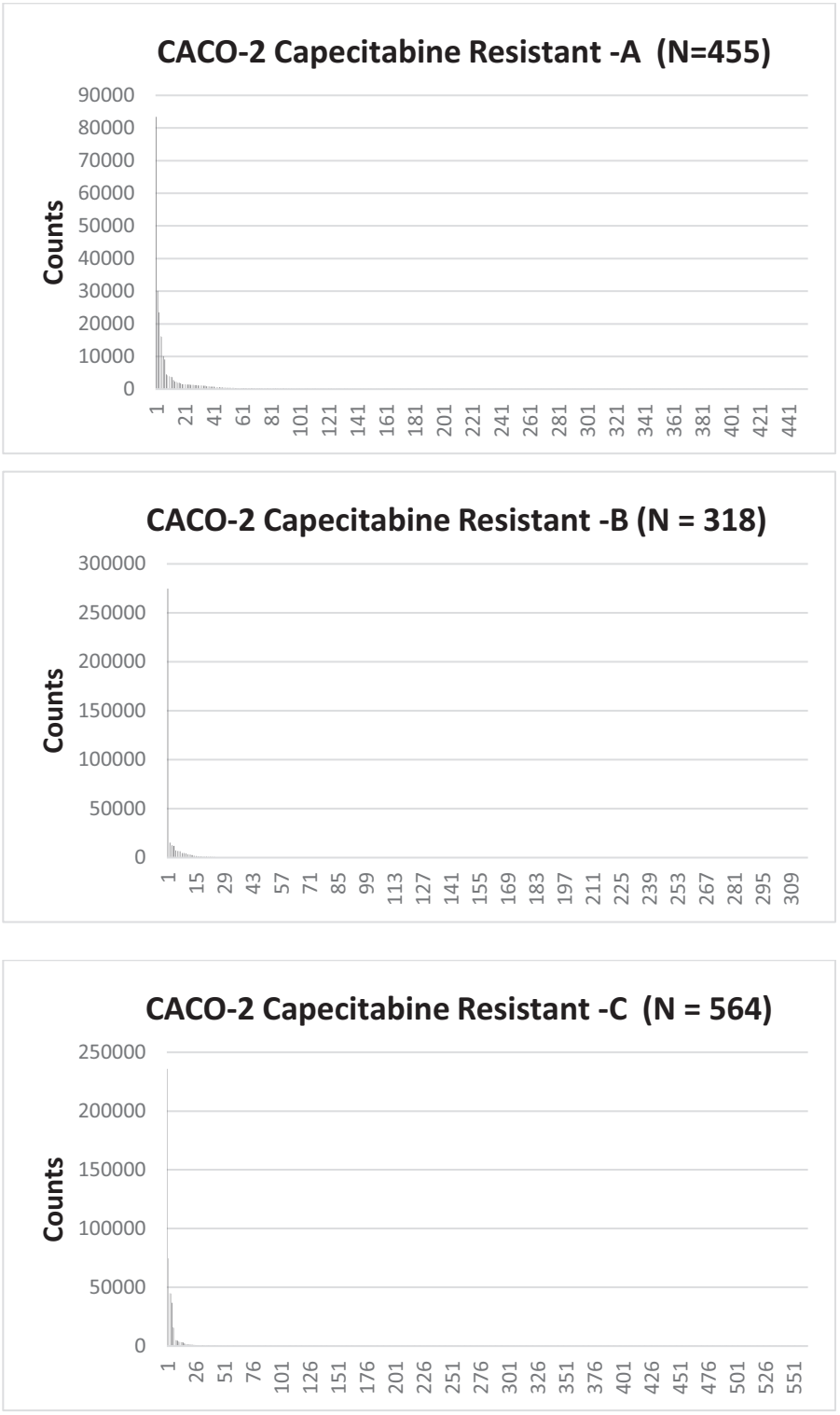

Figure D.1 The number of detected barcodes from barcode sequencing of initial, DMSO Caco-2 control cell lines and capecitabine-resistant Caco-2 replicates

E. THE NUMBER OF DETECTED BARCODES IN BARCODED INITIAL, DMSO AND IRI-RESISTANT HT-29 CELL POPULATIONS

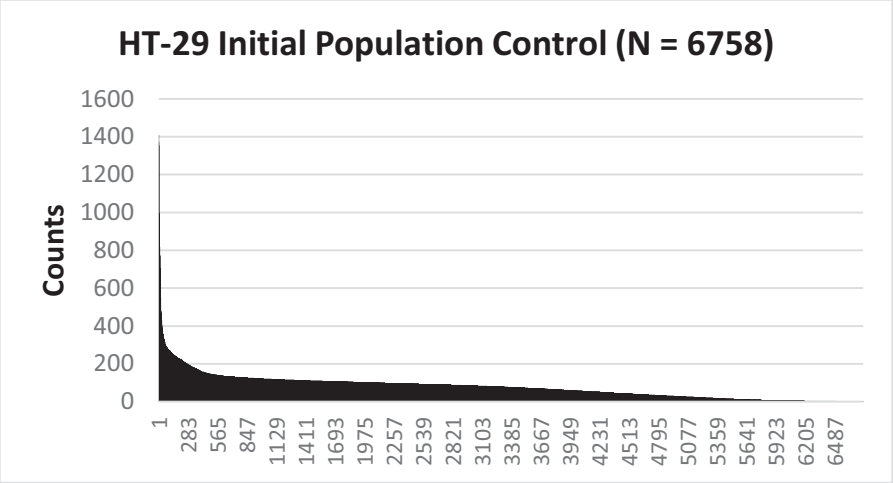

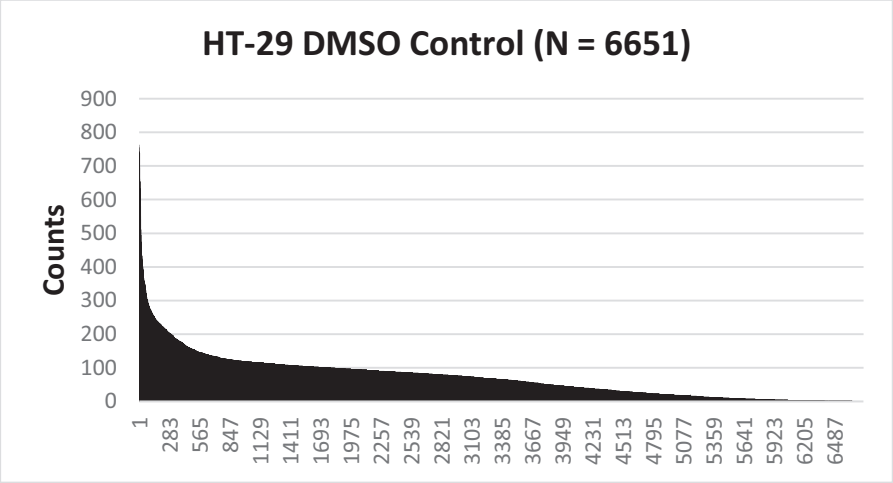

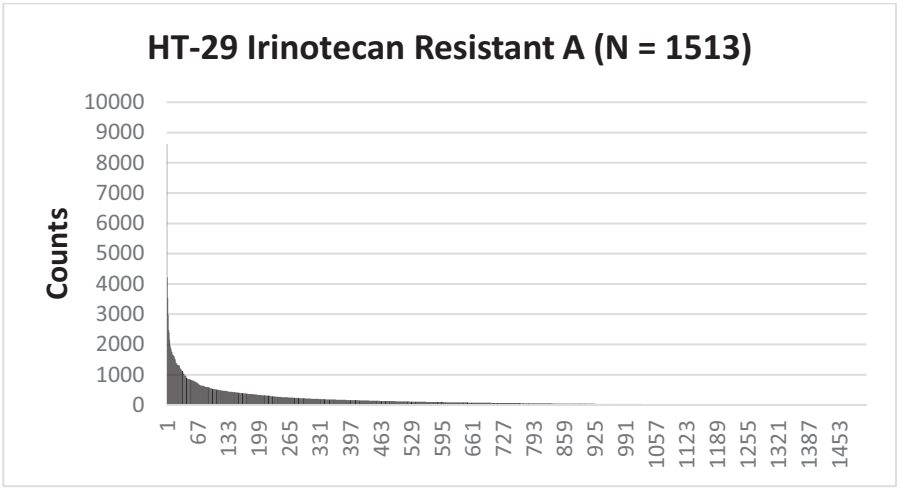

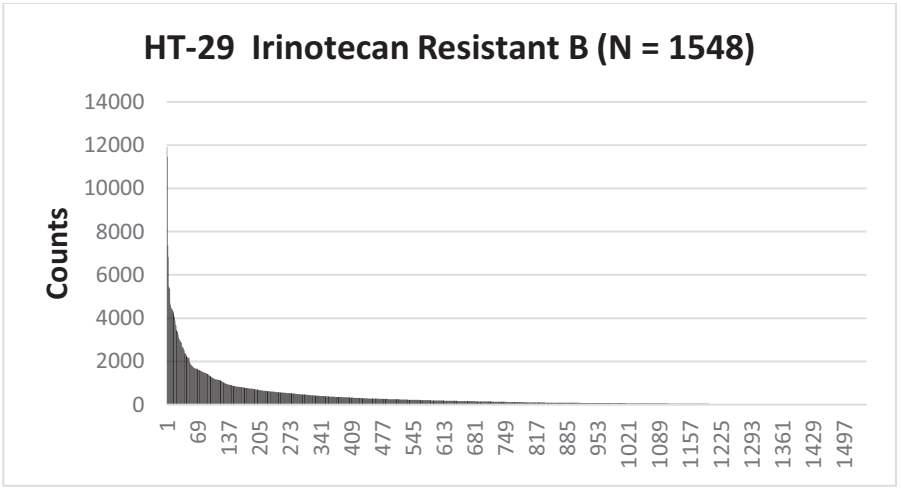

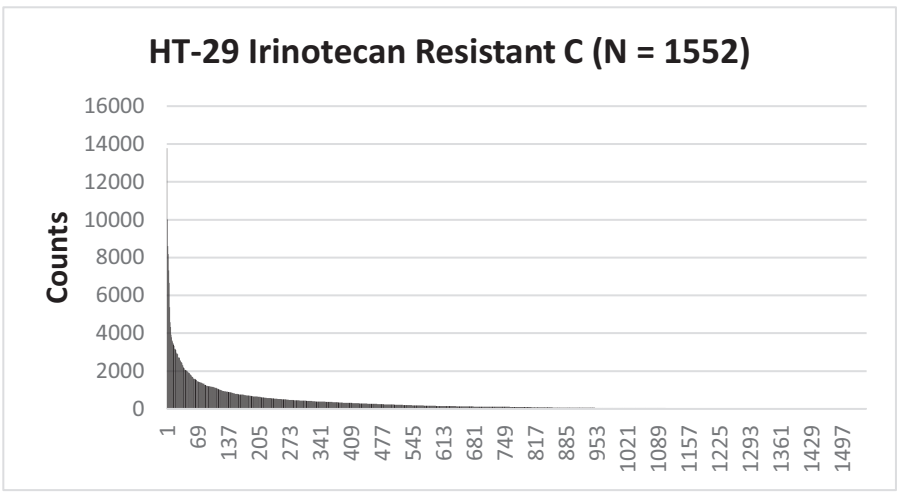

Figure E.1 The number of detected barcodes from barcode sequencing of initial, DMSO HT-29 control cell lines and irinotecan-resistant HT-29 replicates

F. THE WESTERN BLOT ASSAY BUFFERS USED IN THIS STUDY

10X SDS-PAGE RUNNING BUFFER

30.3 g Tris Base

144.4 g Glycine

10 g SDS

Dissolved in distilled water (up to 1 *L*)

100 *mL* 10X Running Buffer are diluted with 900 *mL* distilled water to prepare 1X SDS-PAGE Running Buffer

10X WET TRANSFER BUFFER

0.25 M Tris Base

1.92 M Glycine

Up to 1 *L* pH: 8.3

To prepare 1X Wet Transfer Buffer, 100 *mL* 10X Wet Transfer Buffer are diluted with 700 *mL* distilled , and 200 *mL* methanol are added

TBS-T

20 mM Tris

150 mM NaCl

Up to 1 *L* pH:7.4

To prepare 1X TBS-T , 100 *mL* TBS are diluted with 900 *mL* distilled water and 1 *mL* Tween-20 is added

MILD-STRIPPING BUFFER

15 g Glycine

1 g SDS

10 *mL* Tween-20

Up to 1 *L* pH: 2.2

10% SDS-PAGE SEPERATING GEL MIXTURE

4.05 *mL* distilled water

3.33 *mL* 30% Acryamide/ Bisacrylamide solution

2.5 *mL* 1.5 M Tris-HCL , pH:8.8

100 *µL* APS

100 *µL* SDS (10%)

10 *µL* TEMED

5% SDS-PAGE STACKING GEL MIXTURE

6.8 *mL* distilled water

1.7 *mL* 30% Acryamide/ Bisacrylamide solution

1.25 *mL* 1.5 M Tris-HCL , pH:8.8

100 *µL* APS

100 *µL* SDS (10%)

12 *µL* TEMED